YU ISSN 0372-8633

ŽELEZARSKI ZBORNIK

LETO 25 ŠT. 4–1991
ŽEZB BQ 25 (4) 117–164 (1991)

IZDAJAJO ŽELEZARNE JESENICE, RAVNE, ŠTORE IN METALURŠKI INŠTITUT

ŽELEZARSKI ZBORNIK

Izdajajo skupno Železarne Jesenice, Ravne, Štore in Metalurški inštitut Ljubljana

UREDNIŠTVO

Glavni in odgovorni urednik: J. Arh

Uredniški odbor: A. Kveder, J. Rodič, A. Paulin, F. Grešovnik, F. Mlakar, K. Kuzman, J. Jamar

Tehnični urednik: J. Jamar

Lektor: C. Martinčič

Prevodi: A. Paulin, N. Smajić (angleški jezik), J. Arh (nemški jezik)

NASLOV UREDNIŠTVA: Železarski zbornik, SŽ-Železarna Jesenice, 64270 Jesenice, Yugoslavia

TISK: TK Gorenjski tisk, Kranj

IZDAJATELJSKI SVET:

prof. dr. M. Gabrovšek (predsednik), Železarna Jesenice
dr. B. Brudar, Iskra, Kranj
prof. dr. V. Čižman, Univerza v Ljubljani
prof. dr. D. Drobnjak, Univerza v Beogradu
prof. dr. B. Koroušić, Metalurški inštitut Ljubljana
prof. dr. L. Kosec, Univerza v Ljubljani
prof. dr. J. Krajcar, Metalurški inštitut Sisak
prof. dr. A. Križman, Univerza v Mariboru
dr. K. Kuzman, Univerza v Ljubljani
dr. A. Kveder, Metalurški inštitut v Ljubljani
prof. dr. A. Paulin, Univerza v Ljubljani
prof. dr. Z. Pašalić, Železarna Zenica
prof. dr. C. Pelhan, Univerza v Ljubljani
prof. dr. V. Prosenc, Univerza v Ljubljani
prof. dr. B. Sicherl, Univerza v Ljubljani
dr. N. Smajić, Metalurški inštitut v Ljubljani
prof. dr. J. Sušnik, Zdravstveni dom Ravne
dr. L. Vehovar, Metalurški inštitut Ljubljana
prof. dr. F. Vodopivec, Metalurški inštitut Ljubljana

Published jointly by the Jesenice, Ravne and Štore Steelworks, and The Institute of Metallurgy Ljubljana

EDITORIAL STAFF

Editor: J. Arh

Associate Editors: A. Kveder, J. Rodič, A. Paulin, F. Grešovnik, F. Mlakar, K. Kuzman, J. Jamar

Production editor: J. Jamar

Lector: C. Martinčič

Translations: A. Paulin, N. Smajić (English), J. Arh (German)

EDITORIAL ADDRESS: Železarski zbornik, SŽ-Železarna Jesenice, 64270 Jesenice, Yugoslavia

PRINT: Gorenjski tisk, Kranj

EDITORIAL ADVISORY BOARD:

prof. dr. M. Gabrovšek (Chairman), Iron and Steel Works, Jesenice
Dr. B. Brudar, Iskra, Kranj
Prof. Dr. V. Čižman, University of Ljubljana
Prof. Dr. D. Drobnjak, University of Belgrade
Prof. Dr. B. Koroušić, Institute of Metallurgy, Ljubljana
Prof. Dr. L. Kosec, University of Ljubljana
Prof. Dr. J. Krajcar, Institute of Metallurgy, Sisak
Prof. Dr. A. Križman, University of Maribor
Dr. K. Kuzman, University of Ljubljana
Dr. A. Kveder, Institute of Metallurgy, Ljubljana
Prof. Dr. A. Paulin, University of Ljubljana
Prof. Dr. Z. Pašalić, Iron and Steel Works, Zenica
Prof. Dr. C. Pelhan, University of Ljubljana
Prof. Dr. V. Prosenc, University of Ljubljana
Prof. Dr. B. Sicherl, University of Ljubljana
Dr. N. Smajić, Institute of Metallurgy, Ljubljana
Prof. Dr. J. Sušnik, Health Centre, Ravne
Dr. L. Vehovar, Institute of Metallurgy, Ljubljana
Prof. Dr. F. Vodopivec, Institute of Metallurgy, Ljubljana

Oproščeno plačila prometnega davka na podlagi mnenja
Izvršnega sveta SRS — sekretariat za informacije
št. 421-1/172 od 23. 1. 1974

ŽELEZARSKI ZBORNIK

IZDAJAJO ŽELEZARNE JESENICE, RAVNE, ŠTORE IN METALURŠKI INŠTITUT

LETO 25 LJUBLJANA DECEMBER 1991

Ž E L E Z A R S K I Z B O R N I K
IZDAJAJO ŽELEZARNE JESENICE, RAVNE, ŠTORE IN METALURŠKI INŠTITUT
LETO 25 LJUBLJANA DECEMBER1991

Vpliv varilne tehnologije in izbire dodajnega materiala na lomne lastnosti EPP zvarnega spoja na nizko ogljičnem finozrnatem jeklu

The Influence of Welding Technology and Welding Material Selection on Fracture Properties of Submerged Arc Welded, Low Carbon, Finegrained Steel Plate

I. Rak[1], V. Gliha[2], F. Vodopivec[3], M. Tavčar[2]

1. UVOD

Razvoj nizko ogljičnih jekel, ki so izdelana na termomehanski način ali kaljena in popuščana in ki so uporabljana v konstrukcijah z zahtevnimi obremenitvenimi pogoji, je v veliki meri spremenil varilno tehnologijo. Zaradi nizkega ogljika in nizke vsebnosti difuzijskega vodika v zvaru izdelovalci jekel ne priporočajo več predgrevanja pred varjenjem. Pri tem ni nevarnosti, da bi v TVP nastopila razpokljivost v hladnem, kar je mogoče npr. preveriti z Dürenovim in Suzuki konceptom /1, 2/.

Če navedeno prenesemo na dejanske zvarne spoje (hlajenje pod 50° C po vsakem varku in začetek varjenja brez predgrevanja), ki so zvarjeni z nizko dovedeno toploto (10—15kJ/cm), da bi zajamčili dobro žilavost v grobozrnatem predelu TVP, se lahko v raztopljenem zvaru pojavi nizka žilavost kot posledica tvorbe podolgovatih M/A strukturnih faz glede na kemično sestavo jekla in dodajnega materiala. V primeru napetostnega žarjenja pri 580° C se pojavi neugodni efekt izločevanja Fe_3C iz M/A faz, ki predstavljajo prenasičeno raztopino. Pri tem je žilavost lahko še nižja, če je staljeni zvar občutljiv na reverzibilno popuščno krhkost. V tem prispevku so obravnavane samo lastnosti raztaljenega dela zvarnega spoja.

Zaradi jasnega efekta vpliva znižanega dovoda toplote pri varjenju in zaradi zmanjšanja velikosti zrna in primarnega ferita po kristalnih mejah je bil izbran za raziskavo dodajni material z 0,4% Cr in 0,2% Mo ter z dodatkom Ti-B. Uporabljena je bila metoda elektro varjenja pod praškom - EPP. Žilavost zvara je bila ugotavljana z udarnim Charpijevim kladivom. Zareze v Charpy preizkušancih so bile locirane v kovini in korenski legi X simetričnega zvara pravokotno na debelino. Razlog za to je bilo pričakovano različno razmešanje, predvsem s stališča Nb (NB = 0,01 % v krovni legi in 0,04% v korenski legi). Preizkusi so bili opravljeni na celotni debelini zvara po metodi CTOD z upogibnimi preizkušanci, zarezanimi in utrujanimi pravokotno na debelino v sredini zvara.

Lomne površine so bile preiskane z vrstičnim elektronskim mikroskopom predvsem glede pojava in lokaci-

[1] Tehniška fakultata Maribor, VTO-S,
[2] RRI, Metalna Maribor,
[3] Inštitut za kovinske materiale in tehnologije

1. INTRODUCTION

Development of LC steels, produced on thermomechanical way or by quenching and tempering and used in constructions under sophisticated load conditions, has largely changed the welding technology.

Because of the LC and low diffusible hydrogen content in the weld, the steel producers do not recommend preheating before welding. There is no danger of cold cracking appearance in HAZ what is possible to check up with Düren and Suzuki theory for example /1, 2/ Transferring these statements into the real weldment (interpass temperatures under 50 degrees Celsius and no preheating before welding) welded with low heat input (10-15 KJ/cm) to ensure good toughness in coarse grain area of HAZ, can in the melted part of the weld cause the appearance of low toughness values as the result of oblongated M/A structural phase formation depending on the chemical composition of steel and welding material. In the case of stress relieved heating at 580 degrees Celsius there appears the undesirable effect to Fe_3C precipitation from M/A phases representing a saturated solution. The toughness values can be lowered even more if the sensitivity of the melted part of the weld on a reversible temper brittleness is present.

Because of the clear effects of low heat input at welding and reduced grain size and primary ferrite on crystal boundaries, the welding material with 0,4% Cr and 0,2% Mo and Ti-B additions was chosen in these researches. The SAW welding method was used. The weld toughness was determined by Charpy V-notch impact test. The notchess of Charpy impact specimens were located in face and root location of double V butt type weld, right angled on the thickness of the plate. The reason was in the expected uneven dilution, first of all from the Cb point of view (Cb= 0,01% in the face of the weld and 0,04% in root of the weld). Further tests were carried out on the complete weld thickness by the CTOD method on the bend type specimens notched and fatigued in the rightangled direction to the thickness in the middle of the weld.

Fractured surfaces were examined with line EM, first of all on the appearance of LBZ. Both, line EM and optical microscope were used by the examinations of microstructures in the welded joint. The presented results

je LKP. Mikrostrukture zvara so bile preiskane z optičnim in vrstičnim elek. mikroskopom. Rezultati dokazujejo, da staljeni del zvara kljub drobnemu zrnu in nizki vsebnosti primarnega ferita po kristalnih mejah ni vedno dovolj žilav. Torej ocena struktur z optičnim mikroskopom po priporočilu IIW /3/ ni vedno zadostna za analizo in določitev vzrokov za dobro ali slabo žilavost staljenega zvara. Dodatne metode, kot npr. uporaba vrstičnega mikroskopa, lahko pokažejo dejanski vzrok za nizko ali visoko žilavost v staljenem zvaru v izhodnem in napetostno žarjenem stanju.

2. LASTNOSTI IN MIKROSTRUKTURA NIZKO OGLJIČNEGA EPP STALJENEGA ZVARA

Poznan je odnos med mikrostrukturo zvara in žilavostjo /4/. Razmešanje raztaljenega zvara v času varjenja spreminja transformacijsko kinetiko staljenega zvara, pri čemer imajo lahko vključki znaten vpliv. Gostota, velikost in porazdelitev vključkov narekujejo razvoj velikosti avstenitnih zrn po strditvi. Oksidni in drugi vključki ter koncentracija avstenitne trdne raztopine skupaj s hitrostjo ohlajevanja vplivajo na različne feritne morfologije v času premene (γ/α /5a). Puščičasti ferit se npr. pojavi v EPP zvaru, če je koncentracija O_2 višja od 450 ppm; njegova rast iz primarnega ferita na kristalni meji v zrno je intergranularna. Pri nižjih vsebnostih O_2 se pojavi več ugodnega acikularnega ferita, medtem ko nizke vsebnosti O_2 vodijo do tvorbe bainitne strukture. Poleg vsebnosti O_2 je pomembna velikost in enakomerna porazdelitev vključkov. Vključki velikosti $>0{,}2$ µm bodo povzročili pospešeno tvorbo acikularnega ferita in znižali vsebnost primarnega ferita, pri čemer se povečajo primarna dendritna zrna s fino porazdeljeno intergranularno strukturo /5b/.

V času tvorbe primarnega in puščičastega ferita se preostali avstenit znatno obogati s C ter se lahko transformira v faze, ki vsebujejo zaostali avstenit in martenzit ali bainit-M/A strukturne faze. Takšno strukturo često najdemo pod izrazom ferit s sekundarno fazo. Prisotni vključki so tvorci puščičastega ferita, katerega oblika je odvisna od hitrosti ohlajevanja /6/. Višje hitrosti ohlajevanja pospešujejo tvorbo Widmanstattenskega ferita, ki ga spremlja neugodna porazdelitev M/A faz. Dodatki Nb ta fenomen še pospešujejo, kar se kaže v nižji žilavosti. Na drugi strani dodatki Ti in B izboljšajo žilavost, ker pospešujejo tvorbo acikularnega ferita, ki se pojavi na drobnih intergranularnih vključkih. Večina elementov vpliva na tvorbo in hitrost rasti puščičastega ferita. Dodatki Si in Al pospešujejo tvorbo puščičastega ferita, medtem ko jo Mn in Mo zavirata. Pretvorbo iz acikularnega ferita v ferit s sekundarno fazo, kot npr. M/A fazo, pospešujeta Cr in Mo, ki tudi povišujeta mejo plastičnosti in trdnost /7/.

3. RAZISKAVA SOČELNEGA EPP STALJENEGA ZVARA

3.1. Izbira osnovnega in dodajnega materiala

Raziskave so bile opravljene na EPP zvarnem spoju nizkoogljičnega poboljšanega jekla Niomol 390. Lastnosti osnovnega in dodajnega materiala so navedene v **tabeli 1.** Navedeni dodajni material je bil izbran, da bi poudarili razlike pri nižjem in višjem dovodu toplote zaradi njegove povišane zakaljivosti, kar je razvidno iz višjega Pcm v primerjavi z osnovnim materialom.

V predhodnih raziskavah /8/, kjer je bil uporabljen komercialni dodajni material (z 1 % Ni s Pcm = 0,149 in je bilo varjenje opravljeno prav tako brez predgrevanja, so se pojavila vidna LKP v prelomu CTOD preizkušanca v

show, that the melted part of the weld is not always tough enough in spite of fine grained coarse and low primary ferrite on crystal boudaries. Therefore, the estimation of structures with optical microscope, as it is recommended by IIW /3/, is not always sufficient enough for the analyse and determination of good or bad toughness in the melted part of the welded joint. Additional methods, as line electron microscope for example, can show the real reason for low or high toughness values in the melted part of the welded joint in as-welded or stress relieved conditions.

2. THE PROPERTIES AND MICROSTRUCTURE OF THE LOW CARBON MELTED PART OF THE SUBMERGED ARC WELDED JOINT

The relationship between microstructure and toughness of the welded joint is known /4/. Dilution of the melted part of the welded joint during welding is changing the transformation kinetic of melted weldment and the inclusions can have a significant influence on it. Density, size and distribution of inclusions do dictate the size development of austenitic grains after the solidification. Oxide and other types of inclusions and concentration of austenitic solid solution together with the cooling speed, are influencing upon different ferrite morphologies during the transformation γ/α /5a/. Acicular ferrite can appear for example in the SA welded joint, if the concentration of oxygen is higher than 450 ppm; its growth is intragranular from primary ferrite on crystal boundary into the grain. At the lower oxygen concentrations more favourable acicular ferrite appears, while low oxygen concentration lead to the formation of bainite structure.

Beside the low oxygen concentration the size and uniform distribution of inclusions is important. The inclusion sizes over 0,2µm will cause an accelerated formation of acicular ferrite and reduce the content of primary ferrite increasing at the same time the size of the dendrite grains with fine distributed intragranular structure /5b/.

During the formation of primary and acicular ferrite the remained content of austenite becomes significantly rich with carbon and can transform in phases containing residual austenite and martensite or bainite-M/A structural phases. Such structure we can often find in the expression ferrite with the second phase. Present inclusions are authors of acicular ferrite which shape depends on cooling speed /6/. Higher cooling speed accelerates the formation of Widmanstatt-ferrite accompanied by unfavourable distribution of M/A phases. The additions of Cb accelerates this phenomena what results in the lower toughness. On the other side the additions of Ti and B improve the toughness because they accelerate the formation of acicular ferrite, which appears on intragranular inclusions. The most of elements have their effect on the formation and growth speed of acicular ferrite. The additions of Si and Al accelerate the formation of arrow-shaped ferrite, while Mn and Mo retard it. The transformation from acicular ferrite to ferrite with secondary phase, as for example M/A phase, is accelerated with Cr and Mo which also increase the yield point and strength /7/.

3. RESEARCH OF THE BUTT — SA WELDED MOLTEN JOINT

3.1. The choice of the base and welding material

The researches were carried out on the SA welded, low carbon, quenched and tempered steel plate Niomol

izhodnem in napetostno žarjenem stanju celo pri +20°C. Preiskave na rasterskem mikroskopu so odkrile več kot 10 % M/A strukturne faze.

Dodatek Ti-B je v tej preiskavi bil izbran z namenom preprečiti oz. znižati tvorbo primarnega ferita po kristalnih mejah in pospešiti tvorbo acikularnega ferita v strukturi staljenega zvara /9/.

Vpliv grobega zrna in primarnega ferita na žilavost staljenega zvara je bil tako z izbiro navedenega dodajnega materiala izključen. Namen preiskave je bil ugotoviti vpliv M/A faz z ozirom na njihovo sestavo (visok C), velikost, usmerjenost in gostoto na udarno in lomno žilavost v odvisnosti od hitrosti ohlajevanja in legiranosti staljenega zvara /10, 11/. Nadaljnji namen je bil ugotoviti vpliv napetostnega žarjenja na razpad M/A faz in tako na žilavost staljenega zvara.

Tabela 1: Lastnosti uporabljenih materialov

Lastnosti osnovnega materiala					
Debelina /mm/	R_e /MPa/	R_m /MPa/	σ_5 /%/	Žilavost –60°C /J/	CTODi, –40°C /mm/
30	432	528	25	198,161,149	0,51
Kemična sestava					
0,08C 0,08Sn	0,30Si 0,18Ni	1,11Mn 0,012As	0,006S 0,047Al	0,015P Pcm=0,1-49	0,049Nb CE=0,27-0
Lastnosti čistega dodajnega materiala					
EPP-dod.mat.	R_e /MPa/	R_m /MPa/	σ5 /%/	Žilavost –60°C /J/	CTOD /mm/
OP121TT Fluxocord 35.22	480	520–620	24	>50, varjeno >35, žarjeno	— —
Kemična sestava					
0,05C Ti dod.	0,20Si Pcm=0,1-75	1,2Mn CE=0,37-0	0,04Cr	0,20Mo	0,005B
Kemična sestava dejanskega EPP zvara					
0,05C 0,031Ti 0,009S	0,36Si 0,023Al 0,020P	1,67Mn 0,04Sn 0,022Nb	0,70Cr 0,04Sb	0,41Mo 0,006B	0,025V 0,007As
Pcm=0,2-46	CE=0,55-7	O_2=227p-pm	H_D<2,6 - ml /100 gr		

3.2. Varjenje preizkusnih plošč in priprava preizkušancev

Uporabljeno je bilo večvarkovno varjenje na simetrično pripravljenem X zvarnem žlebu. Keramični vložek je bii uporabljen z izvedbo korenskega varka. Zvarjeni sta bili dve preizkusni plošči z različnima tehnologijama, A-brez predgrevanja in B-s predgrevanjem.

Podatki o varjenju:

debelina plošče — 30 mm
predgrevanje — brez (A), 150°C (B)
vnešena toplota — 15kJ/cm
$\Delta t_{8/5}$ — 5,4s(A), 10,5s(B)
vmesna temp. — 50°C(A), 200°C(B)
pogrevanje — 200°C

390. The properties of base and welding material are given in ***Table 1.*** *Given welding material has been chosen for the reason to point out the differences at lower and higher heat input because of its higher quench capability, what is obvious from higher Pcm value in comparison with base material.*

In previous researches /8/, where commercial welding material (with 1% Ni) was used, with Pcm= 0,149 and where welding was also carried out without preheating, visible LBZ have appeared on fractured CTOD specimen surfaces in as-welded and stress relieved conditions even at + 20 degrees Celsius. Raster microscope examinations have determined more than 10% M/A structural phase. Ti-B addition in this research has been chosen for the reason to prevent or to reduce primary ferrite formation on crystral boundaries and to accelerate the acicular ferrite formation in the structure of molten weld /9/.

With such welding material selection the influence of coarse grain in primary ferrite on molten weld toughness was expelled. The aim of the examination was to find out the influence of M/A phases concerning their composition (high C(, size, orientation and density on fracture toughness of the molten weld depending on its cooling speed and chemical composition /10,11/. Another aim was to find the influence of stress relieving on the disintegration of M/A phases in the molten weld.

Table 1: *Properties of material used*

Base material properties					
Thickness /mm/	R_e */MPa/*	R_m */MPa/*	δ_5 */%/*	*Toughness –60°C /J/*	*CTODI, –40°C /mm/*
30	*432*	*528*	*25*	*198,161,149*	*0,51*
Chemical composition					
0,08C 0,08Sn	*0,30Si 0,18Ni*	*1,11Mn 0,012As*	*0,006S 0,047Al*	*0,015P Pcm=0,1-49*	*0,049Nb CE=0,27-0*
Weld metal properties					
SAW Weld.Mat.	R_e */MPa/*	R_m */MPa/*	δ_5 */%/*	*Toughness –60°C /J/*	*CTOD /mm/*
OP121TT Fluxocord 35.22	*480*	*520—620*	*24*	*>50, as welded >35, stress rel.*	*— — —*
Chemical composition					
0,05C Ti add.	*0,20Si Pcm=0,1-75*	*1,2Mn CE=0,37-0*	*0,04Cr*	*0,20Mo*	*0,005B*
Chemical composition of real weld metal					
0,05C 0,031Ti 0,009S	*0,36Si 0,023Al 0,020P*	*1,67Mn 0,04Sn 0,022Nb*	*0,70Cr 0,04Sb*	*0,41Mo 0,006B*	*0,025V 0,007As*
Pcm=0,2-46	*CE=0,55-7*	*O_2=227p-pm*	*HD<2,6-ml /100 g*		

3.2. Welding of test plates and specimen preparation

A welding technique with more passes was used on double-V grooved steel plate. For the root weld accomplishment a ceramic insert was used. There were two

Po varjenju je bila polovica vsake plošče napetostno odžarjena pri 580°C v času 3 ur, nekaj izrezanih preizkušancev pa še pri 650°C ter s kombinirano termično obdelavo. Preizkušanci so bili izrezani iz zvarnega spoja v izhodnem in napetostno odžarjenem stanju. Pripravljeni so bili metalografski preizkušanci, žilavostni preizkušanci zarezani v krovni in korenski legi ter CTOD preizkušanci iz celotne debeline; vsi zarezani pravokotno na površino plošče v sredini staljenega zvara.

3.3. Udarna in lomna žilavost staljenega zvara

Udarni Charpijevi preizkušanci so bili pretežno odvzeti iz krovne lege zvara in preizkušani v izhodnem in različno termično obdelanih stanjih. Namen je bil ugotoviti vpliv M/A strukturnih faz na udarno žilavost. Nekaj preizkušancev je bilo odvzetih iz korenskega dela zvara z namenom ugotoviti vpliv Nb, ki se je izcejal iz osnovnega materiala v zvar ter ugotoviti, ali je prisotna termična reverzibilna krhkost. Rezultati za udarno in lomno žilavost staljenega zvara v izhodnem stanju, zvarjenega z in brez predgrevanja, so dani v **tabeli 2.**

Tabela 2: Udarna žilavost in vrednosti za CTOD

Stanje	Lokacija zareze	Temperatura /°C/	Žilavost /J/	CTOD /mm/	Trdota /HV5/
1.	2.	3.	4.	5.	6.
Brez predgrevanja, varjeno	krovni sloj, korenski sloj	+20 −20 +20	92 50 88	—	274
	celotna debelina	+20 0 −20		$0{,}148-\sigma_u$ $0{,}094-\sigma_c$ $0{,}064-\sigma_c$	
Brez predgrevanja, žarjeno 580°C	krovni sloj, korenski sloj	+20 −20 +20 −20	72 24 20 8		
	celotna debelina	+20		$0{,}034\sigma_c$	
Brez predgrevanja, žarjeno 650°C	krovni sloj	−20	23		260
Predg. in varjeno	krovni sloj	−20	65		257
Predg. in žar. 580°C	krovni sloj	+20 −20	103 29		
Predg. in žar 650°C	krovni sloj	+20 −20	114 42		236
Brez predgrevanja, varjeno Ref /8/, 1% Ni	krovni sloj	−20	78		
	celotna debelina	+20 0 −20		$0{,}420-\sigma_u$ $0{,}062-\sigma_c$ $0{,}091-\sigma_c$	
Brez predgrevanja, žarjeno, 580°C, Ref. /8/, 1% Ni	krovni sloj	−20	65		
	celotna debelina	+20 0 −20		$0{,}323-\sigma_u$ $0{,}103-\sigma_c$ $0{,}062-\sigma_c$	

test plates prepared, welded with two different technologies; A-without preheating and B-with preheating.

Welding data:

plate thickness	*— 30 mm*
preheating	*— without (A), 150°C (B)*
heat input	*— 15 KJ/cm*
$\Delta t_{8/5}$	*— 5,4 s (A), 10,5 s (B)*
interpass temp.	*— 50oC (A), 200°C (B)*
heating after welding	*— 200°C*

After welding each half of the plate was stress relieved at 580°C in a period of 3 hours but some specimens were heated to 650°C with combinated heat treatment. Test samples were cut from the weld in as welded and stress relieved condition . Test specimens were cut out for metallographic examination, toughness, notched in face and root area of the weld, and CTOD specimens form the whole weld thickness, all notched perpendicular on the plate surface with the notch location in the middle of the molten weld.

3.3. Notch and fracture toughness of the molten weld metal

Table 2: *Notch toughness and CTOD values*

Condition	*Notch location*	*Temperature /°C/*	*Toughness /J/*	*CTOD /mm/*	*Hardness /HV5/*
1.	*2.*	*3.*	*4.*	*5.*	*6.*
Without preheat., as welded	*face weld* *root weld*	*+20* *−20* *+20* *−20*	*92* *50* *88* *16*	*—*	*274*
	whole thickness	*+20* *0* *−20*		$0{,}148-\delta_u$ $0{,}094-\delta_c$ $0{,}064-\delta_c$	
Without preheat., heated, 580°C	*face weld* *root weld*	*+20* *−20* *+20* *−20*	*72* *24* *20* *8*		
	whole thickness	*+20*		$0{,}034-\delta_c$	
Without preheat., heated, 650°C	*face weld*	*−20*	*23*		*260*
Preheated as welded	*face weld*	*−20*	*65*		*257*
Preheated heated 580°C	*face weld*	*+20* *−20*	*103* *29*		
Preheated heated 650°C	*face weld*	*+20* *−20*	*114* *42*		*236*
Without preheat., as welded, Ref. /8/, 1% Ni	*face weld*	*−20*	*78*		
	whole thickness	*+20* *0* *−20*		$0{,}420-\delta_u$ $0{,}062-\delta_c$ $0{,}091-\delta_c$	
Without preheat., heated, 580°C, Ref. /8/, 1% Ni	*face weld*	*−20*	*65*		
	whole thickness	*+20* *2* *−20*		$0{,}323-\delta_u$ $0{,}103-\delta_c$ $0{,}062-\delta_c$	

Za primerjavo so dani rezultati iz reference /8/, kjer je bil uporabljen komercialni dodajni material (1% Ni). Varjeno je bilo z isto nizko vnešeno toploto in brez predgrevanja kakor pri tej preiskavi. Tudi v tem primeru so se pojavila vidna LKP na preloma vrednosti, dobljene pri CTOD preizkusu ob pojavu "pop-in" efekta, so uporabljene različne oznake. Za nastop "pop-in" efekta po počasni rasti razpoke je oznaka (σu), za nastop "pop-in" efekta takoj za otopitvijo razpoke pa (σ_c). Občutljivost na popuščno reverzibilno krhkost /13/ se je določala z Watanabe faktorjem J /14/ in z udarno žilavostjo; rezultati so dani v **tabeli 3.**

Tabela 3: Popuščna krhkost, določana z udarno žilavostjo

Tehnologija varjenja	Brez predgrevanja			Predgrevanje na 150° C		
	Vmesna temp. 50° C			Vmesna temp. 200° C		
Termična obdelava*	Lokacija zareze	T /° C/	Žilavost /J/	Lokacija zareze	T /° C/	Žilavost /J/
550° C	krovna lega,	+20	72	krovna lega,	+20	103
	krovna lega,	−20	23	krovna lega,	−20	30
	korenska lega	−20	10	—	—	—
550° C + 750° C	krovna lega	−20	55	krovna lega	+20	108
550° C + 710° C + 550° C	krovna lega	−20	30	krovna lega	+20	86

*Pri vsaki temperaturi po 4 ure;
Watanabe faktor J = (Si + Mn) + (P + S) × 10⁴; v našem primeru je J = 512
Za J = < 200 je nizka občutljivost na reverzibilno popuščno krhkost
Za J = > 400 je visoka občutljivost na reverzibilno popuščno krhkost

3.4. Metalografske preiskave z optičnim in vrstičnim mikroskopom

Preiskave so bile opravljene na metalografskih obrusih, odvzetih iz plošč, varjenih brez in s predgrevanjem. **Sliki 1 in 2** prikazujeta stebričaste dendrite z drobno intragranularno strukturo in nizko vsebnostjo ferita po kristalnih mejah v staljenem zvaru, zavarjenem brez predgrevanja. Drobna struktura, posneta z vrstičnim mikro-

Slika 1
Brez predgrevanja.

Fig. 1
Without preheating.

Notch toughness specimens were mostly cut out from face area and tested in as welded and different heat treated conditions. The aim was to find out the influence of M/A structural phases on notch toughness. Some specimens were cut out from root area with the aim to find out the influence of Nb, segregated from the base material to the weld and also if the reversible temper embrittlement is present. The result of notch and fracture toughness of the molten weld metal in as welded condition and welded with and without preheating are shown in ***Table 2.***

For comparison, the results from the reference /8/ are given, where the commercial welding material (1% Ni) was used. Welding was carried out with the same low heat input energy and without preheating as in this examination. In this case visible LBZ on the fractured surfaces of the specimen also appeared at + 20 degrees Celsius Different designations are used for the CTOD values at "pop-in" effect appearance. At "pop-in" effect appearance, after the slow crack growth, the designation (δ_u) is used and designation (δ_c) at "pop-in" effect appearance immediately after the crack tip is blunted. The sensitivity on reversible temper embrittlement /13/ was determined with Watanabe factor J /14/ and with notch toughness; the results are shown in ***Table 3.***

Table 3: *Temper embrittlement determined with notch-toughness*

Welding technology	*Without preheating*			*Preheating 150° C*		
	Interpass temp. 50° C			*Interpass temp. 200° C*		
*Heat treatment**	*Notch location*	*T /° C/*	*Toughness /J/*	*Notch location*	*T /° C/*	*Toughness /J/*
500° C	*face weld*	*+20*	*72*	*face weld*	*+20*	*103*
		−20	*23*		*−20*	*30*
	root weld	*−20*	*10*	—	—	—
550° C 750° C	*face weld*	*−20*	*55*	*face weld*	*+20*	*108*
550° C + 750° C + 550° C	*face weld*	*−20*	*55*	*face weld*	*+20*	*108*

**at each temperature 4 hours;*
Watanabe factor J = (Si + Mn) + (P + S) × 10⁴; in our case is J = 512
For J = < 200 is sensibility on reversible temper embrittlement low
For J = > 400 is sensibility on reversible temper embrittlement high

3.4. Metallographic examinations with optic and line microscope

Metalographic specimens were cut out and examined from steel plates, welded without and with preheating. ***Fig. 1*** *and* ***Fig. 2*** *show columnal dendrites with fine intragranular structure and low ferrite content on crystal boundaries in the molten weld, welded without preheating. Fine structure taken off with a line microscope in the face weld area is shown in* ***Fig. 3****; oblong M/A phases along intragranular precipitated ferrite are visible.* ***Fig. 4*** *shows the microstructure after stress relieved heating; several cementite precipitations on the boundary between M/A phase and ferrite are perceived. Microstructure of the molten weld, welded with preheating is shown in* ***Fig. 5****; there are less M/A phases and or-*

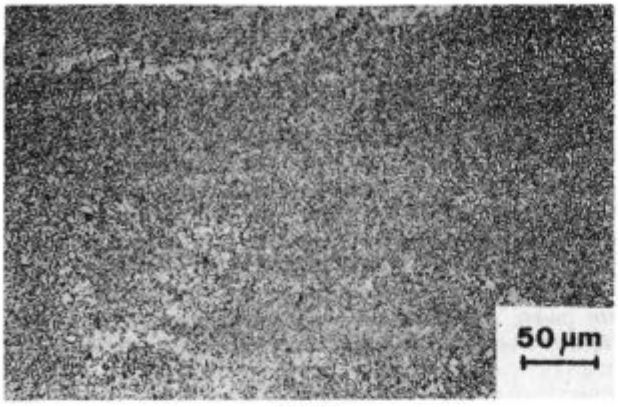

Slika 2
Ista struktura kot slika 1.
Fig. 2
The same structure as in Fig. 1.

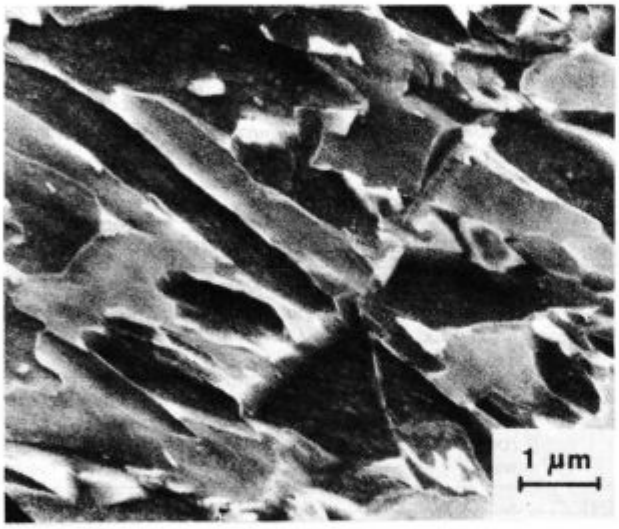

Slika 3
SEM mikrostruktura zvara, brez predgrevanj.
Fig. 3
SEM microstructure of the weld, without preheating.

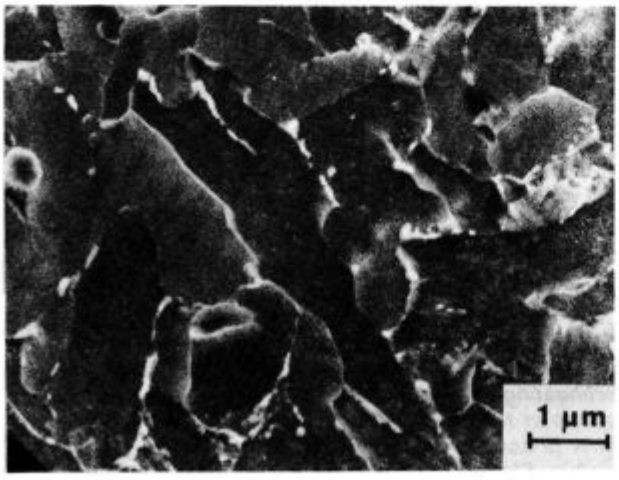

Slika 4
Ista struktura - nap. žarjeno pri 580 °C.
Fig. 4
The same structure - stress - relieved heated at 580°C.

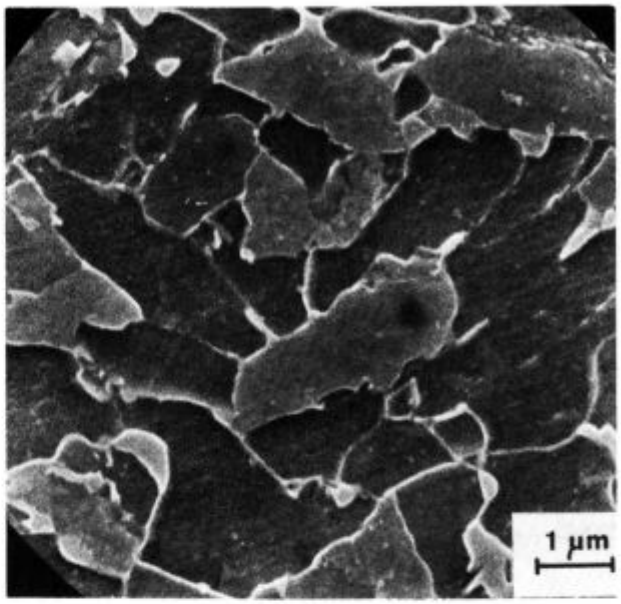

Slika 5
SEM mikrostruktura zvara, s predgrevanjem.
Fig. 5
SEM microstructure of the weld, with preheating.

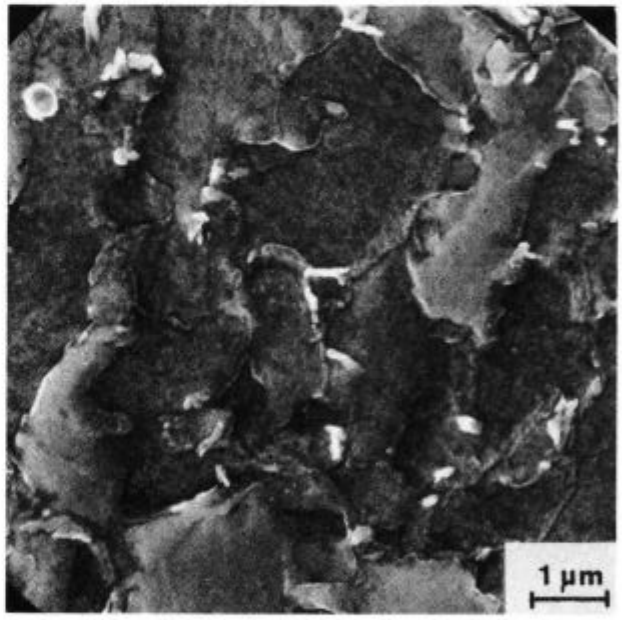

Slika 6
Ista struktura - nap. žarjena pri 580 °C.
Fig. 6
The same structure - stress - relieved heated at 580°C.

ientation is less distinctive. The same microstructure after stress-relieved heating is shown in ***Fig. 6****; a strong tendency of cementite coagulation is visible.*

The examination of LBZ areas has detected a quasi brittle fracture in the fractured area of the specimen in as-welded condition - ***Fig. 7.*** *The fracture area of stress relieved specimen shows besides the quasi brittle fractures also the presence of intergranular brittleness along the columnar dendrites as it is shown in* ***Fig. 8.***

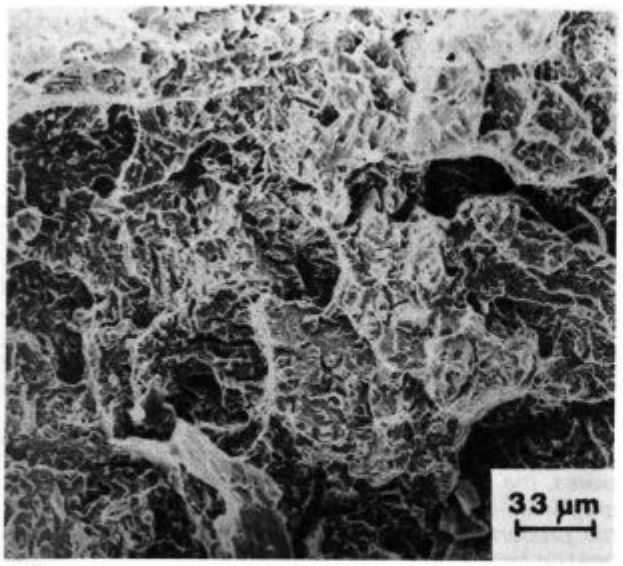

Slika 7
LKP - kvazi krhki transkristalni prelom.

Fig. 7
LBZ - quasi brittle transcrystal fracture.

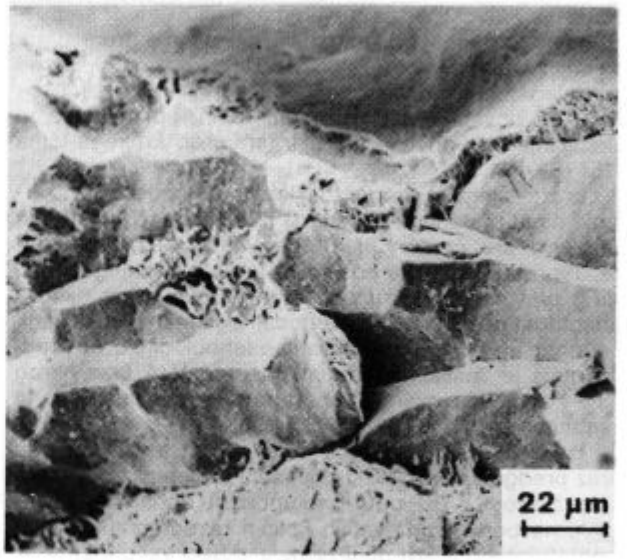

Slika 8
LKP - intergranularni krhki prelom.

Fig. 8
LBZ - intergranular brittle fracture.

skopom v krovni legi, je razvidna iz **slike 3**; vidne so podolgovate M/A faze vzdolž intragranularno izločenega ferita. Mikrostruktura po napetostnem žarjenju je razvidna iz **slike 4**; zaznavni so številni cementitni izločki na meji med M/A fazo in feritom. Mikrostruktura staljenega zvara, zavarjenega s predgrevanjem, je razvidna iz **slike 5**; M/A faz je manj in usmerjenost je manj izrazita. Ista mikrostruktura po napetostnem žarjenju je razvidna iz **slike 6**; vidna je tendenca močnega skepljanja cementita.

Pregled površin LKP je odkril kvazi krhki lom v prelomu preizkušanca v izhodnem stanju — **slika 7.** Površina preloma v napetostno žarjenem preizkušancu je poleg kvazi krhkega preloma pokazala še nastop intergranularne krhkosti vzdolž stebričastih dendritov, kot je razvidno iz **slike 8.**

4. DISKUSIJA REZULTATOV

Preiskave so pokazale bistveno razliko v udarni Charpijevi žilavosti med osnovnim materialom in staljenim zvarom. Kljub dodatkom Ti-B in ugodni vrednosti O_2 (ca. 227 ppm) v zvaru, ki pospešuje tvorbo acikularnega ferita in preprečuje tvorbo primarnega ferita, je bila dosežena udarna žilavost nižja od pričakovane. Lomna žilavost v prisotnosti ostre utrujenostne razpoke pa je pokazala popolno krhkost že pri temperaturah pod 0°C. Vzrok za to je varjenje brez predgrevanja in z nizko dovedeno toploto. Posledica tega je tvorba drobne mikrostrukture, ki vsebuje ferit s sekundarno fazo v obliki M/A strukturne faze namesto acikularnega ferita. Dodatki Cr, Mo in Nb težijo k pospeševanju tvorbe M/A faze, v kateri vsebnost C naraste tudi nad 1% /10/. Razpotegnjene M/A faze vzdolž intrgranularno izločenega ferita so lahko potencialni izvori zgodnjega začetka loma in zato nizke žilavosti. Dodatek Nb in njegovo izcejanje (0,04% v korenu in 0,01% v temenu) imata bistveni vpliv na udarno žilavost.

Kemična sestava staljenega zvara je povišala Watanabe faktor J > 400, tako da je posledica pojava popuščne reverzibilne krhkosti (Sl. 8). Zaradi navedenega ni iz-

4. RESULTS DISCUSSION

The examinations have shown the essential differences in Charpy toughness values of the base material and the molten weld. In spite of Ti-B additions and favourable oxygen content (ca. 227 ppm) in the weld, accelerating the acicular ferrite formation and prevention of primary ferrite formation, the notch-toughness values achieved were lower as it was expected. But the fracture toughness in the presence of sharp fatigue crack has shown the absolute brittleness also at temperatures under 0 degree Celsius. The reason is welding without preheating and with low heat input energy. The result is formation of the fine microstructure containing ferrite with secondary phase in the shape of M/A structural phase in state of acicular ferrite. The addition of Cr, Mo and Nb has a tendency of M/A phase formation in which the carbon content can rich the values greater than 1 % /10/. Oblong M/A phases along the intragranular precipitated ferrite can be the potential sources of early fractures beginning and the reason for low toughness values.

Chemical composition of the molten weld has increased the Watanabe factor J= > 400, so that it results in the reversible temper embrittlement appearance /8/. That is the reason why there is no toughness improvement at heating above 650 degrees Celsius where the causes for temper embrittlement are dissolving, on the other side an intensive precipitating of Fe_3C appears on the boundary between oblong ferrite and M/A phase. The size of Fe_3C precipitates are increasing with elevated temperature under the coagulation mechanism what is the reason for brittle fracture at elevated temperature /15/ (Fig. 4).

From the above we can conclude, that stress-relieved heating does not have a favourable effect on molten weld toughness if M/A structural phases are present into it. M/A phases formation is a consequence of too high alloyment or/and too high cooling speed, so that their presence depends on the weld material selection and welding technology. Using the welding technology without preheating the content of M/A structural phase

boljšanja žilavosti po segrevanju nad 650° C, kjer se povzročitelji za popuščno krhkost raztapljajo, na drugi strani pa se hkrati pojavi intenzivno izločanje Fe_3C na meji med razpotegnjenim feritom in M/A fazo. Velikost izločkov Fe_3C se povečuje s povišanjem temp. po mehanizmu skepljanja, kar privede pri višji temp. do krhkega loma /15/ (Sl. 4).

Iz zgornjega je mogoče sklepati, da napetostno žarjenje nima ugodnega učinka na izboljšanje žilavosti staljenega zvara, če so v njem prisotne M/A strukturne faze. Tvorba M/A faz je posledica previsoke nalegiranosti ali/in previsoke hitrosti ohlajevanja, tako da je njihova prisotnost odvisna od izbire dodajnega materiala in varilne tehnologije. Pri uporabi varilne tehnologije brez predgrevanja je znašala vsebnost prisotne M/A faze okrog 38% v staljenem zvaru. Z uporabo predgrevanja se je ta vsebnost znižala na okrog 33%.

Iz raziskave je mogoče sklepati, da je pri varjenju brez predgrevanja in nizki dovedeni toploti za dosego visoke žilavosti v TVP potrebno uporabiti dodajne materiale, ki ne bodo tvorili večjih količin razpotegnjenih M/A faz. Navedeno lahko dosežemo z nižjimi vsebnostmi Si, Al, Cr in Mo in z dodatki Ti-B, ki pospešujejo tvorbo aciularnega ferita. Na drugi strani je podoben efekt mogoče doseči z uporabo predgrevanja in višjo dovedeno toploto ne glede na prisotnost omenjenih legirnih elementov. Vendar je takšna varilna tehnologija uporabna le, če izberemo jeklo, ki ni občutljivo na rast zrna, ker bomo v nasprotnem primeru dobili nizke vrednosti za žilavost v TVP. Omenjena moderna jekla so izdelana na osnovi TiN in BN izločevalnih efektov s vsebnostjo raztopljenega N pod 10 ppm.

Pri varjenju preizkusnih plošč se vmesna temperatura visoko dvigne in lastnosti staljenega zvara niso primerljive z lastnostmi na dejanskem zvarnem spoju, ki je narejen brez predgrevanja ali z nizkimi $\Delta t^{8/5}$ časi. Namesto da bi se varilo brez predgrevanja, dejansko varimo plošče z visokim predgrevanjem (često $>200^0$ C).

Takšni rezultati niso uporabni za varjenje brez predgrevanja na dejanskih zvarnih spojih, kjer se zaradi dolgih zvarov in velikih površin vmesna temperatura zniža oz. pade celo na sobno. Takšen varilni postopek lahko znatno vpliva na žilavost izhodnih zvarnih spojev in tako na varnost celotne zavarjene konstrukcije. Torej je navedeno vzrok za pazljivo in temeljito izbiro verifikacije varilne tehnologije, ki mora odgovarjati dejanskim pogojem pri izvedbi varjenja v delavnici in na montaži.

5. ZAKLJUČEK

Preiskava EPP zavarjenih raztaljenih zvarov, ki so zavarjeni brez predgrevanja in z nizko dovedeno toploto z uporabo več varkov na nizko ogljičnem finozrnatem jeklu, je odkrila naslednje:

— Udarna in lomna žilavost raztaljenega zvara je odvisna od izbire dodajnega materiala in varilne tehnologije.

— Pri varjenju in preizkušanju zavarjenih plošč morajo biti izpolnjeni pogoji, ki bodo reprezentirali dejanske pogoje v delavnici in na montaži.

— Varilna tehnologija brez predgrevanja in z nizko dovedeno toploto, da bi dosegli dobre žilavostne lastnosti v TVP, lahko povzroči v raztaljenem zvaru v zrnih s primarnim feritom po kristalnih mejah in intragranularnim feritom s sekundarno fazo tvorbo krhkih M/A faz, ki lahko znatno znižajo žilavost. Odločitev, ali uporabiti predgrevanje ali ne, je odvisna od ekvivalenta Pcm osnovnega in staljenega zvara in pričakovanih lastnosti.

in molten weld was 38 %, while with using the preheating this content was decreased to ca. 33 %.

From this examination we can conclude that for welding without preheating and low input energy to achieve high toughness in HAZ it is necessary to use welding materials which will not form higher quantities of oblongated M/A phases. We can achieve that with lower contents of Si, Al, Cr and Mo and with additions of Ti-B, which accelerate the acicular ferrite formation. On the other side we can achieve a similar effect with the use of preheating and higher heat input energy regardless to above mentioned alloying elements. But such welding technology is useful only if we choose steel which is not sensible to grain growth because in the opposite case we will get low toughness values in the HAZ. The above mentioned modern steels are produced on the base of TiN and BN precipitation effects with the nitrogen content under 10 ppm. During the welding of experimental plates, the interpass temperature raise high up and the properties of the molten weld are not comparable with the properties of the actual weld welded without preheating or with low $\Delta t8/5$ time. Instead of welding without preheating we actually weld them with high preheating (often > 200 degrees Celsius).

Such results are not useful for welding without preheating on actual welded joints because of their longness and greatness the interpass temperature decreases or even talls down to room temperature. Such welding process can have a considerable effect on as welded weldments and in this way it effects on security of the whole welded construction. All that has been stated is the reason for a careful and profound choose of verification of welding technology which has to respond to actual welding conditions in the workshop and assembling.

5. CONCLUSION

The examination of SA welded molten welds, welded without preheating and with low heat input energy, with more run technique on low carbon fine grained steel has discovered the following:

— Notch and facture toughness of the molten weld depends on welding material choose and welding technology.

— During welding and testing of welded plates such conditions has to be fulfilled that can represent the actual condition in the workshop and assembling.

— Welding technology without preheating and with low heat input energy can in the molten weld in the grains with primary ferrite with secondary phase, cause the formation of brittle M/A phases, which can considerably decrease the toughness. Decission to use or not to use the preheating depends on Pcm equivalent of base metal and molten weld and on properties expected.

— By CTOD method determinated fracture toughness is otherwise conservative but gives a good insight into the quality estimation of the welded joint.

— The LBZ appearance in the molten weld on the fractured area of CTOD specimens has to be already estimated at room temperature with large test (Wide Plate Tests) with fatigue crack inserted on the surface area. Test has to be carried out at the lowest operating temperature of the future construction /16/.

— Stress releaving with heating has negative consequences because of the M/A structural phases presence. Cementite precipitation on the boundary between ferrite and M/A phase additionally decrease toughness. In the case of stress-releaved heating it is recom-

— Lomna žilavost, določana po metodi CTOD, je sicer konservativna, vendar daje dober vpogled v oceno kvalitete zvarnega spoja.

— Pojav vidnih LKP v staljenem zvaru na lomni površini CTOD preizkušancev že pri sobni temp. je potrebno oceniti z velikimi preizkusi (Wide Plate Tests) s površinsko vgrajeno utrujenostno razpoko. Preizkus je potrebno opraviti pri najnižji temp. obratovanja bodoče konstrukcije /16/.

— Termično sproščanje zaostalih napetosti ima negativne posledice zaradi prisotnosti M/A strukturnih faz. Izločanje cementita na meji med feritom in M/A fazo še dodatno zniža žilavost. V primeru uporabe napetostnega žarjenja je priporočljivo preveriti možnost pojava reverzibilne popuščne krhkosti, ki je odvisna od količine in izcej legirnih elementov ter nečistoč v raztaljenem zvaru.

mended to control the possibility of reversible temper embrittlement appearance, which depends on the quantity and segregations of alloying elements and impurements in the molten weld.

LITERATURA / *REFERENCES*

1. Suzuki, H.: Revised Cold Cracking Parameter PHA and Its Application, IIW IX-1311-84.
2. Durren, C.: Determining the Preheating Temperature for the Field-welding of Large-diameter Pipe, IIW IXG-318-84.
3. Guide to the Light Microscope Examination of Ferrite Steel Weld Metals, IIW IX-1533-88.
4. Cochran, R.C.: Weld Metal Microstructure - a State of the Art Review, Welding in the World, Vol. 21, No. 1/2, p. 16-25, 1983.

5a. Abson, D.J.: Non-metallic Inclusion in Ferritic Steel Weld Metals, A Review IIW IX-1486-87.

5b. Liu, S., Olson, D.L.: The Role of Inclusions in Controlling HSLA Steel Weld Microstructures, Supplement of Welding Journal AWS, June 1986.

6. Easterling, K.: Introduction to the Physical Metallurgy of Welding, Butterworths, 1983, p. 88-103.
7. Evans, G.M.: The Effect of Chromium on the Microstructure and Properties of C-Mn All-weld Metals Deposits, Oerlikon-Schweissmiteilungen 47/89, No. 120.
8. Rak, I., Gliha, V., Sidjanin, L., Petrovski, B.: J-integral Testing of SA Weldments on HSLA Steel Regarding Different Treatments After Welding, European Symposium on Elastic-Plastic Fracture Mechanics, Elements of Defect Assesment, Freiburg, 1989.
9. Okhita, S., Homma, H., Tsushima, Mori, N.: The Effect of Oxide Inclusions on the Microstructure of Ti-B Containing Weld Metal, IIW IX-1070-86.
10. Ikawa, H., Oshige, H., Fukada, Y.: Effects of Martensite Austenite Constituents on HAZ Toughness of a High Strength Steel, IIW IX-1156-80.
11. Komizo, Y., Furusawa, J., Fukada, Y.: Development of High Toughness in Heat Affected Zone, JOM-3 Conference, Helsingor, 1989.
12. Suzuki, H.: Root Cracking and Maximum Hardness in High Strength Steel Welds, IIW IX-1983.
13. Dhooge, A., Ostyn, K., Magula, V., Vinckier, A.: Temper Embrittlement in Modern Off-shore Structural Steels.
14. Komizo, Y.: A Review on Reversible Temper Embrittlement in Cr-Mo Steel Weld Metal, IIW IX-1488-87.
15. Knott, J.K.: Microscopic Aspects of Crack Extention, Advances in Elasto-Plastic Fracture Mechanics, Applied Science Publishers London, 1979.
16. Denys, R.: Incentives for Fracture Toughness Testing, IIW X- 1131-86.

IZDELUJEMO

- ☐ debelo, srednjo in tanko pločevino
- ☐ hladno valjane trakove in pločevino
- ☐ dinamo trakove in pločevino
- ☐ nerjavne trakove in pločevino
- ☐ vlečeno, brušeno in luščeno jeklo
- ☐ valjano in vlečeno žico
- ☐ patentirano žico
- ☐ pleteno patentirano žico za prednapeti beton
- ☐ hladno oblikovane profile
- ☐ kovinske podboje za vrata
- ☐ dodajni material za varjenje
- ☐ žičnike
- ☐ jeklene odlitke
- ☐ tehnične pline

NUDIMO TUDI USLUGE

- ☐ prevaljanja, vlečenja, iztiskanja in toplotne obdelave pločevin in žice

120 let TRADICIJE ZNANJA in KAKOVOSTI naših izdelkov

ŽELEZARNA JESENICE

64270 Jesenice, Cesta železarjev 8
telefon: (064) 81-231, 81-341, 81-441
telex: 34526 ZELJSN, Jugoslavija
telefax: 83 395

Kobaltove zlitine v lesni industriji
Cobalt Base Alloys in Woodcutting Industry

J. Rodič*[1]

1. UVOD

Več kot dve desetletji je v praksi dobro poznan ugoden učinek navarjanja rezilnega dela zob s kobaltovimi zlitinami-steliti* za izboljšanje rezilne sposobnosti in povečanje vzdržljivosti različnih vrst žag v lesni industriji **(slika 1)**.

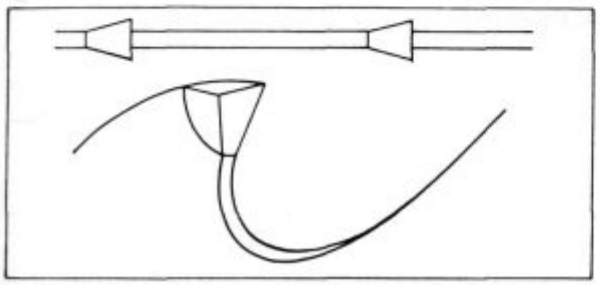

Slika 1
Stelitiranje
Obloga konice zoba s posebno kobaltovo zlitino, odporno proti obrabi, omogoča bistveno podaljšanje vzdržljivosti in rezne sposobnosti žag.
Stelitiranje je posebno priporočljivo pri žaganju svežega lesa z mnogoštevilnimi kremenčevimi vključki.

Fig. 1
Stellite Tipping
Tooth tipping with special cobalt base alloy resistant against abrasion enables significant prolongation of lifetime and cutting ability of saws.
Stellite tipping is especially recommended for sawing fresh, nontreated wood with many inclusions of silicon oxides.

Postopek prostega ročnega navarjanja zob na žagah se kljub poznanemu in dokazanemu zelo ugodnemu učinku dolga leta ni širše uveljavil. To ugotovitev lahko v veliki meri povezujemo s potrebo zahtevnega, zamudnega in zelo strokovnega dela, s slabim materialnim izkoristkom drage zlitine in z zahtevnostjo brušenja zob.

V strokovnih krogih se je za postopek nanašanja kobaltovih zlitin na zobe žag udomačilo ime "stelitiranje". Ta postopek je bil dolgo skoraj izključno prepuščen uporabnikom za vzdrževanje in obnavljanje žag v vsakodnevni praksi.

Specializirani proizvajalci žag so se za nekatere vrste žag usmerili na obloge z lotanjem trdokovinskih ploščic na zobe. Z razvojem specializiranih polavtomatskih in

* Stellite je prva blagovna znamka Cabot Corporation - Stoody Deloro za kobaltove zlitine, odporne proti obrabi in povišanim temperaturam. To ime je danes za veliko skupino kobaltovih zlitin splošno uporabljeno in udomačeno v praksi.

*[1] Prof. dr. Jože Rodič, dipl. inž. metalurgije, direktor podjetja MIL-PP d.o.o., Ljubljana za razvoj in proizvodnjo specialnih zlitin

1. INTRODUCTION

Beneficial effects of saw teeth tipping with cobalt base alloys - stellites for improving cutting ability and lifetime of saws in woodcutting industry are well known more than two decades (**Fig. 1**).*

Although these beneficial effects were known for many years the stellite tipping was not extensively used due to the disadvantages of manual welding procedure which is time consuming and requires a lot of experience in welding and sharpening. Furthermore, this practice is associated with low yield of expensive material. The stellite tipping was therefore applied only by users for maintenance and resharpening of saws. Specialized producers on the other hand introduced hard metal tipping by soldering process. The new progress of stellite tipping arrised with the development of automatic machines for welding and sharpening which were recently introduced by three companies ALLIGATOR (France), ISELI (Switzerland) and VOLLMER (Germany).

Due to the increased productivity achieved by automatic stellite tipping a new network of servicing centers for maintainance of all types of band, gang and circular saws is growing. This professional maintainance technology assures better quality and life time of saws which has direct impact on productivity and economy of saw mill production while at the same time the quality of cut surfaces is improved.

The stellite tipped saws enable an uninterrupted eight-hour sawing with cut length 80-100 km and production over 20 m^3 per shift so that interruptions and changes of saws during one shift are an exception.

This promising progress has encouraged a systematic applied research. With the growing exploitation of stellites in wood cutting technology a need for development of special assortment of alloys devoted to this application is emerging. The need for intensive research in this area is also supported with results of comparative studies which are presented in Section 7. These studies show that cobalt base alloys have a high priority for this application so that optimisation is expected within these grades.

Three grades of stellites (12, 1, 6) are the most frequently used in woodcutting and the most important is grade 12 (See Tab. 1).

The grade 1 was commonly applied for hard wood for many years, but recently the use of this grade has considerably decreased due to experience.

The grade 6 has appeared in general woodcutting technology very recently. Some saw mills applied this

** Stellite is a registered trade mark of Cabot Corporation - Stoody Deloro for cobalt base alloys which are abrasion resistant at room and elevated temperatures. This designation is commonly used for a vide variety of cobalt base alloys.*

polno avtomatiziranih strojev za stelitiranje žag, ki so jih razvile v zadnjem obdobju tri firme ALLIGATOR - Francija, ISELI - Švica in VOLLMER - Nemčija, se je začela situacija na področju stelitiranja žag bistveno spreminjati.

Logična posledica visoke produktivnosti, dosežene z razvojem avtomatskega strojnega stelitiranja, je nastajanje vse širše mreže specializiranih servisnih centrov za stelitiranje in ostrenje vseh vrst žag, tračnih, gaterskih in krožnih.

Vzdrževanje in obnova žag v takih servisnih centrih dosega vrhunsko in zanesljivo kakovost, kar se neposredno odraža v izrednem povečanju produktivnosti žaganja, v ekonomiki proizvodnje z zniževanjem stroškov, ob istočasnem napredku kakovosti rezanih površin in močnem podaljšanju življenske dobe kvalitetnih žag.

Neprekinjeno osemurno žaganje hlodovine z dolžino poti rezanja 80—100 km in s storilnostjo razreza nad 20 m^3 na izmeno, je danes za žago kar normalni normativ in zastoji zaradi nepričakovanih menjav žag so ob rednem vzdrževanju in kvalitetni obnovi žag že kar izjemen pojav.

Razumljivo je, da je ta napredek vzpodbudil tudi intenzivnejše in bolj sistematične razvojne raziskave.

Dosedanja uporaba standardnih vrst stelitov že napoveduje razvoj optimirane sestave teh zlitin za potrebe stelitiranja žag v lesni industriji in to v nekaj namenskih variantah glede na vrsto rezanega lesa in tehniko žaganja s specifičnimi parametri v proizvodnji.

Tudi primerjalne raziskave stelitiranih žag in tistih z zobmi iz trdih kovin, ki jih bomo na kratko povzeli v poglavju 7, so privedle do presenetljivih spoznanj, ki močno uveljavljajo pomen stelitov v nadaljnjem razvoju.

Kobaltove zlitine so se v primerjalnih raziskavah[1] izkazale za najboljše, zato optimiranje asortimenta dodajnih materialov za stelitiranje žag pričakujemo med njimi.

Dosedanji tipični asortiment stelitnih zlitin za lesno industrijo lahko omejimo na tri standardne vrste, med katerimi daleč prevladuje poznana zlitina št. 12. (Glej tabela 1)

Za nekatere trde vrste lesa je bila močno uveljavljena in je še veliko uporabljana zlitina št. 1, vendar se prav v zadnjem obdobju na podlagi izkušenj v praksi vloga in pomen stelita 1 v uporabi na tem področju očitno zelo zmanjšuje.

Ob preusmerjanju razvoja, ki izhaja iz bogatih izkušenj zadnjega obdobja izgleda očitno, da so lesarski strokovnjaki v splošnem preveč pomena pripisovali samo trdoti stelitiranih zob[5]. Nekateri "žagarji", ki jim notranji raziskovalni nagon preprosto ni dopuščal, da bi se povsem prepuščali tradicionalnim pravilom pri izboru stelitov, so uspešno z zelo vzpodbudnimi rezultati zamenjali standardni stelit 12 s stelitom 6 in še naprej raziskujejo nove ideje z industrijskim preizkušanjem vzdržljivosti različno stelitiranih žag.

Zelo zanimivi rezultati teh industrijskih raziskav v kombinaciji z metalurškim razmišljanjem o sestavah, lastnostih uporabljenih zlitin in z metalografskimi študijami že nakazujejo nove smeri razvoja z modifikacijami k optimalni sestavi kobaltovih zlitin za stelitiranje žag v dveh ali treh variantah glede na značilnosti vrste rezanega lesa.

S pilotnimi napravami horizontalnega kontinuirnega litja[7,8,9] in z razvojem novih spremljajočih tehnoloških postopkov[10] že poteka projekt specializacije v proizvodnji kobaltovih zlitin za specifične potrebe v lesni industriji. Razvojne raziskave potekajo v tesni povezavi s proizvajalci strojev za stelitiranje žag, s proizvajalci žag in s servisnimi centri za stelitiranje in ostrenje žag. V tem razvoju želimo zajeti in upoštevati čimveč praktičnih iz-

grade which was not commonly used purely for research interest. The encouraging results confirmed opinion of some researchers[5] that the hardness itself should not be considered as the only decisive property of stellites for cutting ability. The research along these lines which is out of traditional practice is in progress. However, those saw mills which tried grade 6 instead of grade 12 prefer the former one for standard use.

These observations in woodcutting practice in combination with metallurgical knowledge of chemical composition and material properties with respect to metallographic studies of microstructures should provide optimal assortment of stellites for cutting of various woods.

The applied research project in the area described above is being undertaken in pilot plant for horizontal continuous casting (HCC)[7,8,9] and subsequent thermomechanical treatment[10]. This research is performed in cooperation with producers of stellite tipping machines, producers of saws and with service centers for stellite tipping and sharpening. It is expected that this joint research programme which considers expertises gained in industry related to woodcutting will result in metallurgical development of products for stellite tipping.

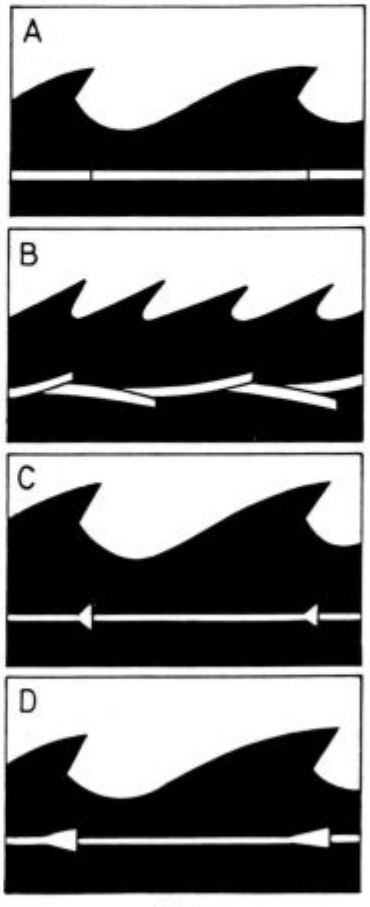

Slika 2
Trakovi žag, zvarjeni in napeti.
A - surovo ozobljeni trak, B - Razperjanje in brušenje zob, C - Nakrčenje vrhov zob in brušenje, D - Stelitiranje in brušenje zob.

Fig. 2
Saw bands, welded and tensioned
A - Saw band with raw teeth, B - Setting and grinding of teeth, C - Swagging of tooth tips and grinding, D - Stellite tipping and grinding of teeth.

kušenj, zbranih v zadnjih letih in le-te usmeriti v metalurški razvoj zlitine za specifične namene in potrebe.

Poleg razvoja asortimenta za optimalni izbor vrste uporabljenih zlitin je pomemben tudi razvoj samih postopkov stelitiranja in posebnih oblik preseka HKL-palic, dodajnih materialov za stelitiranje zob. Ti proizvodi so poznani pod imenom FORM-STELITI in so se doslej izdelovali samo po tehnologiji metalurgije prahov (PM). Danes se kot pomembna dopolnitev asortimenta že uveljavlja tudi uporaba HCC-FORM-STELITOV.

2. VRSTE ŽAG, OBLIKE IN GEOMETRIJA ZOB

Pri stelitiranju enakovredno obravnavamo vse tri osnovne vrste žag, tračne, gaterske in krožne.

Na **sliki 2** je shematično prikazano surovo ozobljenje trakov, razperjanje ali nakrčevanje zob pri klasičnih in stelitiranje zob pri modernih tračnih žagah.

Slika 3 prikazuje geometrijo stelitiranega zoba z vsemi koti, ki so pomembni za ostrenje z ravnim in poševnim brušenjem.

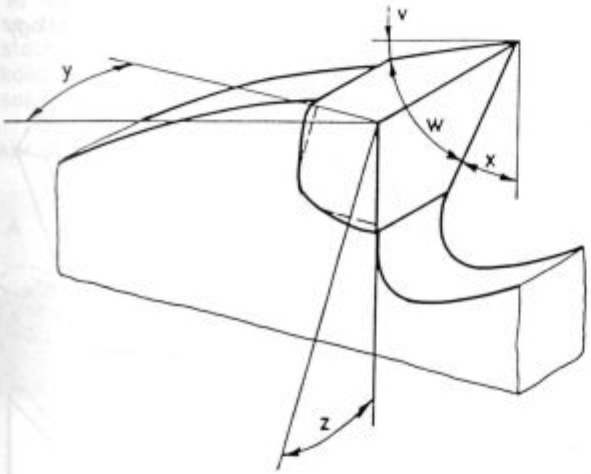

Slika 3
Geometrija zoba žage
X - Cepilni kot, V - Prosti kot.

Fig. 3
Geometry of saw tooth
X - Rake angle, V - Clearance angle.

3. RAZVOJ STELITIRANJA ŽAG

Pri tem moramo omeniti dva bistevno različna pristopa k stelitiranju žag. Od tega je odvisna seveda tudi konstrukcija in način delovanja strojev za stelitiranje.

Postopek I.: Navarjanje zob s TIG postopkom ali s plazmo

Pri postopku stelitiranja z dodajanjem kobaltove zlitine na zob z navarjanjem preko tekoče faze uporabljamo okrogle HCC palice tankih presekov. Daleč največ se uporablja palice standardne dimenzije ∅O3,2 mm. Podajalni mehanizem stroja podaja palico za taljenje nad kokilo.

Pri tem postopku avtomat stroja obda zob žage z bakreno kokilo **(slika 4)**, ki ima določeno obliko zoba in stelit se po TIG postopku ali s plazmo natali v kokilo na vrh zoba. Po strditvi je vrh zoba s stelitom ustrezno oblikovan in stelit trdno zvarjen z osnovo zoba.

Uvedba plazma gorilcev pri teh strojih omogoča povečanje storilnosti stelitiranja in tudi uporabo nekoliko

Besides the development of optimal assortment of applied alloys the development of welding procedures in stellite tipping and application of special shapes of cross section for adding the material in welding is also important. These so called FORMSTELLITES are mainly produced by powder technology but recently HCC is considered as an alternative technology.

2. SAW TYPES, FORMS AND TOOTH GEOMETRY

Stellite tipping is equally treated with all three general types of saws: band saws, gang saws and circular saws.

***Figure 2** represents schematically a saw band with raw teeth, setting and swagging of teeth with conventional saws and stellite tipping of teeth. The geometry of stellite tipped tooth with all important angels for sharpening with straight and bevel grinding is shown in **Fig. 3**.*

3. DEVELOPMENT OF STELLITE TIPPING

Two essentially different procedures have been introduced in the approach to stellite tipping of saw teeth. The construction and operational characteristics of stellite tipping machines are adjusted to special requirements of the process.

Procedure I.: Stellite tipping with TIG or plasma welding

For stellite tipping with welding through liquid phase HCC rods of small sections are usually used where ∅O3.2 mm is the most commonly applied dimension. The stellite tipping machine automatically supplies the rod to the appropriate position above the mould for melting.

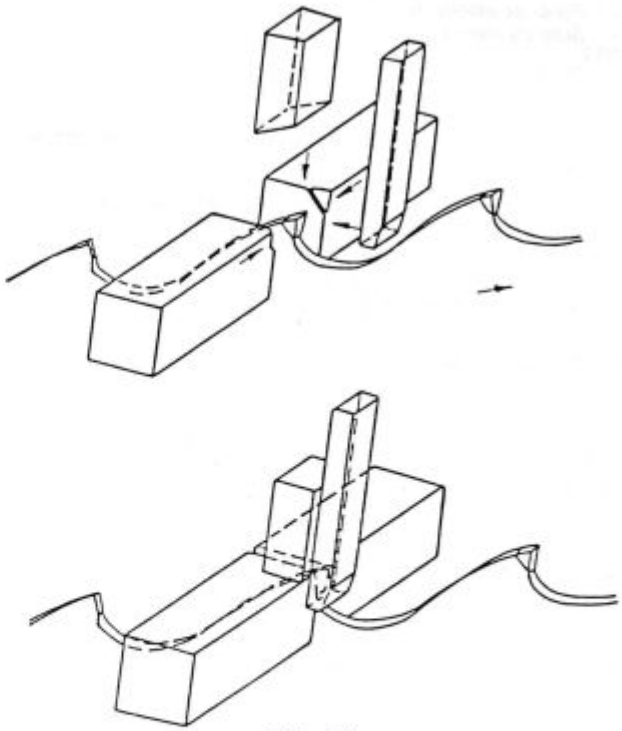

Slika 4[1)]
Skica naprave, ki kot kalup daje zahtevano obliko konice zoba pri stelitiranju.

Fig. 4[1)]
Schematic drawing of a jig which performs the moulding action to give the tip the desired geometry.

debelejših palic, kar se pomembno pozna pri ceni dodajnih materialov oziroma pri stroških stelitiranja v celoti.

Slika 5 prikazuje stelitiran zob in brušenje[3].

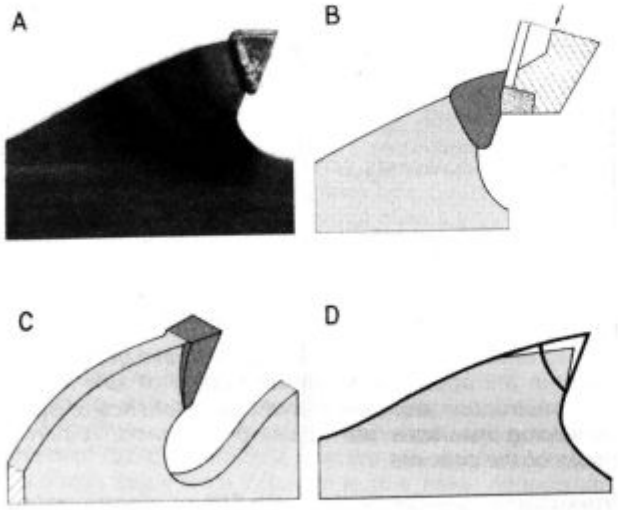

Slika 5[3]
Stelitiranje in brušenje zob
A - Oblika stelitiranega zoba, B - Brušenje cepilnega kota, C - Stranske ploskve se brusijo samo na novo stelitiranem zobu,
D - Večkratno prebrušenje cepilnega in prostega kota.

Fig. 5[3]
Stellite tipping and sharpening of teeth
A - Form of stellite tipped tooth, B - Grinding of rake angle, C - Side clearance surfaces are ground only after stellite tipping,
D - Repeated sharpening of rake and clearance angle.

Postopek II.: Uporovno navarjanje stelitnih delcev na zobe

Po drugem osnovnem postopku stelitiranja žag z več variantami se dodajni material-stelit določene oblike v avtomatu uporovno segreje, na stičišču z osnovnim materialom žage natali in vtisne točno v ustrezen položaj na zobu žage. Za ta postopek privarjanja so že ponudili tržišču tudi precizne ulitke stelitov, ali pa oblikovance iz stelitnega prahu, vsestransko oblikovane. S tem naj bi posnemali izkušnje iz uporabe trdokovinskih ploščic, ki se lotajo na zobe žag.

Uporaba teh predoblikovanih koščkov se po začetnih korakih razvoja v stelitiranju žag ni veljavila po pričakovanjih in danes že prevladuje mnenje, da ta prvotno zelo obetajoča pot v nadaljnjem razvoju stelitiranja žag nima perspektive.

Več uporabljajo palice z različnimi oblikami preseka, ki jih avtomat reže ravno ali poševno med postopkom stelitiranja pri podajanju palice. Avtomat lahko delček prej odreže, pa ga nato privari ali pa konec palice privari in jo nato avtomatsko odreže.

Razvoj dodajnih stelitov v obliki palic različnih dimenzij s posebnimi oblikami preseka je odvisen od sistema dodajanja palic za stelitiranje zob pri avtomatskem ali ročnem podajanju na stroju.

Najprej se je razvil postopek z uporabo palic okroglega preseka, ki jih avtomatsko ali ročno krmiljeni stroj za stelitiranje podaja z vrha ali od strani pred cepilno ploskev zoba kot kaže **slika 6**.

*In this procedure the blocks of cooper are moved to embrace the saw tooth in order to form a mould for the desired geometry. The mould is then filled up by either TIG or plasma melting. After the solidification a preform of the tooth which is welded to the base is obtained (**Fig. 4**).*

The introduction of plasma welding enabled the improvement of productivity and the application of stellite rods of larger section which are considerably cheaper so that plasma welding is reducing the overall production cost of stellite tipping.

***Figure 5** illustrates stellite tipping and sharpening of saw teeth.*

Procedure II.: Resistance welding in stellite tipping

In resistance welding approach the adding material in the form of stellite tip is heated up in automatic machine to melt both materials at the interface between tip and saw base. The machine is then pressing the tip to the exact position on the tooth. For tips used in this approach precision cast stellite pieces or pieces of pressed powder stellites were introduced by analogy with hard metal tipping.

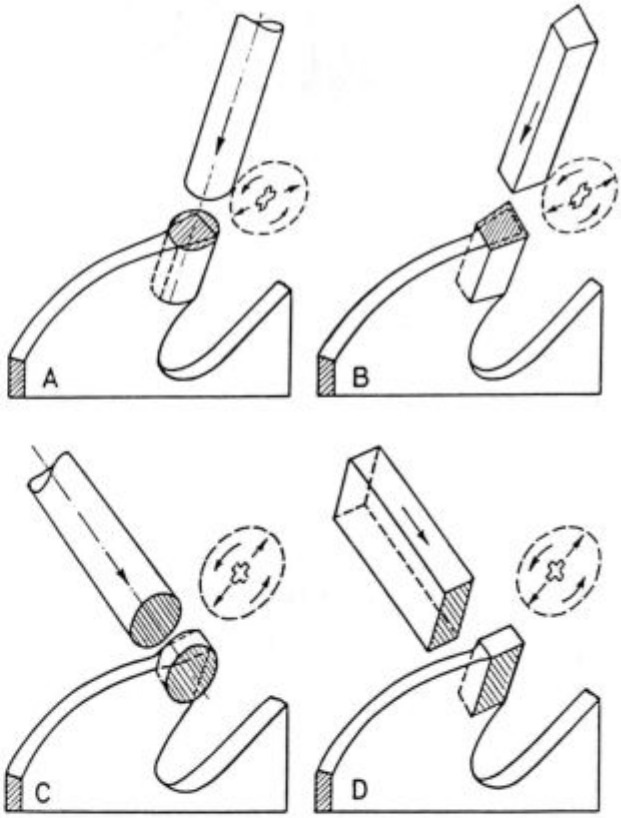

Slika 6
Električno uporovno navarjanje stelitnih delcev na vrh zoba
A - Vertikalno podajanje okroglih stelitnih palic, B - Vertikalno podajanje stelitnih palic trapeznega preseka, C - Horizontalno podajanje okroglih stelitnih palic, D - Horizontalno podajanje stelitnih palic paralelo gramskega preseka.

Fig. 6
Electric resistance welding of stellite tips
A - Vertical adding of round stellite rods, B - Vertical adding of form-stellite rods with trapeze section, C - Horizontal adding of round stellite rods, D - Horizontal adding of form-stellite rods with parallelogram section.

*** 1. varianta: Vertikalno podajanje palic**

Pri tem načinu stelitiranja žag s podajanjem palic okroglega preseka od vrha pred zob žage je povsem razumljivo v fazi brušenja prišlo do ideje za uporabo palic kvadratnih ali pravokotnih in končno trapeznih presekov, tako da ima zob že takoj po stelitiranju nastavljeno ravno cepilno ploskev in predoblikovani stranski ploskvi s prostim kotom. Palico se odreže poševno pod kotom, ki ustreza prostemu kotu zoba. Na ta način se doseže velik prihranek brušenja zob.

*** 2. varianta: Horizontalno podajanje palic**

Za drugo varianto postopka stelitiranja z uporovnim navarjanjem se uporablja dodajanje palic stelitov od strani. Namesto okroglih palic večjega preseka (**slika 7**[3]) imajo precejšnjo prednost palice s presekom paralelograma (**slika 8**[3]).

Nekaj nevšečnosti pri postopku uporovnega navarjanja form stelitov povzročajo ostanki iztisnjenega materiala. Odstranjevanje teh brad je lahko neprijetna ovira normalnega postopka.

Po stelitiranju se morajo konice zob popuščati, kar se z modernimi stroji opravi v toku samega postopka stelitiranja. Izkušnje kažejo, da med vsemi form-steliti po količini daleč prevladuje uporaba tistih s trapeznim presekom.

Uporaba form-stelitov je kljub višji ceni upravičena, ker omogoča

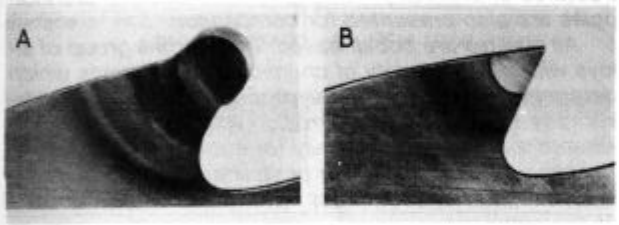

Slika 7[3]
Uporovno navarjanje zob z okroglim stelitom
A - po stelitiranju, B - po končnem brušenju.

Fig. 7[3]
Stellite tipping with electric resistance welding of round stellite rod
A - after stellite tipping, B - after final sharpening.

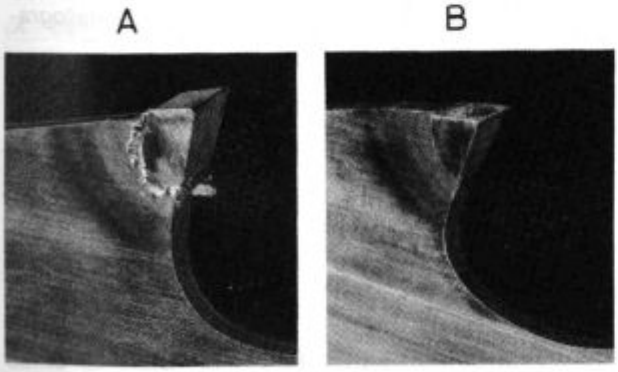

Slika 8[3]
Uporovno navarjen zob s form-stelitom paralelogramskega preseka
A - po stelitiranju; B - po končnem brušenju.

Fig. 8[3]
Stellite tipping with electric resistance welding of form-stellite rod with parallelogram section
A - after stellite tipping, B - after final sharpening.

The application of these preformed tips was expected to be successful but very recently more economic procedures are proposed in which rods of various dimensions and cross-sections are automatically supplied and cut at appropriate angles during the process. There are two alternatives: The piece of rod for tooth tip is cut off first and then welded or the end of rod is welded first and then cut off.

The development of stellite rods in various sections and forms depends on adding system of the stellite tipping machine.

At the beggining round section rods were supplied either from the top or side to the face of the tooth as shown in ***Fig. 6****.*

**** Alternative 1: Vertical supply of rods***

In this alternative of stellite tipping the round section rod is supplied from the top and cut at clearance angle. To reduce the waste of material and grinding costs square and rectangular sections were introduced but finally trapeze form sections were accepted as standard. After stellite tipping with trapeze-form rods all main angles of the tooth are close to the final sharpening geometry. Side clearance surfaces are ground only after stellite tipping while repeated sharpening is performed only for rake and clearance angles.

**** Alternative 2: Horizontal supply of rods***

In this alternative of stellite tipping with resistance welding rods of larger sections are supplied from the side and cut at side clearance angle. Initially round rods ***(Fig. 7)*** *were used but later parallelogram sections were introduced to reduce the waste of material and grinding costs* ***(Fig. 8)****.*

The difficulties can arrise in resistance welding where the material which is pressed to the side needs to be removed.

After stellite tipping the teeth must be tempered. Modern machines include this in automatic procedure.

Production practice shows that number of various forms is reducing towards a limited number of standard forms and that trapeze section forms are preferred.

Although the stellite forms are expensive their application is justified by subsequent costs such as reduced consumption of stellites, up to 60 % shorter sharpening times and lower consumption of abrasive tools.

4. PRODUCTION TECHNOLOGY FOR ADDITIVE MATERIALS IN STELLITE TIPPING

Stellite rods can be produced by two different technologies:

- *Horizontal Continuous Casting (HCC), (**Fig. 9**);*
- *Powder Metallurgy (PM).*

Almost all round section rods are produced by HCC while form stellites on the other hand were until now produced only by PM.

The first samples of form stellites produced in pilot plant MILPP represent a new technology and are now tested by users. The initial results show that this technology will be introduced in practice as complementary rather then competitive to the existing PM technology. The PM form stellites can not be replaced by HCC for special applications and chemical compositions but for common stellite tipping at lower price level and larger quantities an additional market can be opened for the HCC form stellites.

— manjšo porabo stelitov
— do 60 % krajši čas brušenja, ker sta prosti in cepilni kot zoba že podana in
— manjšo porabo brusnih plošč.

4. TEHNOLOGIJA IZDELAVE DODAJNIH MATERIALOV ZA STELITIRANJE ZOB

Za proizvodnjo stelitnih palic sta v uporabi dve osnovni tehnologiji:
— horizontalno kontinuirno litje (HCC),
— metalurgija prahov (PM).

Skoraj vse okrogle palice za stelitiranje so izdelane po HCC tehnologiji (**slika 9**).

Za proizvodnjo form-stelitov v glavnem prevladuje metalurgija prahov.

Prvi vzorci HKL-formstelitov iz pilotne proizvodnje MIL-PP predstavljajo novost in so že na preizkušanju v uporabi. Po prvih izkušnjah pričakujemo, da se bo uporaba HKL-formstelitov v praksi uveljavila bolj kot pomembna dopolnitev in ne toliko kot konkurenčna aktenativa dosedanjega asortimetna formstelitov, izdelanih po tehnologiji metalurgije prahov. Cenejši HKL-formsteliti bodo omogočili širšo uporabo te tehnologije stelitiranja, PM-formsteliti pa bodo še naprej nepogrešljivi za specialna področja uporabe.

5. ASORTIMENT ZLITIN ZA STELITIRANJE ŽAG

Ker gre pri stelitiranju za tipično interdisciplinarno področje med metalurgijo, lesarstvom, strojništvom in kemijo (korozijo) je prav, če na kratko predstavimo sicer poznane vrste in specifične lastnosti kobaltovih zlitin pod skupnim imenom "steliti". Tudi nekaj primerov mikrostruktur stelitov iz HKL in PM tehnologije zanimivo prikazuje značilnosti teh posebnih zlitin in obeh postopkov.

Skupina stelitov obsega zlitine s precej širokim območjem variacij kemijske sestave. Skupna značilnost vseh stelitov je osnovna sestavina, kobalt. Dodatki drugih kovin v različnih kombinacijah vplivajo na značilne mehanske lastnosti, in s tem tudi neposredno na obstojnost proti obrabi ter na odpornost proti koroziji, ki je pri rezanju svežega lesa izredno pomembna.

Žilavost stelitov, čeprav slaba, je mnogo boljša od izredno krhkih WC-trdin.

Lastnosti stelitov so dobro obstojne tudi pri povišanih temperaturah.

Steliti se odlikujejo z nizkimi koeficienti trenja.

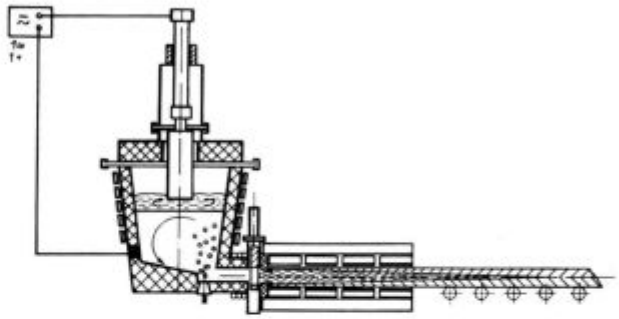

Slika 9
Shema postopka horizontalnega kontinuirnega litja (HKL) tankih palic.

Fig. 9
Scheme of the proces for horizontal continuous casting (HCC) of thin rods.

5. ASSORTMENT OF ALLOYS FOR STELLITE TIPPING

*Since development of stellite tipping requires interdisciplinary cooperation between metallurgists, mechanical and chemical (corrosion) engineers and woodcutting experts it is appropriate to recall well known properties, chemical compositions (**Tab. 1**) and hardness of typical grades for this application. Some typical microstructures of stellites produced by HCC and PM technologies are also presented for comparison.*

All stellites are cobalt based. They form a group of alloys with a wide variety of chemical compositions which determine their mechanical properties, cutting ability, abrasive resistance and corrosion which is recently considered as decisive especially for cutting fresh wood.

Although the toughness of stellites is low it is always much higher then toughness of tungsten carbide grades of hard metals.

Many properties of stellites remain almost unchanged even at elevated temperatures.

The friction caused by stellites is much lower then friction produced by tungsten carbide grades of hard metals.

6. METALLOGRAPHY OF HCC- AND PM- STELLITES[11]

At MIL-PP a modification of standard grade 12 was introduced with designation MILIT 12 W. A metallogra-

Tabela 1: Kemijska sestava in trdota preizkušanih zlitin

Table 1: *Chemical composition and hardness of tested alloys*

	Co %	Ni %	Cr %	W %	Si %	B %	Fe %	C %	HRC
I. Štiri zlitine primerjane v raziskovalnem projektu FORINTEK CANADA CORP.[1)]									
I. Four alloys compared in research project by FORINTEK CANADA CORP.[1)]									
STELLITE 12	59	—	29	9	—	—	—	1.8	47–51
STELLITE 20	45	—	33	18	—	—	—	2.5	55–59
DELORO 50	—	77	10	—	4	1.5	4	0.4	49–52
DELORO 60	—	70	15	—	4.5	3	4.5	0.5	59–62
II. Druge zlitine, uporabljane za rezanje lesa									
II. Other alloys, applied in wood cutting									
STELLITE 1	54	—	30	12	—	—	—	2.5	51–58
STELLITE 6	65	—	28	4	—	—	—	1.1	39–43
(STELLITE F)	39	22	25	12	—	—	—	1.7	40–45

6. METALOGRAFIJA HKL- IN PM-STELITOV[11]

MIL-PP je za stelitiranje žag razvil specialno HKL varianto stelita pod imenom MILIT 12 W s posebno kemijsko sestavo. Za ilustracijo prikazujemo nekaj metalografskih posnetkov HKL-palice ∅O3,2 mm v surovem litem stanju.

Sliki 10 A in B prikazujeta značilno površino HKL palice, posnete z rasterskim elektronskim mikroskopom (REM). Vidi se sled koraka, katere globina znaša poprečno 0,1 mm.

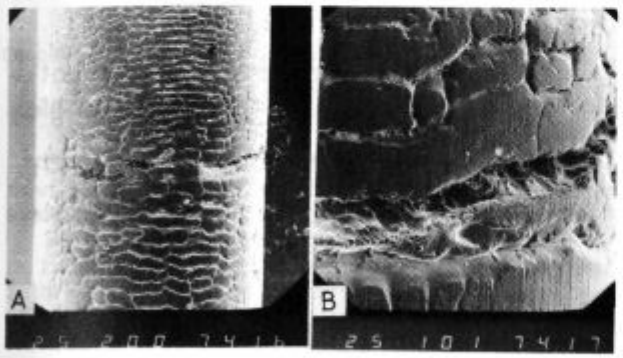

Slika 10
Površina HKL-palice ∅O3,2 mm - Kobaltove zlitine MILIT 12 W
(A - REM 20x, B - REM 100x).

Fig. 10
Surface of HCC-rod ∅O3.2 mm - Co base alloy grade MILIT 12W (A - SEM 20x, B - SEM 100x).

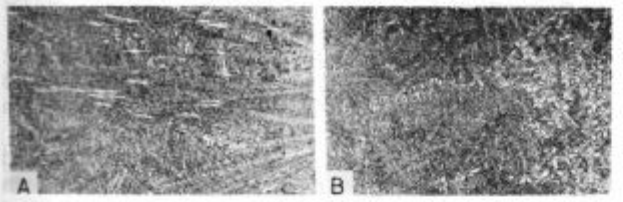

Slika 11
Značilna strjevalna mikrostruktura HKL palice ∅O3,2 mm - MILIT 12 W - v litem stanju
(A-prečno 200x; B-vzdolžno na sredini preseka 200x).

Fig. 11
Characteristic solidification microstructure of HCC-rod ∅O3.2 mm - MILIT 12 W - as cast
(A - transverse 200x, B - longitudinal in the middle of section 200x).

Naslednji dve **sliki 11 A in B** kažeta mikrostrukturo istega vzorca na prečnem in vzdolžnem preseku. Značilna strjevalna mikrostruktura dendritnega tipa s primarnimi in sekundarnimi vejami je izredno fina, kar je posebna prednost HKL-tehnologije.

Nov specialni postopek termomehanske konsolidacije HCC palic[10], ki ga razvija MIL-PP v okviru posebnega projekta specializacije proizvodnega programa kobaltovih zlitin za stelitiranje žag v lesni industriji, obeta še dodatne kakovostne prednosti.

Za razliko od tipične mikrostrukture HKL vzorcev vidimo na naslednjih slikah **12 A, B in C** mikrostrukturo PM-vzorca paralelogramskega preseka, ki je bil izdelan po tehnologiji metalurgije prahov. Očitna je značilna porazdelitev karbidov v matrixu.

Slika 13 prikazuje značilnosti porazdelitve elementov med osnovo in karbidi PM form-stelita.

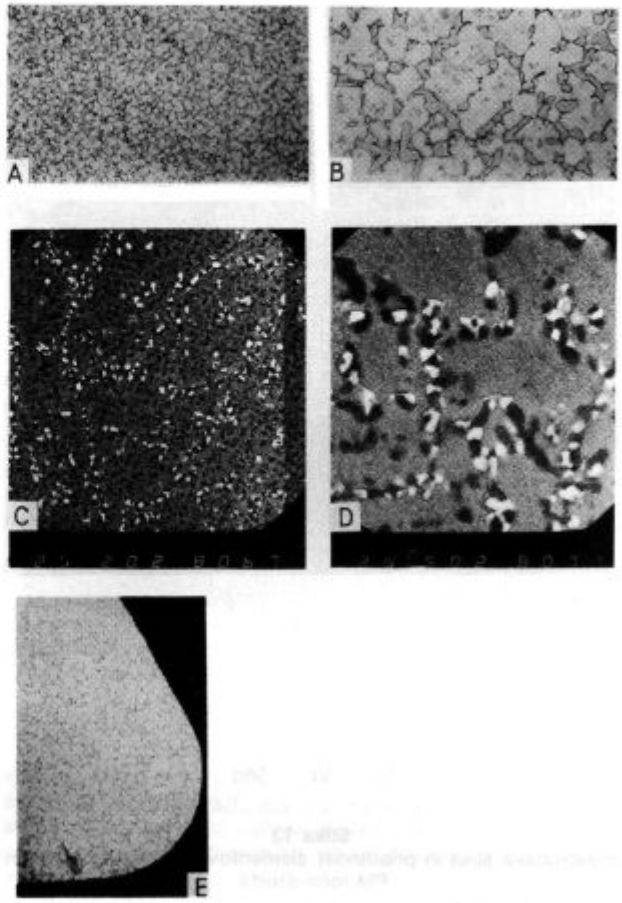

Slika 12
Značilna mikrostruktura paralelogramskega formstelita izdelanega po tehnologiji metalurgije prahov
(A - pov. 200x, B - pov. 500x, C - REM 2000x, D - REM 5000x, E - pov. 200x ob ostrem kotu paralelograma).

Fig. 12
Characteristic microstructure of parallelogram formstellite produced with powder metallurgy
(A - magn. 200x, B - magn. 500x, C - SEM 2000x, D - SEM 5000x, E - magn. 200x at the sharp angle of parallelogram).

*phic illustration of HCC stellite ∅O3.2 mm in as cast condition made by scanning electron and optical microscope is presented in **figures 10 and 11**, respectively.*

The depth of witness mark on the surface of HCC rods is usually 0.1 mm. The solidified microstructure of dendritic type with primary and secondary branches is very fine which is characteristic for HCC technology.

A new thermomechanical consolidation of HCC rods is being developed by MIL-PP and is expected to enable improved quality of stellites for tipping of saws.

*A typical microstructure of PM form stellite with parallelogram cross-section is presented in **Fig. 12** with optical and SEM photographs where characteristic distribution of carbides in the matrix is evident.*

*In **Fig. 13** presence of chemical elements in the matrix and car- bides of PM form stellite is presented.*

7. COMPARATIVE RESEARCH[1,2]

The research and development center FORINTEK CANADA CORP, published results of a comprehensive research which had a decisive influence on further development of stellite tipping for woodcutting.

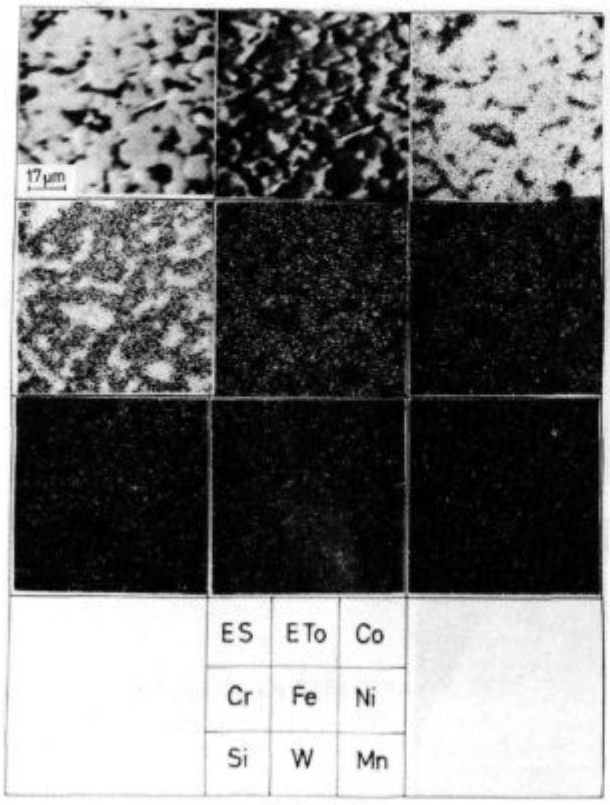

Slika 13
Elektronska slika in prisotnost elementov v osnovi in karbidih PM form-stelita.

Fig. 13
Electron picture and distribution of elements in the matrix and carbides of PM form-stellite.

7. PRIMERJALNE RAZISKAVE[1,2)]

V laboratorijih raziskovalno-razvojnega centra FORINTEK CANADA CORP. so opravili obsežne raziskave[1)], ki so odločilno vplivale na nadaljnji razvoj stelitiranja žag v lesni industriji.

V prvi seriji poskusov so primerjali štiri zlitine odporne proti obrabi pri žaganju svežega lesa. (Tabela 1)

Na **sliki 14** je prikazan način merjenja otopitve rezalnega roba s fotomikroskopijo[1)].

Glede na otopitev rezalnega roba je dal najboljše rezultate nanos zlitine stellite 12 (**slika 15**[1)]).

Otopitev zob po 35 km reza, kar ustreza približno 4 uram žaganja, je bila pri jeklenih zobeh kar dvanajstkrat večja kot pri stelitiranih z zlitino stellite 12. Še pomembnejša je ugotovitev, da so jekleni zobje dosegli že po 1 km reza ali 6 minutah tako stopnjo otopitve kot stelitirani zobje po 35 km reza ali 4 urah žaganja.

Krivulja obrabe pri jeklu za žage kaže, da so standardni zobje žage že po eni uri rezanja močno obrabljeni. Zaradi zmanjševanja zastojev je žal kar običajno, da se s tako otopelimi zobmi žaganje nadaljuje. Posledica tega je slaba kvaliteta površine rezanega lesa, neenakomerna debelina in netočnost reza ter seveda močno povečana poraba energije.

Obe zlitini na osnovi niklja DELORO 50 in 60 po ugotovljenih rezultatih ne moreta konkurirati zlitini stellite 12.

Zlitine stellite 20 že zaradi slabih rezultatov uporabe na žagi z meritvami v laboratoriju sploh niso preizkušali.

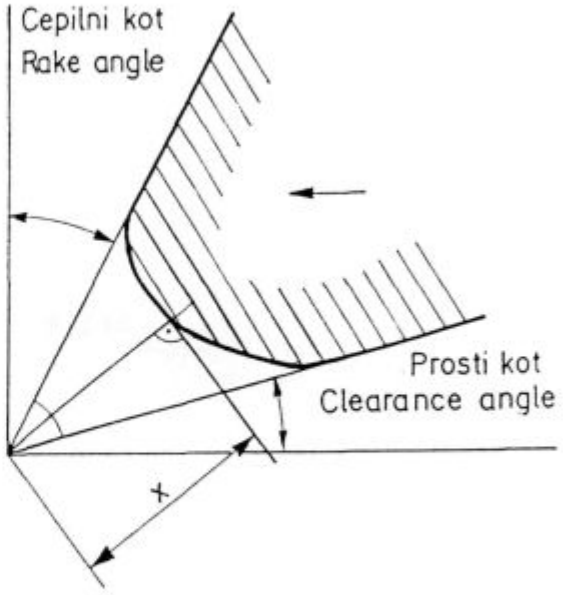

Slika 14[1)]
Meritev otopitve na zobu žage.

Fig. 14[1)]
Measurement of cutting edge retreat on saw tooth.

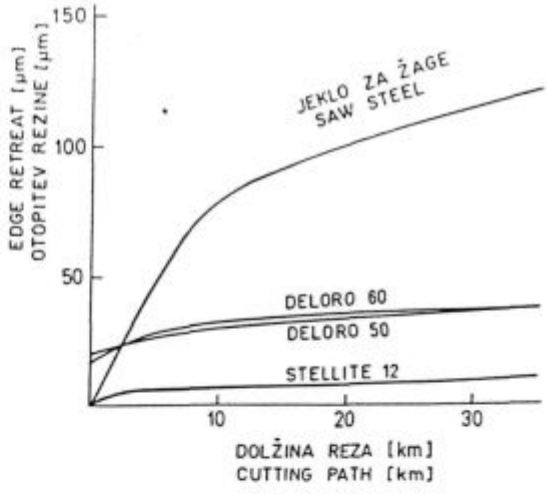

Slika 15[1)]
Otopitev konvencionalnih in obloženih zob na žagah.

Fig. 15[1)]
Dulling of conventional and tipped saw teeth.

*In the first set of experiments four grades of abrasion resistant alloys for cutting fresh wood were tested (**Tab. 1**).*

*In **Fig. 14** a method for measuring dulling of cutting edge with photomicroscopy is presented[1].*

*The best results with respect to dulling of tooth cutting edge were obtained by tipping of stellite grade 12 (**Fig. 15**).*

The dulling of teeth after cut length of 35 km, which corresponds to approximately 4 hours of sawing, was measured for saw steel and stellite 12. The value of cutting edge retreat for saw steel was found to be twelve times higher than for stellite 12. Even more important is the observation that the measured dulling of stellite 12

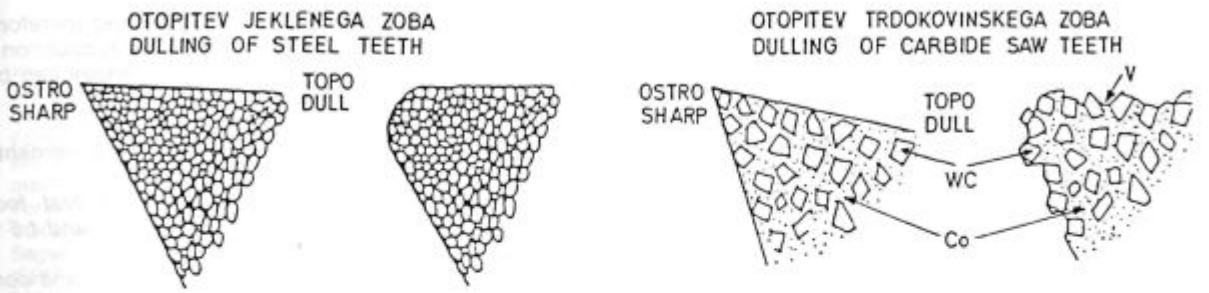

Slika 16[1)]

Otopitev jeklenih in trdokovinskih zob WC - volframov karbid, Co - osnova, V - prazen prostor, ki je bil prej zapolnjen s kobaltom.

Fig. 16[1)]

Dulling of saw steel teeth and carbide tips WC - tungsten carbide, Co - matrix, V - empty space, formerly occupied by cobalt.

Zanimiva je ugotovitev, da je obstojnost žage v veliki meri odvisna tudi od sposobnosti zlitine na zobeh za kvalitetno brušenje.

Zaključek te serije raziskav je bilo priporočilo uporabe zlitine stellite 12 za stelitiranje vseh vrst žag, ne samo zato, ker je ta zlitina pokazala najboljše rezne sposobnosti, najboljšo obrabno in korozijsko obstojnost, ampak tudi zaradi najboljšega obnašanja pri brušenju. Pri brušenju te zlitine je dosežena najboljša začetna ostrina zob, kar pomembno vpliva na celotno izdržljivost žage.

V drugi seriji posebnih laboratorijskih poskusov z natančnimi meritvami so primerjali obrabo rezalnega roba zlitine stellite 12 z dvema vrstama karbidnih trdin in s standardnim jeklom za žage. Raziskave so opravili za tri tipične vrste lesa. Pri teh poizkusih je bila dolžina reza 80 km, kar ustreza normalno žaganju 7-8 obratovalnih ur.

Slika 16[1)] shematično prikazuje značilnosti otopitve na rezalnem robu jeklenega oziroma trdokovinskega zoba. Obraba oziroma otopitev stelitiranih zob je po mehanizmu podobna jeklenim zobem.

Stelitirani zobje so pokazali v primerjavi z obema karbidnima trdinama (volframov karbid - 6 % Co in volframov karbid - 18 % Co) najmanjšo obrabo in bistveno boljšo vzdržljivost. To pomeni, da imajo stelitirane žage precejšnje prednosti pred trdokovinskimi, posebno pri rezanju svežega lesa in pri tankih rezih. Ta raziskovalna ugotovitev je bila potrjena tudi v industrijski praksi žaganja zadnjih let. Korozijska odpornost zlitine in spoja z osnovo v veliki meri ugotovitev dodatno pojasnjuje. Kislinski ekstrakti svežega lesa napadajo kobalt v osnovni masi in s tem poslabšajo odpornost proti izpadanju volframovih karbidov.

Stelitirane žage bodo pri rezanju svežega lesa popolnoma izpodrinile žage s trdokovinskimi zobmi.

Trdokovinske žage se bodo še naprej obdržale v pohištveni in drugi finalizacijski lesni industriji. Tudi tam ima zaradi problemov odpadanja trdokovinskih ploščic pri velikih hitrostih ter ob udarnih obremenitvah na zob vez med oblogo zoba in osnovno kovino, ki jo dosežemo pri stelitiranju določene prednosti v primerjavi z nalotano trdo kovino.

8. POVZETEK PREDNOSTI STELITIRANJA ŽAG

(a) **v primerjavi z uporabo standardnih jeklenih žag:**

- Rezna zmogljivost stelitiranih žag je v primerjavi z žagami z razperjenimi zobmi večja, ker reže vsak zob na obeh straneh.
- Hitrost pomika se lahko poveča do 30 %.
- Povečana obstojnost rezalnega roba zob in zmanjšanje zastojev

at 35 km is reached by saw steel already after first kilometre of cut length which corresponds to approximately six minutes of sawing.

Thus the dulling of saw steel teeth is very intensive in initial stages so that sawing after few kilometres of cut length is performed by relatively dull teeth which cause bad surface quality of cut wood, nonuniform thickness and increased energy consumption.

The stellite 12 was found to be superior in comparison to stellite 20 and both nickel base alloys which were considered in these dulling tests.

On the basis of this comparative research a conclusion was made that stellite 12 is highly recommended for all types of saws not only because of its best cutting ability, abrasion and corrosion resistance but also because of its best grindability which enables good sharpening of teeth.

In the second set of laboratory experiments the stellite 12 was compared with two grades of tungsten carbide hard metals for three typical sorts of wood. In these tests a cut length of 80 km was considered.

*In **Fig. 16** the mechanism of dulling is schematically illustrated and compared between saw steel and hard metal. The dulling mechanism of stellite teeth is similar to that of saw steel.*

The results obtained by stellite tipped teeth were better then both tungsten carbide grades with 6 % and 18 % of cobalt. Stellite tipped saws are superior to hard metal saws especially for cutting fresh woods and thin cut. This was also confirmed in practice. The corrosion resistances of stellite 12 and its welding junction are both better than tungsten carbide grades and their soldering junctions. The acid extracts of fresh wood are chemically interacting with cobalt matrix and in this way badly influence the resistance of carbides against separation from cobalt matrix.

Stellite tipped saws will replace hard metal saws in cutting fresh wood while they will retain their position in furniture and other finalising industries employing treated woods. However, even in these applications the stellite tipping has certain advantages especially in the case where high speed cutting causing high impact loads is present.

8. SUMMARIZED ADVANTAGES OF STELLITE TIPPING

*(a) **Advantages with respect to conventional steel saws:***

- *The stellite tipping enables higher cutting productivity with respect to the saws with teeth setting;*
- *The cutting speed can be up to 30 % higher;*

— Manjša hrapavost površin rezanega lesa in večja natančnost reza po daljšem trajanju žaganja. Povečan je izplen rezanega lesa.
— Zmanjšanje potrebne energije. Pri standardnih jeklenih žagah se poraba moči po štiriurnem žaganju v povprečju poveča za 15 %, pri uporabi stelitiranih žag pa samo za 1,5 %.
— Ostrenje žag je bolj ekonomično in poraba žagnih trakov ali diskov je manjša.
— Poprečni proizvodni stroški žaganja so manjši.
Vse naštete prednosti se dosežejo v glavnem brez povečanja stroškov, ker se stroški stelitiranja skoraj v celoti izravnajo s tem, da ni več potrebno delo z nakrčevanjem in razperjanjem zob.

(b) **v primerjavi z uporabo trdokovinskih žag:**
— Povečana obstojnost rezalnega roba zob.
— Izboljšanje možnosti za žaganje s tanjšim rezom. Varjeni spoj med stelitom in nosilnim jeklom je v splošnem precej trdnejši od lota med karbidno trdino in jeklom.
— Konice stelitov so manj občutljive za poškodbe in nastale poškodbe se dajo lažje popravljati.
— Stroški brušenja so nekoliko manjši, zaradi možnosti uporabe cenejših plošč.
— Nižja cena stelitnih konic.
Poraba časa in stroški dela za trdokovinske ali stelitne konice zob v praksi ne predstavljajo pomembnih razlik.

(c) **nekaj dodatnih razlogov za uvedbo stelitiranja žag**
— Rezanje trdih in zelo neenakomerno rastočih lesov (exotov) in lesov z mineralnimi vključki je mogoče samo s stelitiranimi žagami.
— V zadnjem času se je izkazalo, da prinaša stelitiranje velike prednosti tudi pri rezanju mehkih lesov.
— Z relativno majhnimi dodatnimi ukrepi za stelitiranje se dosežejo veliki ekonomski uspehi.

9. ZAKLJUČEK

Stelitiranje žag močno podaljšuje življensko dobo zob in ima posebno pri žaganju nesušenih lesov pomembne prednosti pred vsemi danes razpoložljivimi načini zmanjševanja obrabe, vključno z oblaganjem zob s trdokovinskimi konicami. Tehnologija stelitiranja omogoča precejšnje zmanjšanje proizvodnih stroškov ob istočasnem povečevanju produktivnosti in izboljšanju kakovosti. Nabava potrebne opreme za stelitiranje se v večini žagarskih obratov amortizira v kratkem času.

Zelo priporočljivo tehnično, kvalitetno in ekonomsko rešitev predstavlja organiziranje servisnih centrov za stelitiranje in ostrenje vseh vrst žag.

Nadaljnji razvoj na področju stelitiranja žag bo usmerjen v kompletiranje proizvodnih programov kobaltovih zlitin s posebnim poudarkom na specializaciji ponudbe, pri čemer bo imelo optimiranje sestave zlitin za določena področja in namene uporabe prav gotovo vse večji pomen.

— *The life time of cutting edge is longer and therefore enables reduction of interruptions in the production;*
— *A low cut roughness and narrow tolerances can be retained for a longer time;*
— *The yield of wood is higher;*
— *The energy consumption and power requirements are lower.*
— *The increase of power consumption in first four hours is approximately 15 % for steel saws and 1.5 % for stellite tipped saws;*
— *The sharpening of teeth is more economic and consumption of saw bands or discs is lower;*
— *The average production costs are lower.*

All above mentioned advantages can be achieved without additional costs because stellite tipping cost are comparable to the costs related to swagging and setting of conventional steel saws.

(b) ***Advantages with respect to hard metal saws:***
— *The life time of cutting edge of teeth is longer;*
— *A better possibility for sawing with thin cut because the welded stellite junction is stronger than soldered hard metal junction;*
— *The stellite tips are less sensitive to damages and can be easier repaired;*
— *The sharpening costs are lower because cheaper grinding plates can be used;*
— *The price of stellite tips is lower.*

The time consumption and labour costs for hard metal and stellite tipping are approximately the same.

(c) ***Some additional reasons for introduction of stellite tipping***
— *The sawing of certain hard and irregularly grown woods (exots) and woods with mineral inclusions is often possible only with stellite tipped saws;*
— *Recent production experience confirms advantages of stellite tipping also for cutting soft woods;*
— *With modest investments for stellite tipping relatively high savings and improvements can be achieved.*

9. CONCLUSION

The stellite tipping of saws enables longer life time of teeth and has many advantages especially in sawing untreated woods. It is superior to all today known approaches for reduction of teeth wear including hard metal tipping. The technology of stellite tipping enables considerable lowering of production costs while at the same time quality and productivity are improved.

It is expected that stellite tipping and sharpening will be organized in servicing centers. Further developments in stellite tipping will be aimed to an optimized assortment of alloys and forms of products for specialized applications.

LITERATURA / *REFERENCES*

1. Kirbach E., T. Bona: Stellit-bestuckung von Weichholzsagen (prevod), Lumber Manufacturing Update - Seminar, 26.–28. Oct. 1981, Seattle, WA - Technical Report No.17, FORINTEK CANADA CORP., Aug.1981.
2. Kirbach E.: Methods of improving wear resistance and maintenance of saw teeth. Technical Report No. 3/1979. Forintek Canada Corp.
3. VOLLMER - prospekti: Das Stellitieren und Sharfen von Sagezahnspitzen.
4. ISELI - privatna informacija/*privat communication*
5. ALLIGATOR - privatna informacija/*privat communication*
6. STN-W. Niggl: Priporočila za stelitiranje žag/*Recommendation for stellitizing of saws*
7. Rodič J.: Skrajševanje tehnološkega postopka od taline do žice/*Shortenings of Technological Procedures from Melt to Wire;* Železarski zbornik 22, dec. 1988, str. 101-109
8. Rodič J., W. Holzgruber, M. Haissig: Development of a new CW&BP* - Process for Specialty Steels and Superalloys, EUROMAT 89 - Conference, Aachen, Nov. 1989
9. MIL-PP d.o.o., Ljubljana: Posebne zlitine na osnovi Co za lesno industrijo/*Special Co-base alloys for wood cutting;* 1991
10. Rodič J.: Development of a New Process-Thermomechanical Consolidation of HCC Rods, not published
11. Rodič A.: Internal reports of metallographic examination of samples, Institute of metals and technologies, Ljubljana 1991

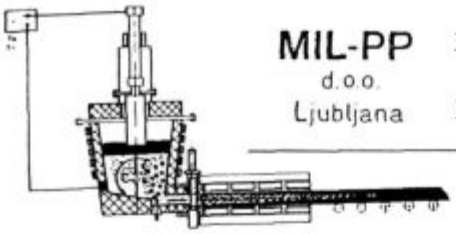

MIL-PP d.o.o. Ljubljana

RAZVOJ IN PROIZVODNJA SPECIALNIH ZLITIN

DEVELOPMENT AND PRODUCTION OF SPECIAL ALLOYS

61000 Ljubljana, Slovenija
p.p. 431 - Lepi pot 11
Tel. +38 61 151 161, 216 709
Fax. (061)-213-780

HORIZONTALNO KONTINUIRNO LITJE - HKL
HORIZONTAL CONTINUOUS CASTING - HCC

HCC PROGRAM "MILIT"

POSEBNE ZLITINE NA OSNOVI Co ZA LESNO INDUSTRIJO
SPECIAL Co-BASE ALLOYS FOR WOOD CUTTING

	MILIT 6H	MILIT 12H	MILIT 12WH	MILIT 1H	MILIT FH	MILIT 21H
C	1,2	1,4	1,6	2,5	1,8	0,3
Si	1	1	1,5	1	1	0,5
Mn	0,5	2,5	2,5	0,5	0,5	0,5
Cr	29	30	29	30	25	28
Ni	2	1,5	1,5	-	23	3
W	4,5	8	10	13	12	-
Mo	0,5	-	-	-	-	6
Co	60	54	53	50	35	60
HRC	**42**	**48**	**54**	**55**	**42**	**30**

OBLIKE FORMS	DIMENZIJE DIMENSIONS	DOLŽINE LENGTHS	DOBAVNO STANJE DELIVERY CONDITION
	2.0 mm ÷ 8.0 mm	L = 8 mm ÷ 16 mm 350 mm ÷ 4000 mm	lito ali brušeno as cast or grinded
	2.0 mm ÷ 6.5 mm	L = 8 mm ÷ 16 mm 1000 mm	brušeno - grinded
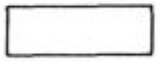	F = 8 mm² ÷ 50 mm²	L = 8 mm ÷ 16 mm 1000 mm	brušeno - grinded
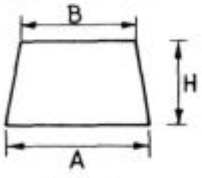	B = 2.7 mm ÷ 6.0 mm H = 2.5 mm ÷ 4.0 mm A = 3.2 mm ÷ 6.5 mm	L = 1000 mm	brušeno - grinded
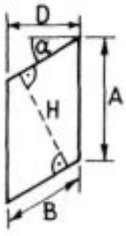	A = 4.0 mm ÷ 7.5 mm B = 3.0 mm ÷ 5.0 mm D = 2.8 mm ÷ 4.5 mm H = 3.5 mm ÷ 6.5 mm α = 30°	L = 1000 mm	brušeno - grinded
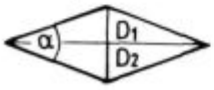	D_1 = 11 mm D_2 = 5 mm α = 50°	L = 1000 mm	brušeno - grinded
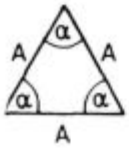	A = 4.0 mm ÷ 6.5 mm α = 60°	L = 1000 mm	brušeno - grinded

Faktor mejne intenzitete napetosti pri počasnem natezanju navodičenega jekla z visoko trdnostjo

Threshold Stress Intensity Factor at Slow-Strain-Rate Tension of High-Strength Hydrogen-Charged Steel

B. Ule[1], F. Vodopivec[1], L. Vehovar[1] and L. Kosec[2]

Konstrukcijska jekla z visoko trdnostjo in visoko napetostjo tečenja se vedno bolj uporabljajo celo za izdelavo manj zahtevnih strojnih delov. Zaradi razmeroma nizke žilavosti tovrstnih jekel in slabo izraženega prehoda v krhko stanje postajajo toliko pomembnejše njihove lomne značilnosti.

Na izgubo lomne duktilnosti močno vpliva zlasti vodik v jeklu, čeprav pri tem ne učinkuje bistveno na napetost tečenja. Poslabšanje lomne duktilnosti pa je izrazito le pri počasnem natezanju navodičenega jekla, medtem ko ga pri konvencionalnem nateznem preizkusu skoraj ne zaznamo. Male koncentracije vodika v jeklu z visoko trdnostjo torej ne vplivajo na lomno žilavost takšnega jekla, peč pa imajo za posledico pojavljanje faktorja mejhne intenzitete napetosti.

1. UVOD

Ena od znanih oblik porušitve jekel z visoko trdnostjo je tako imenovani zapozneli lom statično obremenje-

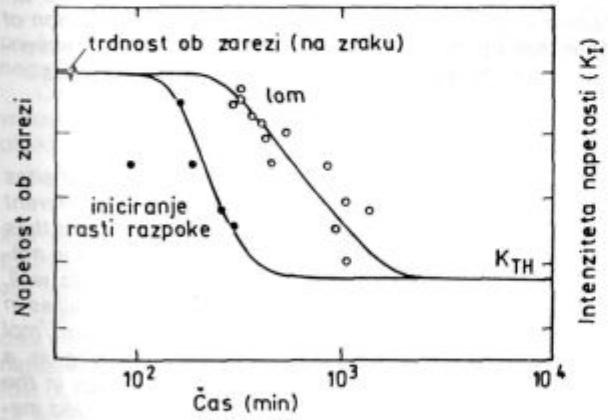

Slika 1:
Tipičen zapis pojava zapoznelega loma na nateznem preizkušancu z zarezo, obremenjenem s konstantno obremenitvijo. Zapis velja za vodičeno jeklo, vrisana pa je tudi trdnost ob zarezi za jeklo brez vodika (preizkušano na zraku) /lit. (1)/.

Fig. 1:
Typical delayed-failure phenomenon for hydrogen-charged notched tensile specimens at constant load. The notch tensile strength of uncharged steel (measured in air) is also shown (Ref. 1).

[1] *Inštitut za kovinske materiale in tehnologije, Lepi pot 11, 61000 Ljubljana*
[2] *Fakulteta za naravoslovje in tehnologijo, Oddelek za montanistiko, 61000 Ljubljana*

The use of structural steels with high-tensile and high-yield strength is increasing even in the manufacture of less demanding machine parts. Because of their relatively low toughness and poorly expressed transition into brittle state, their fracture properties are of major importance.

The decrease in fracture ductility is in particular strongly influenced by hydrogen content in steel, although hydrogen does not essentially affect its yield strength. However, the deterioration of fracture ductility is distinctive only at slow-strainrate tension of hydrogen-charged steel, whereas it practically cannot be detected in a conventional tensile test. Consequently, the low concentration of hydrogen in high-strength steel does not influence its fracture toughness, but results in the appearance of a threshold stress intensity factor.

1. INTRODUCTION

*Delayed fracture caused by stress-induced hydrogen segregation is one of the known types of fracture of high-strength steel. This problem is characterised by the nucleation of a microcrack, which then grows until it achieves a critical size, resulting in an abrupt fracture (**Fig. 1**). The incubation period, as well as the delayed time to failure occurrence, are prolonged with the decrease in load until, at a sufficiently low load, the delayed failure does not occur. Therefore, we can speak of threshold of applied stress or threshold stress intensity factor K_{TH}, which can be considerably lower than the critical stress intensity factor or fracture toughness K_{IC} of steel. In the case of hydrogen embrittlement the threshold stress intensity factor is likewise denoted as K_{HE}.*

The threshold stress intensity factor is inversely proportional to the hydrogen concentration in steel, which leads to the idea that the mutual effect of hydrogen and applied stress provokes the nucleation of microcracks. It was also found that the incubation period strongly depends on the hydrogen concentration in steel, while the effect of the applied stress magnitude is coniderably lower.

Since the effect of hydrogen on the mechanical properties of high-strength steel is manifested by the decreased fracture ductility at slow-strain-rate tension and since such decrease depends on crack nucleation as well as on crack propagation, it is therefore logical that a slow-strain-rate tension test will by all means prove to

* *Institute of metals and Technology, Lepi pot 11, 61000 Ljubljana*
** *University of Ljubljana, Fac. of natural Science, Metal. dept., 61000 Ljubljana*

nega jekla, ki je posledica napetostno induciranega segregiranja vodika v jeklu. Pri tem pojavu pride najprej do iniciiranja prve mikrorazpoke, ki nato počasi raste, vse dokler ne doseže kritične velikosti, kar povzroči hipno porušitev (**sl. 1**)[1]. Inkubacijski čas kot tudi čas do loma se podaljšujeta z zniževanjem statično delujoče obremenitve, vse dokler pri neki dovolj nizki obremenitvi zapozneli lom izostane. Govorimo torej lahko o pragu delujoče napetosti oziroma o faktorju mejne intenzitete napetosti K_{TH} (threshold stress intensity factor), ki je lahko tudi občutno nižji od faktorja kritične intenzitete napetosti, to je od lomne žilavosti jekla K_{IC}. V razmerah vodikove krhkosti označimo faktor mejne intenzitete napetosti tudi kot K_{IHE}.

Z znižanjem koncentracije vodika v jeklu se faktor mejne intenzitete napetosti zvišuje, kar napeljuje na misel, da je porajanje mikrorazpok posledica vzajemnega učinkovanja vodika in delujoče napetosti. Ugotovili so tudi[2], da je inkubacijski čas zelo odvisen od koncentracije vodika v jeklu, le malo pa od velikosti delujoče napetosti.

Ker se učinek vodika na mehanske lastnosti visokotrdnega jekla manifestira z izgubo lomne duktilnosti pri počasnem natezanju in ker je lomna duktilnost jekla odvisna tako od porajanja kot tudi napredovanja razpok, je logično, da bo počasni natezni preizkus vsekakor primernejši za ugotavljanje vpliva vodika na lastnosti jekla kot pa konvencionalni natezni preiskus. Če je hitrost deformacije pri natezanju tako velika, da pride do loma v času, ki je krajši od inkubacijskega časa, učinek vodika na lastnosti jekla ne bo zaznaven.

Poleg statičnih preizkusov s konstantno obremenitvijo (static delayed failure test) se za določevanje občutljivosti jekla za lom, induciran z vodikom, še največ uporablja natezni preizkus s cilindričnimi preizkušanci z zarezo po obodu. O tem priča opis Pollockove metode v reviji Metals Progress[3]. Pollock določa občutljivost jekla za lom, induciran z vodikom, z merjenjem sile loma cilindričnih preizkušancev z zarezo po obodu pri hitrosti nateznaja 2×10^{-4} mm s^{-1}. Trdnost zarezanega preizkušanca je namreč v takšnih primerih manjša od trdnosti gladkega, kar neposredno odseva izgubo duktilnosti zaradi učinkovanja vodika.

V strokovni literaturi je opisanih še več različnih načinov kvalitativnega določevanja občutljivosti jekla za lom, induciran z vodikom, ki pa vsi temeljijo v glavnem na enostavnem merjenju stopnje poslabšanja kontrakcije pri natezanju jekla[4,5].

Ker določevanje faktorja mejne intenzitete napetosti K_{TH} le na osnovi rezultatov nateznega preizkusa v literaturi še ni ustrezno obdelano, smo raziskali rešitev tega problema. Izkoristili smo merljivo poslabšanje lomne duktilnosti jekla pri počasnem natezanju kot nadomestku za dolgotrajni statični natezni preizkus pri konstantni obremenitvi. Ob tem smo upoštevali hipotezo, po kateri poslabšanje lomne duktilnosti pri počasnem natezanju dejansko potrjuje obstoj faktorja mejne intenzitete napetosti, če se lomna žilavost takšnega jekla - merjena pri običajnih hitrostih natezanja - le malo ali pa sploh ne spremeni.

Razvoj in teoretična utemeljitev te metode omogočata določanje faktorja mejne intenzitete napetosti kar na osnovi rezultatov nateznega preizkusa, s tem pa je določevanje občutljivosti jekla za lom, induciran z vodikom, bistveno bolj objektivno, kot je pri sedaj uporabljanih metodah.

2. TEORETIČNI DEL

Vodik je v železu v atomarni obliki bodisi na intersticijskih mrežnih mestih bodisi vezan v večji ali manjši me-

be more convenient in determining the influence of hydrogen on steel properties than a conventional tension test. If the deformation rate at tension is so large that failure occurs in a period shorter than the incubation one, the influence of hydrogen on the properties of steel will not be cognizable.

Besides static test at constant load (static delayed failure test), the tension test on cylindrical specimens with a circumferential notch is more frequently used for the determination of hydrogen induced fracture of steel. This is evident in the description of Pollock s method in Metals Progress[3]. Pollock determines the sensitivity of steel to hydrogen-induced fracture by measuring the fracture load at a crosshead speed of 2×10^{-4} mm s^{-1} using cylindrical notched tensile specimens. In this case the strength of notched specimens is lower than that of smooth specimens, which directly reflects the decrease of ductility due to the effect of hydrogen.

Many more methods for qualitative determination of hydrogen induced fracture of steel have been described in professional literature. However, all of these are mainly based on the measurement of the decrease of reduction of area at tension test of steel[4,5]. Since the determination of threshold stress intensity factor K_{TH} only on the basis of the results of a tensile test has not been adequately treated in literature, our attempts were aimed at finding a solution to this problem.

Instead of a long-term static test at constant load, we used the slow-strain-rate tension test for determining the measurable decrease in fracture ductility of steel. We followed the hypothesis that the decrease in fracture ductility at slow-strain-rate tension test actually confirms the existence of a threshold stress intensity factor if the fracture toughness of such steel - measured at conventional strain rate - changes only slightly or doesn't change at all.

The development and theoretical justification of this method prove its usefulness in determining the threshold stress intensity factor on the basis of results attained in a tensile test. In this way, the determination of steel sensitivity to hydrogeninduced fracture is essentially more objective than in currently used methods.

2. THEORY

Hydrogen is present in iron either at interstitial sites at the lattice or bound as trapped hydrogen to different discontinuities of the cristall lattice - "traps" - and thus referred to as trapped hydrogen. Some hydrogen in molecular form is always found in the microvoids as well. The partial molal volume of hydrogen in iron as well as in most other metals is surprisingly high (appr. 2 cm^3/mol of hydrogen or 0,33 nm^3/atom)[6-8]. This results in a strong interaction between hydrogen intersticials in the cristal lattice and elastic-stress fields of the loaded metal lattice.

A thermodynamic analysis of this process, based on the assumption that hydrogen is a completely mobile component, was performed by Li, Oriani and Darken[9], who found the following relation:

$$\mu - \mu_0 = \sigma_{ij} E_{ij} dV \qquad (1)$$

The distortion field around the hydrogen atom is described by the deformation tensor E_{ij}; ρ_{ij} is the stress tensor which determines the stress state originating from external loads acting on cristal lattice. μ_0 is the chemical potential of hydrogen in the absence of external stress, while u represents the chemical potential of hydrogen under external stress. The difference between

ri na različne diskontinuitete kristalne mreže, ki jih imenujemo s skupnim imenom pasti in od tod v pasteh ujeti vodik (trapped hydrogen). Nekaj vodika je v železu vedno tudi v porah v molekularni obliki. Parcialni molski volumen vodika v železu in večini drugih kovin je presenetljivo velik (približno 2 cm^3/mol vodika, oziroma 0,33 nm^3/atom)[6–8]. Posledica tega je močna interakcija med vodikovimi intersticijami v kristalni mreži ter polji elastičnih napetosti v obremenjeni kristalni mreži kovin.

Li, Oriani in Darken[9], so s termodinamično analizo tega problema, pri čemer so vodik v železu obravnavali kot povsem mobilno komponento, prišli do izraza:

$$\mu - \mu_0 = \sigma_{ij} E_{ij} dV \qquad (1)$$

Deformacijski tenzor E_{ij} opisuje deformacijsko polje okrog intersticijskega atoma vodika, $\mu\sigma_{ij}$ je napetostni tenzor, ki opredeljuje napetostno stanje, izvirajoče od zunanje mehanske obremenitve kristalne mreže. Z μ_0 je v zgornjem izrazu (1) označen kemijski potencial vodika v neobremenjeni kristalni mreži kovine, μ pa je kemijski potencial vodika v mehansko obremenjeni mreži kovine. Razlika potencialov je zato enaka delu, ki je potrebno za vgnezdenje intersticijskega vodika v polje delujočih napetosti.

Gradient napetosti torej povzroči gradient kemijskega potenciala vodika, le-ta pa predstavlja gonilno silo za difuzijo intersticijsko raztopljenega vodika. Rezultat tega je segregiranje vodika v neenakomernem polju napetosti: vodik se zaradi reverzibilne dilatacije kristalne mreže s pripadajočo pozitivno spremembo volumna, ki spremlja vgnezdenje vodikovih intersticij, koncentrira v področjih prevladujočih nateznih napetosti, medtem ko se področja s prevladujočimi tlačnimi napetostmi z vodikom osiromašijo. Prerazporejanje vodika v obremenjeni kristalni mreži poteka toliko časa, dokler ni dosežena v vseh točkah mreže ravtežna koncentracija vodika, določena z izrazom:

$$[H] = [H]_0 \exp \frac{\sigma_{ij} E_{ij} dV}{RT} \qquad (2)$$

pri čemer je $[H]_0$ koncentracija enakomerno porazdeljenega vodika v neobremenjeni kristalni mreži.

Če upoštevamo le volumsko spremembo v okolici vrinjenih vodikovih atomov, lahko izraz (2) zapišemo v obliki:

$$[H] = [H]_0 \exp \frac{\sigma_m \bar{V}_H}{RT} \qquad (3)$$

kjer je z σ_m označena hidrostatična komponenta napetostnega tenzorja [$\sigma_m = 1/3\ (\sigma_x + \sigma_y + \sigma_z)$], $\bar{V}_H$ pa je parcialni molski volumen vodika v železu.

Z enačbo (3) je mogoče izračunati koncentracijo vodika v lokaliziranem področju, na primer v zoženem vratu nateznega preiskušanca, kjer deluje hidrostatična napetost σ_m. Ko koncentracija vodika [H] na tem mestu doseže kritično vrednost $[H]_{cr}$, ko je torej $K_I = K_{TH}$, moramo računati z iniciiranjem mikrorazpok in zapoznelim lomom jekla. Problem je analitično rešil Gerberich[10], ki je za faktor mejne intenzitete napetosti izpeljal izraz:

$$K_{TH} = \frac{R\,T}{\alpha V_H} \ln \frac{[H]_{cr}}{[H]_0} - \frac{\sigma_{ys}}{2\,\alpha} \qquad (4)$$

pri tem ima α eksperimentalno ugotovljeno vrednost 2/5 $mm^{-1/2}$.

Odvisnost (4) je eksperimentalno dobro potrjena, vendar pa pri napetostih tečenja, ki so nižje od 1200 MPa, pogosto prihaja do neujemanja med enačbo (4) in rezultati eksperimentov. To neujemanje lahko deloma razložimo z odvisnostjo razmerja $[H]_{cr}/[H]_0$ od napetosti tečenja jekla. Farrell and Quarrell[4] sta namreč ugo-

the potentials is the work needed to place the hydrogen into the active stress field.

The gradient of chemical potential of hydrogen is therefore caused by the stress gradient and represents the driving force for the diffusion of interstitially dissolved hydrogen, resulting in hydrogen segregation in non-uniform stress field. Hydrogen concentrates in the areas of predominantly tensile stresses due to the reversible dilatations of the cristal lattice with the corresponding volume changes accompanied by the insertion of hydrogen interstitials, while the compressively strained regions become impoverished with hydrogen. The redistribution of hydrogen in the strained cristal lattice takes place until an equilibrium concentration of hydrogen is achieved in all points of the cristal lattice. This is expressed by:

$$[H] = [H]_0 \exp \frac{\sigma_{ij} E_{ij} dV}{RT} \qquad (2)$$

where $[H]_0$ is the concentration of hydrogen, uniformly distributed within the unstrained cristal lattice.

If only the volume change around the inserted hydrogen atoms is considered, the equation (2) may be expressed as:

$$[H] = [H]_0 \exp \frac{\sigma_m d\bar{V}_H}{RT} \qquad (3)$$

where σm is the hydrostatic component of stress tensor $\sigma_m = 1/3\ (\sigma_x + \sigma_y + \sigma_z)$ and $\bar{V}_H$ is the partial molal volume of hydrogen in iron.

Equation (3) may be used to calculate the concentration of hydrogen in a localised area, as for example in the narrowed neck of tensile specimens with hydrostatic stress σ_m.

Microcracks nucleation and delayed fracture of steel can be expected when the hydrogen concentration [H] in this region achieves the critical value $[H]_{cr}$, i.e. when $K_I = K_{TH}$. This problem was solved analytically by Gerberich[10], who expressed the threshold stress intensity factor in the form of:

$$K_{TH} = \frac{R\,T}{\alpha \bar{V}_H} \ln \frac{[H]_{cr}}{[H]_0} - \frac{\sigma_{ys}}{2\,\alpha} \qquad (4)$$

where factor a reaches the experimentally determined value of 2/5 $mm^{-1/2}$.

The relation (4) is experimentally well confirmed, although some discrepancies can often be observed between Eq. (4) and the experimental results at yield strength below 1200 MPa. These discrepancies can be partly explained by the dependance of the $[H]_{cr}/[H]_0$ ratio on the yield point. Namely Farrell and Quarrell[4] ascertained that larger concentrations of hydrogen are needed to produce embrittlement in steel with lower yield strength, which they expressed with the relation $[H]_{cr} \propto 1/\sigma_{ys}$.

Kim and Loginow11 proved that the content of soluble hydrogen in steel was proportional to the yield strength, thus $[H]_0 \propto \sigma_{ys}$. If both statements are taken into account this can be written as:

$$\frac{[H]_{cr}}{[H]_0} \simeq \frac{\beta}{\rho_{ys}} \qquad (5)$$

where β is a constant for specific types of steel with determined hydrogen concentration.

By substituting (5) for (4), we arrive at the well-known Gerberich equation for threshold stress intensity factor in its final form:

$$K_{TH} = \frac{R\,T}{\alpha \bar{V}_H} \ln \frac{\beta}{\sigma_{ys}} - \frac{\sigma_{ys}}{2\,\alpha} \qquad (6)$$

tovila, da so ze doseganje krhkosti v jeklih z nižjo napetostjo tečenja potrebne višje koncentracije vodika, kar sta zapisala kot $[H]_{cr} \infty 1/\sigma_{ys}$. Kim and Loginow[11] pa sta dokazala, da se v jeklih z višjo napetostjo tečenja topi več vodika, torej $[H]_0 \infty \sigma_{ys}$. Z upoštevanjem obeh navedenih ugotovitev lahko zapišemo:

$$\frac{[H]_{cr}}{[H]_0} \simeq \frac{\beta}{\rho_{ys}} \qquad (5)$$

pri čemer je β konstanta za posamično vrsto jekla in za določeno vsebnost vodika v njem.

Ko substituiramo (5) v (4), dobimo znano Gerberichovo enačbo za faktor mejne intenzitete napetosti v njeni končni obliki:

$$K_{TH} = \frac{R\,T}{\alpha \bar{V}_H} \ln \frac{\beta}{\sigma_{ys}} - \frac{\sigma_{ys}}{2\alpha} \qquad (6)$$

Ker vodik v jeklu še najbolj vpliva na lomno duktilnost jekla pri počasnem natezanju, je za nadaljnjo teoretično analizo smiselno poiskati soodvisnost med lomno žilavostjo K_{IC} in parametri nateznega preizkusa. Takšno soodvisnost poznamo pod imenom Hahn-Rosenfieldova korelacija[12, 13], ki ima naslednjo obliko:

$$K_{IC} = \sqrt{\frac{0{,}05\, E_f\, n^2\, E\, \sigma_{ys}}{3}}\ (\mathrm{MPa\ m^{1/2}}) \qquad (7)$$

Pri tem je E_f lomna duktilnost, ki jo izračunamo iz znane kontrakcije jekla Z po formuli:

$$E_f = \ln[1/(1-Z)] \qquad (8)$$

medtem, ko eksponent deformacijskega utrjevanja n izračunamo iz enakomernega raztezka e_u po formuli:

$$n = \ln(1 + e_u) \qquad (9)$$

Ker pri običajnih hitrostih obremenjevanja, kakršne uporabljamo pri merjenju faktorja kritične intenzitete napetosti K_{IC}, ne zaznamo opaznejšega poslabšanja duktilnosti jekla, ki bi ga sicer lahko pripisali vplivu majhnih koncentracij vodika v jeklu (okoli 1 ppm)[4, 14], se zdi utemeljena hipoteza, da poslabšanje lomne duktilnosti jekla pri počasnem natezanju dejansko odraža eksistenco faktorja mejne intenzitete napetosti K_{TH}.

V skladu s to hipotezo bi lahko Hahn-Rosenfieldovo korelacijo (7) uporabili kar za izračunavanje faktorja K_{TH}, potem ko bi v enačbo (7) vstavili vrednosti, izmerjene pri počasnem natezanju. Ker pa je poznana tudi teoretično izpeljana Gerberichova enačba za K_{TH} (6), v kateri je neznana le vrednost β, je mogoče po izenačenju enačb (6) in (7) vrednost β izraziti eksplicitno:

$$\beta = \sigma_{ys} \exp \frac{\alpha \bar{V}_H}{R\,T} \left\{ \sqrt{\frac{0{,}05\, E_f\, n^2\, E\, \sigma_{ys}}{3}} + \frac{\sigma_{ys}}{2\alpha} \right\} \qquad (10)$$

V izrazu (10) so veljavne vrednosti za σ_{ys}, E_f ter n, kot že rečeno, izmerjene pri počasnem nateznem preizkusu.

Verificiranje postavljene hipoteze se bo torej reduciralo na ugotavljanje konstantnosti veličine β, ki mora biti neodvisna od napetosti tečenja jekla σ_{ys}. Konstantna vrednost β pomeni, da je postavljena hipoteza pravilna in da s podatki počasnega nateznega preizkusa lahko izračunamo K_{TH} kar z enačbo (7).

3. EKSPERIMENTALNI DEL

Za eksperimentalno delo smo izbrali jeklo Č.4751 z naslednjo kemijsko sestavo: 0,38% C, 0,99% Si, 0,38% Mn, 0,012% P, 0,010% S, 5,19% Cr, 1,17% Mo ter 0,23% V. Po homogenizacijskem žarjenju in normalizaciji smo iz kovanih palic s premerom 16 mm za natezni preizkus

Since hydrogen in steel mostly affects the fracture ductility at slow-strain-rate tension, it would therefore seem adequate for further analysis to determine the relation between fracture toughness K_{IC} and the parameters of tensile test. Such a relation, known as the Hahn-Rosenfield correlation[12, 13], is given by:

$$K_{IC} = \sqrt{\frac{0{,}05\, E_f\, n^2\, E\, \sigma_{ys}}{3}}\ (\mathrm{MPa\ m^{1/2}}) \qquad (7)$$

where E_f is the fracture ductility, calculated from the actual reduction of area Z using the equation:

$$E_f = \ln[1/(1 - Z)] \qquad (8)$$

whereas the strain hardening exponent n can be calculated from the uniform elongation e_u using the equation:

$$n = \ln(1 + e_u) \qquad (9)$$

Since the evident worsening of fracture ductility, which may be attributed to the small amounts of hydrogen in steel (appr. 1 ppm), cannot be detected[4, 14] by conventional strain-rate used in measurements of critical stress intensity factor K_{IC}, it therefore seems that the hypothesis according to which the decreased fracture ductility at slow-strain-rate tension reflects the existence of threshold stress intensity factor is justified.

In accordance with this hypothesis, the Hahn-Rosenfield correlation (7) could be used for the calculation of K_{TH} after the values measured at slow-strain-rate have been inserted into equation (7). Since Gerberich s theoretically developed equation for K_{TH} (6) is also known (β being the only unknown value), it is therefore possible to express the value of β explicitly after the balance of Eq. (6) and (7):

$$\beta = \sigma_{ys} \exp \frac{\alpha \bar{V}_H}{R\,T} \left\{ \sqrt{\frac{0{,}05\, E_f\, n^2\, E\, \sigma_{ys}}{3}} + \frac{\sigma_{ys}}{2\alpha} \right\} \qquad (10)$$

As already mentioned, the relevant values of σ_{ys}, E_f and n in Eq. (10) are measured in a slow-strain-rate tension test.

The verification of the postulated hypothesis will thus be reduced to the measurement of constancy of the β value, which has to be independent of the yield stress σ_{ys} of steel. The constant β value means that the hypothesis is correct and that K_{TH} can be calculated using the Eq. (7) on the basis of slow-strain-rate tensile test data.

3. EXPERIMENTAL

Steel Č.4751 containing (wt-%) 0,38% C, 0,99% Si, 0,38% Mn, 0,012% P, 0,010% S, 5,19% Cr, 1,17% Mo and 0,23% V has been chosen for experimental work. Cylindrical tensile specimens with a diameter of 10 mm, gauge length of 100 mm and total length of 250 mm were machined from the forged rod after it had been homoneously annealed and normalized. Specimens were thermally treated in a vacuum annealing furnace. They were austenitised at 980° C for a short period, quenched in a flow of gaseous nitrogen and then tempered at temperatures of 620° C, 640° C and 670° C respectively. Thus, three separate and distinct classes of yield strength - 1220 MPa, 1020 MPa and 900 MPa respectively were achieved.

The cathodic charging of thermally treated tensile specimens was carried out for 1 hour in 1 N sulfuric acid at a current density of 0,3 mA/cm². The experimental set-up for cathodic polarisation of tensile specimens, as shown in ***Fig. 2****, is composed of a potentiostat and corrosion cell with electrodes.*

izdelali 250 mm dolge cilindrične preiskušance s premerom 10 mm in dolžino 100 mm. Preiskušance smo toplotno obdelali v vakuumski žarilni peči, tako da smo jih po kratkotrajni austenitizaciji pri 980°C kalili v toku plinastega dušika, nato pa popuščali pri temperaturah 620°C, 640°C oziroma 670°C. Na ta način smo dobili tri ločene in dobro definirane trdnostne razrede z napetostjo tečenja 1220 MPa, 1020 MPa oziroma 900 MPa.

Toplotno obdelane preiskušance za natezni preizkus smo navodičili z enournim katodnim polariziranjem v 1 N raztopini žveplene kisline pri gostoti toka 0,3 mA/cm². Eksperimentalni sklop s katodnim polariziranjem preizkušancev, sestavljen iz potenciostata in korozijske celice z elektrodami, je prikazan na **sliki 2.**

Natezne preizkuse smo opravili na nateznem trgalnem stroju INSTRON, potem ko smo natezne preizkušance po končanem navodičenju 24 ur zadrževali na zraku, da so se koncentracije vodika v jeklu približale residualnim vrednostim (približno 0,7 ppm), ki se nato časovno skoraj niso več spreminjale.

Za hitrost natezanja smo izbrali tako hitrost 1 mm/min, značilno za običajni natezni preizkus, kot tudi hitrost 0,1 mm/min, značilno za počasno natezanje. Merili smo napetost tečenja σ_{ys} (MPa), natezno trdnost σ_{TS} (MPa), maksimalni enakomerni raztezek e_u (× 100 %) ter kontrakcijo jekla Z (× 100 %).

Lomno duktilnost E_f in eksponent deformacijskega utrjevanja n smo izračunali z enačbama (8) in (9).

Mikrofraktografske preiskave prelomnih površin vodičenih in pri hitrosti natezanja 0,1 mm/min obremenjevanih nateznih preizkušancev smo opravili s scanning elektronskim mikroskopom JEOL JSM-35 (SEM).

4. REZULTATI

Izmerjene mehanske lastnosti navodičenega jekla kot tudi jekla brez vodika (pod 0,05 ppm) so zbrane v **tabeli 1.** V tej tabeli so zbrane še lomne žilavosti K_{IC} jekla, izračunane s Hahn-Rosenfieldovo korelacijo (7) na osnovi rezultatov običajnih nateznih preizkusov pri hitrosti natezanja 1 mm/min ter nadalje še faktorji mejne intenzitete napetosti K_{TH} vodičenega jekla, izračunani z isto enačbo (7), vendar na osnovi rezultatov počasnega natezanja pri hitrosti 0,1 mm/min.

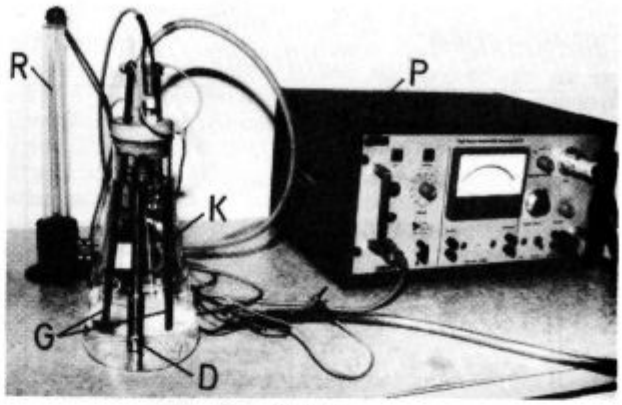

Slika 2:
Eksperimentalni sklop za vodičenje nateznih preiskušancev s katodnim polariziranjem.
(P-potenciostat, D-natezni preizkušanec, G-grafitni protielektrodi, K-kalomelova elektroda in R-rotometer).

Fig. 2:
Experimental set-up for hydrogen charging of tensile specimens with cathodic polarisation.
(P-potenciostat, D-tensile specimen, G-graphite electrodes, K-kalomel electrode, R-rotameter).

The tension tests were made on an INSTRON testing machine, after hydrogen charging of specimens was completed and the specimens exposed to air for 24 hours. This enabled the concentrations of hydrogen in steel to approach the residual values (appr. 0,7 ppm), which remained nearly time-independent.

The tension tests were performed at conventional strain rate i.e. at a crosshead speed of 1 mm/min as well as at lower-strain-rate i.e. at a crosshead speed of 0,1 mm/min. The yield strength σ_{ys} (MPa), tensile strength σ_{TS} (MPa), max. uniform elongation e_u (x100%) and the reduction of area Z (x100%) were measured. The fracture ductility E_f and the strain hardening exponent n were calculated using equations (8) and (9) respectively.

The fracture surfaces of tensile specimens tested at a crosshead speed of 0,1 mm/min were examined in the scanning electron microscope JEOL JSM-35 (SEM).

Tabela 1: Mehanske lastnosti jekla brez vodika in istega jekla po navodičenju
Table 1: *Mechanical properties of uncharged and hydrogen-charged steel*

Hitrost natezanja 1 min/min *Crosshead speed 1 mm/min*			Lomna žilavost *Facture toughness*	Hitrost natezanja 0,1 mm/min *Crosshead speed 0,1 mm/min*			Faktor mejne inten. napet. *Threshold stress inten. factor*	Konstanta *Constant*
Napetost tečenja *Yield strength*	Enakomerni raztezek *Uniform elongation*	Kontrakcija *Reduction of area*	K_{IC}	Napetost tečenja *Yield strength*	Enakomerni raztezek *Uniform elongation*	Kontrakcija *Reduction of area*	K_{TH}	β /En (10)/ /Eq. (10)/
σ_{ys}(MPa)	e_u × 100 %	Z × 100 %	MPa. $m^{1/2}$	σ_{ys}(MPa)	e_u × 100 %	Z × 100 %	MPa · $m^{1/2}$	MPa
Jeklo brez vodika, *uncharged steel*								
924	8,7	52	126,9	910	8,5	51		
1010	7,4	51,3	112,5	1027	6,5	50,3		
1270	6,4	50	107,5	1214	6,2	50,3		
Navodičeno jeklo, *hydrogen charged steel*								
885	8,4	50,3	117,2	899	8,1	47,7	109,8	4005
1082	7,2	49,3	110,1	1078	6,5	42,7	90,1	4223
1209	6,1	47,3	96,3	1226	6,0	27,3	67,4	4037

V tabeli 1 so prikazane tudi vrednosti za konstanto β, izračunane s pomočjo enačbe (10) na osnovi rezultatov počasnega natezanja.

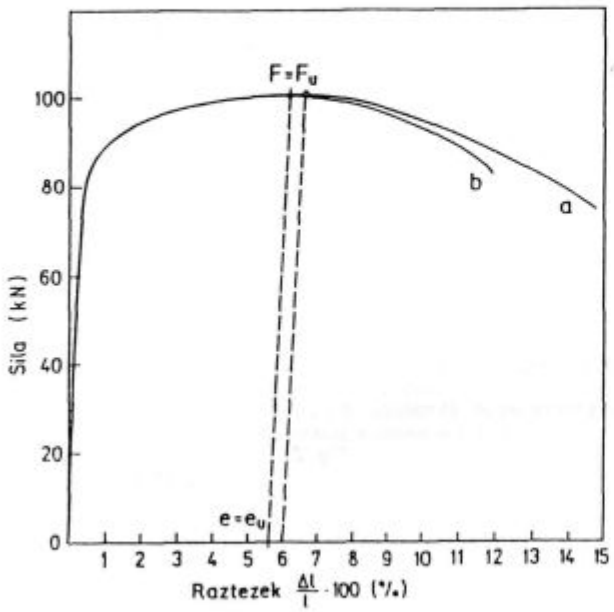

Slika 3:
Diagram sila-deformacija pri počasnem natezanju jekla trdnostnega razreda 1300 MPa; a) brez vodika (pod 0,05 ppm) in b) 24 ur po vodičenju (ca. 0,7 ppm vodika).

Fig. 3:
Load-deformation diagram obtained at slow-strain-rate tension test of steel with yield strength of 1300 MPa.
(a) without hydrogen (less than 0,05 ppm) and (b) 24 hours after hydrogen charging (appr. 0,7 ppm hydrogen).

V diagramu sila-deformacija na **sliki 3** je prikazana odvisnost med silo in raztezkom pri počasnem natezanju jekla s trdnostjo ca. 1300 MPa. Odvisnost, označena z a), velja za jeklo brez vodika (pod 0,05 ppm), z napetostjo tečenja 1070 MPa, trdnostjo 1286 MPa, enakomernim raztezkom $e_u = 6\%$ in kontrakcijo $Z = 49\%$, medtem ko velja odvisnost, označena z b), za jeklo istega trdnostnega razreda, ki pa je bilo natezano 24 ur po vodičenju (ca. 0,7 ppm vodika). V tem primeru smo namerili napetost tečenja 1090 MPa, trdnost 1284 MPa, enakomerni raztezek $e_u = 5{,}6\%$ ter kontrakcijo $Z = 39\%$.

Mikrofraktografske preiskave prelomnih površin navodičenih nateznih preizkušancev kažejo, da z vodikom inducirani lom pri počasnem natezanju takšnih preizkušancev ne ostane povsem duktilnega tipa, celo pri preizkušancih z relativno nizko napetostjo tečenja ne (**slika 4**). Pri višji napetosti tečenja so prelomne površine navodičenega ter počasi natezanega jekla mešane narave; poleg kvazicepilnih ploskev najdemo na prelomnih površinah tudi jamičasta duktilna področja ter številne grebene, nastale s trganjem (**slika 5**).

5. RAZPRAVA

Analiza rezultatov mehanskih preizkusov (**Tabela 1**) kaže, da je lomna žilavost K_{IC}, s katodnim polariziranjem navodičenega jekla z visoko trdnostjo, le malo manjša od lomne žilavosti enakega jekla brez vodika, kot o tem tudi sicer lahko sklepamo iz diagrama na sliki 1.

Počasnejše natezanje pri jeklu brez vodika ne povzroči kakšnih opaznejših sprememb, medtem ko se pri

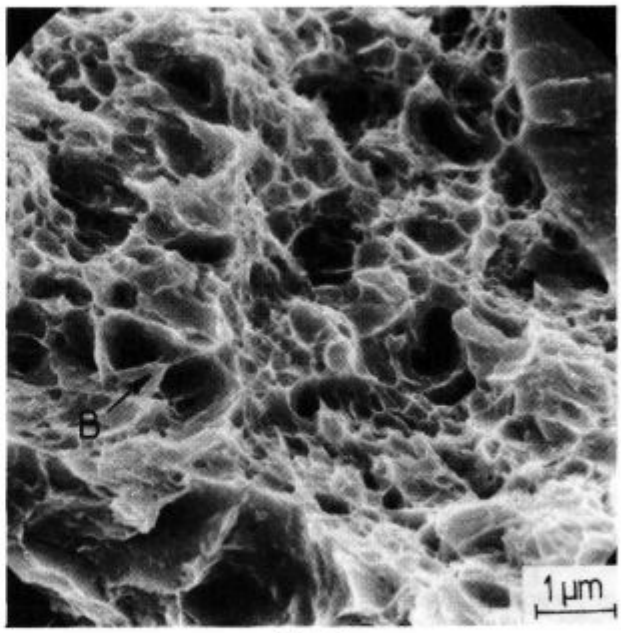

Slika 4:
Jamičasta duktilna prelomna površina s posameznimi kvazicepilnimi detajli (B) pri vodičenem in počasi natezanem jeklu z napetostjo tečenja ca. 900 MPa.

Fig. 4:
Dimpled ductile fracture area with some quasicleavage details (B) in hydrogen-charged and slow-strain-rate tested steel with yield strength of 900 MPa.

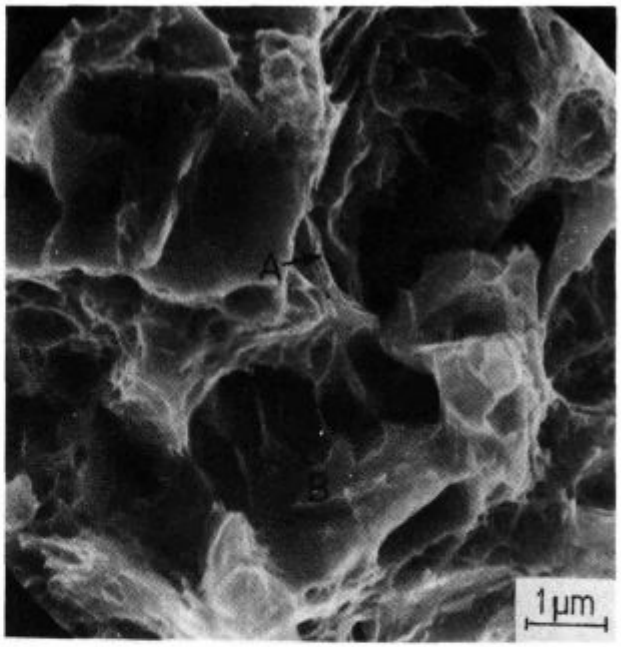

Slika 5:
Mešana oblika preloma vodičenega jekla z napetostjo tečenja ca. 1070 MPa.
Poleg cepilnih oziroma kvazicepilnih ploskev (B) je na prelomni površini moč zaslediti tudi jamičasta duktilna področja ter številne grebene, nastale s trganjem.

Fig. 5:
Mixed fracture mode on hydrogen-charged steel with yield strength of 1070 MPa.
Besides cleavage and quasicleavage facets (B), dimpled ductile areas and many tear ridges can also be observed.

navodičenem jeklu močno poslabša lomna duktilnost, t.j. kontrakcija jekla, ne pa tudi enakomerni raztezek, trdnost in napetost tečenja takšnega jekla. Poslabšanje lomne duktilnosti navodičenega jekla pri počasnem natezanju dejansko kaže na obstoj faktorja mejne intenzitete napetosti K_{TH} (K_{HE}). S Hahn-Rosenfieldovo korelacijo (7) izračunane vrednosti K_{TH} dajejo namreč, po substituciji v Gerberichovo enačbo (6), za konstanto β vrednost približno 4100 MPa. Ta vrednost je neodvisna od napetosti tečenja jekla in zato v okviru eksperimentalne natančnosti merjenja res konstantna količina, skladno z Gerberichovim modelom.

Eksperimenti so nadalje pokazali, da je bila uporabljena hitrost natezanja 0,1 mm/min že dovolj majhna, da smo lahko iz poslabšanja lomne duktilnosti navodičenega jekla izračunali take vrednosti faktorja mejne intenzitete napetosti K_{TH}, za katere je β konstanta.

Če upoštevamo, da velikost plastične cone v trenutku loma navodičenega preizkušanca dosega velikost približno polovice vratu preiskušanca ($l = 3$ mm), dobimo za $\dot{E}_c$, upoštevaje hitrost natezanja $v = 1{,}6 \times 10^{-3}$ mm s^{-1} (0,1 mm/min), vrednost $\dot{E}_c = v/l = 5{,}3 \times 10^{-4}$ s^{-1}.

V strokovni literaturi[15] navajajo za nerjavna jekla nekoliko višje vrednosti $\dot{E}_c$, približno 10^{-3} s^{-1}. Raziskave Nakana in sodelavcev[16], opravljene s počasnim natezanjem vodičenega jekla z napetostjo tečenja 500 MPa, pa kažejo, da se pri zadostni koncentraciji vodika v jeklu kontrakcija jekla asimptotično približa neki znižani vrednosti že pri kritični hitrosti deformacije $\dot{E}_c = 10^{-4}$ s^{-1}, to pa je že velikostni red naših izmerjenih vrednosti. Ta hitrost deformacije je namreč že dovolj majhna, da Cottrellovi oblaki vodikovih atomov lahko potujejo skupaj z dislokacijami globoko v plastično cono nateznih preizkušancev.

Diagram na sliki 3 potrjuje, da vodik ne vpliva bistveno na mobilnost dislokacij v zgodnjih fazah deformacijskega procesa pri natezanju, saj skoraj ne učinkuje na napetost tečenja, trdnost in enakomerni raztezek jekla, pač pa le na kontrakcijo jekla. Vodik torej spreminja obliko diagrama sila-deformacija šele od pojavljanja plastične nestabilnosti dalje, kar se dobro ujema z navedbami iz različnih literaturnih virov[17–25]. Po teh navedbah vodik ne vpliva niti na zgodnje nukleiranje mikropor, niti na gostoto mikropor, ko se stopnja deformacije približuje lomni deformaciji. Očitno je zato vpliv vodika zaznaven šele v fazi rasti mikropor in/ali fazi njihovega združevanja. Do pospešene rasti in koalescence mikropor v tej fazi pa lahko pride tudi z mehanizmom ločevanja prostih površin, na katerih je adsorbiran vodik[26]. Na **sliki 6** je shematsko prikazana rast in koalescenca mikropor vzdolž meje dveh kristalnih zrn. Mehanizem koalescence mikropor z ločevanjem prostih površin, na katerih je adsorbiran vodik, prične delovati, ko se oblikuje troosno napetostno stanje v zoženem delu nateznega preizkušanca. Posledica tega je že opisano "zgoščevanje" zadnje faze plastične deformacije pri počasnem natezanju navodičenega jekla.

Mikrofraktografske preiskave samo še ilustrirajo pravkar opisani mehanizem loma. Pojasnjujejo namreč lome jamičaste duktilne vrste, pri katerih pa kažejo stene in dna jamic posamične mikromorfološke značilnosti cepilnega oziroma kvazicepilnega loma. Res smo tudi pri naših raziskavah vodičenega in počasi natezanega jekla višjega trdnostnega razreda opazili poleg duktilnih jamičastih področij še trganja (tearing), ki so sicer značilna za jekla z zadostno duktilnostjo in dovolj majhno napetostjo tečenja, da do porušitve lahko pride s plastično deformacijo. Poleg detajlov takšne vrste pa smo opazili na prelomnih površinah tudi področja kvazicepilne narave, često na samem obrobju večjih in globjih, lijakasto

4. RESULTS

The mechanical properties of hydrogen-charged as well as hydrogen uncharged steel (less than 0,05 ppm) are presented in ***Table 1****. The fracture toughness of steel K_{IC}, calculated according to the Hahn-Rosenfield correlation (7) on the basis of conventional tension tests made at a crosshead speed of 1 mm/min, as well as the threshold stress intensity factor K_{TH} of cathodic charged steel, also calculated using equation (7), but on the basis of results obtained at a crosshead speed of 0,1 mm/min, are also shown in Table 1.*

The values of constant β are also given in ***Table 1.*** *These were calculated using equation (10), on the basis of slow-strain-rate tensile test data.*

*The load-deformation diagram (****Fig. 3****) shows the relation between load and elongation at slow-strain-rate tension of steel with a tensile strength of appr. 1300 MPa. Curve a) denotes the uncharged steel (less than 0,05 ppm hydrogen), having a yield strength of 1070 MPa, tensile strength of 1286 MPa, uniform elongation $e_u = 6\%$ and reduction of area $Z = 49\%$, whereas Curve b) denotes hydrogen-charged steel (appr. 0,7 ppm hydrogen) of the same strength class, being tested 24 hours after it had been charged. In this case the yield strength of 1090 MPa, tensile strength of 1284 MPa, uniform elongation $e_u = 5{,}6\%$ and reduction of area $Z = 39\%$ were measured.*

*The microfractographic examinations of fracture surfaces of hydrogen-charged specimens confirm that hydrogen-induced fracture at slow-strain-rate tension does not remain predominantly ductile, even in specimens with a relatively low yield strength (****Fig. 4****). The fracture surfaces of hydrogen-charged steel with higher yield strength, stretched at slow-strain-rate tension, are of mixed mode. In addition to quasicleavage details, ductile dimpled areas and numerous tear ridges have also been observed (****Fig. 5****).*

5. DISCUSSION

The analysis of mechanical testing data (Table 1) shows that the fracture toughness K_{IC} of hydrogen-charged high-strength steel is only slightly lower than that of the uncharged steel, which can also be concluded from the diagram in Fig. 1.

The slow-strain-rate tension of uncharged steel does not provoke any noticeable changes, whereas that of hydrogen-charged steel strongly decreases the fracture ductility, i.e. the reduction of area, but does not affect the uniform elongation, tensile strength and yield strength of such steel. The deterioration of fracture ductility of hydrogen-charged steel at slow-strain-rate tension indicates the existence of the threshold stress intensity factor K_{TH} (K_{HE}). Namely, the K_{TH} - values, calculated with the Hahn-Rosenfield correlation (7) after being substituted into Gerberich's equation (6), give an approximate value of 4100 MPa for the β-constant. Within the experimental error of the measure- ments, the obtained value is constant and, in accordance with Gerberich's model, independent of the yield strength of steel.

The experiments further showed that the applied crosshead speed of 0,1 mm/min was sufficiently low to enable the calculation of K_{TH} - values from the decrease in fracture ductility of hydrogen-charged steel, i.e. the calculation of K_{TH} - values for which β is a constant.

Considering that the size of the plastic zone of a hydrogen- charged specimen is approximately half of the neck diameter ($l = 3$ mm) at fracture, the crosshead speed is $v = 1{,}6 \times 10^{-3}$ mm s^{-1} (0,1 mm/min), then a value of $\dot{E}_c = v/l = 5{,}3 \times 10^{-4}$ s^{-1} is obtained.

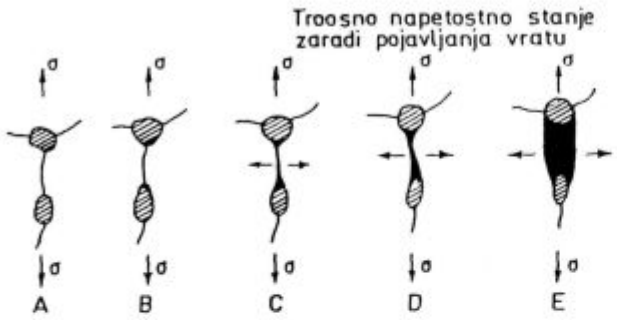

Slika 6:
Shematski prikaz nastajanja por, njihove rasti in koalescence vzdolž meja zrn, na katerih je adsorbiran vodik /lit. (26)/.

Fig. 6:
Schematic representation of microvoid formation, growth and coalescence along grain boundaries where hydrogen is adsorbed (Ref. 26).

oblikovanih jamic (slika 4, detajl B), pa tudi kot povsem samostojna plitvejša področja.

6. SKLEPI

Na osnovi opravljenih raziskav smo ugotovili, da izgubo lomne duktilnosti pri počasnem natezanju navodičenega jekla z visoko trdnostjo lahko uspešno izkoristimo za kvantitativno določevanje faktorja mejne intenzitete napetosti K_{TH} (K_{HE}). Ugotovili smo namreč, da majhne koncentracije vodika (pod 1 ppm) v jeklu, ki je bilo navodičeno s katodnim polariziranjem, ne vplivajo bistveno na lomno žilavost, merjeno pri običajnih hitrostih natezanja (1 mm/min). Počasno natezanje (0,1 mm/min) navodičenega jekla z visoko trdnostjo pa poslabša lomno duktilnost, kar nakazuje obstoj faktorja mejne intenzitete napetosti K_{TH}. Z izračunanjem faktorjev K_{TH} s pomočjo Hahn-Rosenfieldove korelacije (7) in vstavljanjem teh vrednosti v Gerberichovo enačbo (6) smo ovrednotili parameter β /enačba (10), tabela 1/. Dobili smo konstantno vrednost okoli 4100 MPa, neodvisno od napetosti tečenja jekla, kot to tudi zahteva Gerberichov model za K_{TH}.

Mikrofraktografske preiskave prelomnih površin počasi natezanega vodičenega jekla z visoko trdnostjo kažejo, da je prelom lokalno še vedno tudi duktilne vrste. Kljub detajlom kvazicepilne narave smo v vseh primerih našli še duktilne grebene, nastale s trganjem, in jamičasta področja duktilnega tipa. Kvazicepilna oblika loma na obrobju večjih in globjih lijakasto oblikovanih jamic dokazuje, da so le-te rasle in se medsebojno zlivale tudi z mehanizmom ločevanja prostih površin, na katerih je bil adsorbiran vodik.

Professional literature[15] quotes somewhat higher $\dot{E}_c$ - values for stainless steels, approximately 10^{-1} s^{-1}. However, the investigations performed by Nakano and coworkers[16] on hydrogen-charged steel with yield strength of 500 MPa using slow-strain-rate measurements show that at sufficient concentration of hydrogen in steel the reduction of area asymptotically approaches the reduced value already at a critical deformation rate of $\dot{E}_c = 10^{-4}$ s^{-1}, whose magnitude is of the same order as found in our investigations. This deformation rate is, in fact, low enough to enable the Cottrell atmosphere of hydrogen atoms pinned on dislocations to penetrate deep into the plastic zone of tensile specimens.

The diagram on Fig. 3 confirms that hydrogen has no essential influence on the mobility of dislocations in earlier phases of the deformation process at tension. It has almost no effect on the yield strength, tensile strength and uniform elongation of steel, but only on the reduction of area. Thus hydrogen changes the shape of a load-deformation diagram only after the appearance of plastic instability, as already found by a number of authors[17–25]. According to these sources, hydrogen has no effect on the early nucleation of microvoids, nor on microvoid density, when the deformation approaches the fracture deformation. Therefore, the effect of hydrogen becomes obvious only at the stage of microvoid growth and/or during their coalescence. The growth of microvoid and their coalescence can also be accelerated by a mechanism of separation of internal interfaces where hydrogen is adsorbed[26]. The growth and coalescence of microvoids along the grain boundary are schematically shown in ***Figure 6.*** *The mechanism of microvoid coalescence and the separation of internal interfaces due to adsorbed hydrogen becomes operative when the triaxial stress state in the narrow neck of the tensile specimen is formed, resulting in the previously described "condensation" of the last stage of plastic deformation at slow-strain-rate tension of hydrogen-charged steel.*

The microfractographic investigations are an additional illustration of above-mentioned fracture mechanism. They explain the ductile-dimpled types of fracture in which the walls and bottoms of dimples exhibit individual micromorphological characteristics of the cleavage or quasi-cleavage type of fracture. It is true that our investigations of hydrogen-charged high-strength steel at slow-strain-rate also showed, in addition to ductile-dimpled areas, tearing regions typical for steels with sufficiently high ductility and yield strength low enough that the fracture may be the result of plastic deformation. Besides the details of such ductile types, we also observed quasicleavage areas on fracture surfaces, most often on the very periphery of larger, deeper funnel-type dimples (Fig. 4, detail B) and also as entirely independent shallow regions.

6. CONCLUSIONS

On the basis of the performed investigations, we have ascertained that the loss of fracture ductility at slow-strain-rate tension of hydrogen-charged high-strength steel can be successfully used for the quantitative determination of the threshold stress intensity factor K_{TH} (K_{HE}). It was established that small concentrations of hydrogen (less than 1 ppm) in cathodically-charged steel have no substantial influence on the fracture toughness, as measured at conventional strain-rate (1 mm/min). However, the slow-strain-rate (0,1 mm/min) of hydrogen-charged high-strengthsteel weakens the fracture ductility, which reflects the existence of the threshold stress intensity factor K_{TH}. The parameter β

/Eq. (10), Table 1/ was determined by inserting the K_{TH} - values, calculated using the Hahn-Rosenfield correlation (7), into Gerberich s equation (6). We thus obtained a constant value of about 4100 MPa, independent of the yield strength of steel, as requested by Gerberich s model for K_{TH}.

Microfractographic investigations of fracture surfaces of highstrength hydrogen-charged steel tested at slow-strain-rate indi- cate that, locally, the fracture is still of ductile type. Despite the quasicleavage details, ductile ridges as a result of tearing as well as ductile dimpled areas were found in all cases. The quasicleavage type of fracture on the periphery of larger, deeper and funnel-type dimples proves that the growth and coalescence of voids are also the consequence of the mechanism causing the separation of internal interfaces where hydrogen is adsorbed.

LITERATURA / *REFERENCES*

1. C.S. Kortovich in E.A. Steigerwald, Eng. Fract. Mech., 4, 637 (1972).
2. G.L. Hanna, A.R. Troiano in E.A. Steigerwald, Trans. of the ASM, 57, 658-671 (1964).
3. New hydrogen-embrittlement test, Advanced Materials and Processes inc., Metal Progress, 7, 10-11 (1988).
4. K. Farrell in A.G. Quarrell, J. Iron Steel Inst., 202, 1002 (1964).
5. H. Morimoto in Y. Ashida, Trans. ISIJ, 23, B-352 (1983).
6. H. Wagenblast in H.A. Wriedt, Metall. Trans., 2, 1393-1397 (1971).
7. J.O'M. Bockris, W. Beck, M.A. Genshaw, P.K. Subramanyan in F.S. Williams, Acta metall., 19, 1209-1218 (1971).
8. H. Peisl v Hydrogen in Metals, Topics in Applied Physics, Ed.: G. Alefeld and J. Volkl, vol. 28, 53-74 (1978).
9. L.C.M. Li, R.A. Oriani in L.S. Darken, Z. Phzsik. Chem., 49, 271 (1966).
10. W.W. Gerberich v Effect of Hydrogen in high-strength and martensitic steels, Hydrogen in Metals, ASM-Ohio, 115 (1974), kot tudi:

W.W. Gerberich in S.T. Chen, Metall. Trans., 6A, 271 (1975).

11. C.D. Kim in A.W. Loginow, Corrosion, 24, 313 (1968).
12. G.T. Hahn in A.R. Rosenfield, Sources of Fracture Toughness: The Relation between KIC and the Ordinary Tensile Properties of Metals, Applications Related Phenomena in Titanium Alloys, ASTM STP 432, 5-32, Philadelphia, (1968).
13. G.T. Hahn in A.R. Rosenfield, Metall. Trans., 6A, 653-668 (1975).
14. G.T. Hahn in A.R. Rosenfield, Trans., ASM, 59, 909 (1966).
15. M.B. Whiteman in A.R. Troiano, Corrosion, 21, 53-56 (1965).
16. K. Nakano, M. Kanao in T. Aoki, Trans. of National Research, Institute for Metals, 29, No. 2, 34-43 (1987).
17. R. Garber, M. Bernstein in A.W. Thompson, Scr. Metall., 10, 341-345 (1976).
18. A.S. Argon in J. Im, Metall. Trans., 6A, 839-851 (1975).
19. J.R. Rice in D.M. Tracey, J. Mech. Phys. Solids, 17, 201-217 (1969).
20. D.M. Tracey, Eng. Fract. Mech., 3, 301-315 (1971).
21. A.S. Argon, J. Im in R. Safoglu, Metall. Trans., 6A, 825-838 (1975).
22. C.D. Beachem, Metall. Trans., 3, 437-451 (1972).
23. T.D. Lee, T. Goldenberg in J.P. Hirth, Metall. Trans., 10A, 199-208 (1979).
24. In-Gyn Park in A.W. Thompson, Metall. Trans., 21A, 465-477 (1990).
25. D. Kwon in R.J. Asaro, Metall. Trans., 21A, 117-134 (1990).
26. H. Cialone in R.J. Asaro, Metall. Trans., 10A, 367-375 (1979).

PRIKAZ

Izdelava jekel v elektro obločni peči, sekundarna rafinacija v vakuumski napravi, kontinuirno vlivanje jekla, vlivanje jekla v kokile, vlivanje odlitkov v livarni, valjanja gredic, slabov in predtrakov na valjalnem stroju bluming, valjanje žice in profilov, valjanje debele pločevine

PROIZVODNJE

Toplo valjanje trakov na valjalnem stroju (štekel), hladno vlečenje žice, hladno vlečenje profilov, hladno valjanje trakov, proizvodnja žebljev, proizvodnja dodajnih materialov, izdelava hladno oblikovanih profilov, izdelava vratnih podbojev

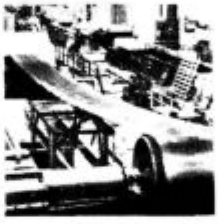

SLOVENSKE ŽELEZARNE

ŽELEZARNA JESENICE

64270 Jesenice, Cesta železarjev 8, telefon: (064) 81 231, 81 341, 81 441
teleks: 34526 ZELJSN, Jugoslavija, telegram: Železarna Jesenice

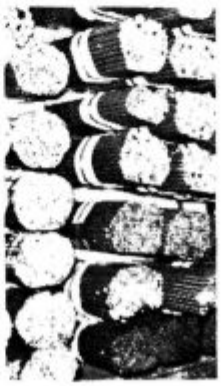

V proizvodnem programu so naslednji izdelki:

gredice, toplo valjana debela, srednja, in tanka pločevina, hladno valjana pločevina in trakovi, toplo valjana žica, hladno vlečena žica, hladno vlečeno, luščeno in brušeno paličasto jeklo, hladno oblikovani profili, kovinski vratni podboji, dodajni materiali za varjenje, žeblji, jekleni ulitki, tehnični plini

Poleg navedenih izdelkov pa nudimo tudi storitve:

valjanje v pločevino ali trak, vlečenje v žico ali paličasto jeklo, toplotne obdelave, raziskave oziroma meritve lastnosti jekla, računalniške obdelave, psihološke, sociološke in ekološke študije, tehnološki inženiring

Kompjutorska simulacija skrućivanja odljevaka kompleksne geometrije

Computer Simulation of Solidification of Complex Geometry Castings

V. Grozdanić*[1], J. Črnko*[1]

1. UVOD

Pri proizvodnji odljevaka složene geometrije od velike su pomoći modeli kojima se simulira njihovo skrućivanja jer je već za kompjutorskim terminalom moguće odrediti tok njihova skrućivanja, vrijeme skrućivanja, mjesta moguće pojave defekta u odljevcima, te utjecati na njihov dizajn kako bi se proizvedli zdravi odljevci. Međutim, raznolikost i kompleksnost oblika odljevaka umnogome otežavaju simulaciju skrućivanja jer je potrebno primijeniti kompleksan matematički aparat da bi se proces opisao matematičkim modelom koji uz osnovnu diferencijalnu jednadžbu provođenja topline sadrži početne i granične uvjete. Diferencijalna jednadžba rješava se numerički primjenom metode konačne razlike ili konačnog elementa. Metoda konačne razlike može biti eksplicitna i implicitna a po svojoj matematičkoj formulaciji nešto je jednostavnija od metode konačnog elementa, što je uvjetovalo da se ta metoda prije koristila pri rješavanju kućivanja odljevaka. Ne ulazeći u prednosti ili nedostatke navedenih metoda općenito je prihvaćeno da se kod modeliranja skrućivanja odljevaka manje složene geometrije za numeričko rješavanje parcijalne diferencijalne jednadžbe koristi metoda konačne razlike. Primjer odljevka relativno složene geometrije predstavlja kućište ventila **(slika 1)**, čiji matematički model skrućivanja sadrži numeričko rješenje parcijalne diferencijalne jednadžbe implicitnom metodom promjenljivog smjera.

2. MATEMATIČKI MODEL

Pri operacionalizaciji matematičkog modela potrebno je riješiti parcijalnu diferencijalnu jednadžbu provođenja topline koja odgovara geometrijskom uzoru kućišta ventila (slika 1)[1]:

$$\frac{\delta T}{\delta t} = a\left(\frac{\delta^2 T}{\delta r^2} + \frac{1}{r}\frac{\delta T}{\delta r} + \frac{\delta^2 T}{\delta z^2}\right) \qquad (1)$$

Kako u horizontalnoj osi simetrije kućišta ventila vrijedi da je $r = 0$, jednadžbu (1) potrebno je modificirati pomoću L'Hospitalovog pravila nakon čega se dobije diferencijalna jednadžba slijedećeg oblika:

$$\frac{\delta T}{\delta t} = a\left(2\frac{\delta^2 T}{\delta r^2} + \frac{\delta^2 T}{\delta z^2}\right) \qquad (2)$$

Početni uvjeti. Temperatura kalupa i njegove vanjske strane jednaka je T_s, dok je temperatura metala u kalupu jednaka temperaturi lijevanja T_L. Početna temperatura na

*[1] Institut za metalurgiju, Sisak

1. INTRODUCTION

Computer simulation of solidification is very helpful for castings of complex geometry since it enables reliable determination of the course of solidification, the time required for complete solidification and the points of potential casting defects. The simulation can also contribute to improve casting design in order to assure sound castings. However, the simulation is very difficult in the case of complex geometrical shape because it requires the elaboration of a sophisticated mathematical model which beside basic differential equation of heat flow must include initial and boundary conditions also.

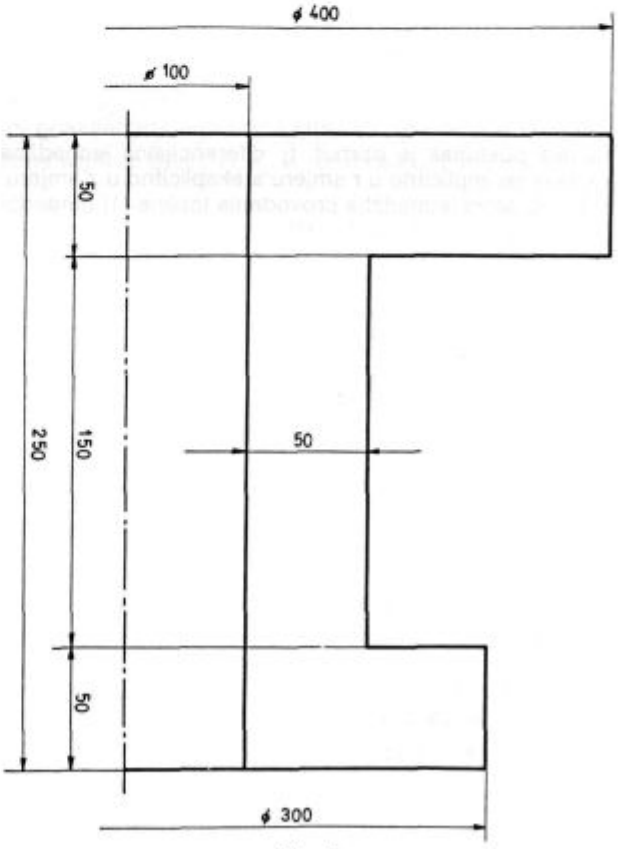

Slika 1
Kućište ventila s odgovarajućim dimenzijama.

Fig. 1
Valve housing with corresponding dimensions.

graničnoj plohi između odljevka i kalupa dobije se rješavanjem Fourierove diferencijalne jednadžbe provođenja topline u slučaju kontakta dvaju polubeskonačnih medija:

$$T_j = T_s + \frac{T_L - T_s}{1 + \frac{k_k}{k_m}\sqrt{\frac{a_m}{a_k}}} \qquad (3)$$

Izvod jednadžbe (3) dan je u Dodatku 2.

Granični uvjeti. Vanjska strana kalupa drži se pri konstantnoj temperaturi T_s. Na dodirnoj plohi kalup-metal, metal-jezgra i kalup-jezgra postoji kontinuitet toplinskog toka odnosno vrijedi granični uvjet četvrte vrste:

$$k_m \frac{\delta T_m}{\delta n} = k_k \frac{\delta T_k}{\delta n} \qquad (4)$$

$$k_m \frac{\delta T_m}{\delta n} = k_j \frac{\delta T_j}{\delta n} \qquad (5)$$

$$k_k \frac{\delta T_k}{\delta n} = k_j \frac{\delta T_j}{\delta n} \qquad (6)$$

Toplofizička svojstva materijala. Pri simulaciji skrućivanja kućišta ventila toplinska svojstva kalupa, metala i jezgre uzeta su kao funkcija temperature[2] (Dodatak 3).

3. IMPLICITNA METODA PROMJENLJIVOG SMJERA

Diferencijalna jednadžba provođenja topline (1) odnosno (2) s odgovarajućim početnim i graničnim uvjetima riješena je numeričkom metodom konačne razlike - implicitnom metodom promjenljivog smjera[3]. Metoda se sastoji u tome da se vremenski interval podijeli na dva koraka. U prvoj polovini vremenskog intervala diferencijalna jednadžba rješava se implicitno u z smjeru, a eksplicitno u r smjeru. Za drugu polovinu vremenskog intervala postupak je obrnut, tj. diferencijalna jednadžba rješava se implicitno u r smjeru a eksplicitno u z smjeru. Diferencijalna jednadžba provođenja topline (1) numerički se rješava na slijedeći način:

— za prvi $\Delta t/2$ vrijedi

$$\frac{T^n_{i,j-1} - 2T^n_{i,j} + T^n_{i,j+1}}{(\Delta r)^2} + \frac{T^n_{i,j+1} - T^n_{i,j-1}}{2 r_j \Delta r} + \frac{T^{n+1/2}_{i-1,j} - 2T^{n+1/2}_{i,j} + T^{n+1/2}_{i+1,j}}{(\Delta z)^2} = \frac{1}{a_{i,j,n}} \frac{T^{n+1/2}_{i,j} - T^n_{i,j}}{\Delta t/2} \qquad (7)$$

— za drugi $\Delta t/2$ vrijedi

$$\frac{T^{n+1}_{i,j-1} - 2T^{n+1}_{i,j} + T^{n+1}_{i,j+1}}{(\Delta r)^2} + \frac{T^{n+1}_{i,j+1} - T^{n+1}_{i,j-1}}{2 r_j \Delta r} + \frac{T^{n+1/2}_{i-1,j} - 2T^{n+1/2}_{i,j} + T^{n+1/2}_{i+1,j}}{(\Delta z)^2} = \frac{1}{a_{i,j,n}} \frac{T^{n+1/2}_{i,j} - T^{n+1/2}_{i,j}}{\Delta t/2} \qquad (8)$$

Diferencijalna jednadžba provođenja topline (2) numerički se rješava na slijedeći način:

— za prvi $\Delta t/2$ vrijedi

$$2\frac{2T^n_{i,2} - 2T^n_{i,1}}{(\Delta r)^2} + \frac{T^{n+1/2}_{i-1,1} - 2T^{n+1/2}_{i,1} + T^{n+1/2}_{i+1,1}}{(\Delta z)^2} = \frac{1}{a_{i,1,n}} \frac{T^{n+1/2}_{i,1} - T^n_{i,1}}{\Delta t/2} \qquad (9)$$

Differential equation can be solved numerically by the method of finite difference or finite elements. The method of finite difference can be explicit or implicit. In respect to mathematical formulation it is more simple than the method of finite element therefore it has been used more frequently for the solving of solidification problem. Without consideration of shortages and advantages of the both methods it has generally been accepted that for modelling of solidification of casting with less complex shape the method of finite difference is more suitable for numerical solution of corresponding partial differential equation. Valve housing ***(Fig. 1)*** *is an example of a casting with comparatively complex geometry. Mathematical model of its solidification contains numerical solution of partial differential equation by implicit method of variable direction.*

2. MATHEMATICAL MODEL

In the elaboration of mathematical model the following partial differential equation of heat flow corresponding to valve housing (Fig. 1)[1] should be solved:

$$\frac{\delta T}{\delta t} = a\left(\frac{\delta^2 T}{\delta r^2} + \frac{1}{r}\frac{\delta T}{\delta r} + \frac{\delta^2 T}{\delta z^2}\right) \qquad (1)$$

Since for horizontal axis of valve housing symmetry $r = 0$ equation (1) should be modified according to L'Hospital's rule which results in the equation:

$$\frac{\delta T}{\delta t} = a\left(2\frac{\delta^2 T}{\delta r^2} + \frac{\delta^2 T}{\delta z^2}\right) \qquad (2)$$

Initial conditions. Mold temperature and temperature of its outer side is equal to T_s whereas the temperature of metal is equal to casting temperature T_L. Initial temperature at the mold/casting boundary interface can be obtained by solving Fourier's differential equation for heat flow through the contact area of two semiinfinite medias:

$$T_j = T_s + \frac{T_L - T_s}{1 + \frac{k_k}{k_m}\sqrt{\frac{a_m}{a_k}}} \qquad (3)$$

Derivation of eq. (3) is given in Appendix 2.

Boundary conditions. Outer mold surface maintains constant temperature T_S. On contact mold/metal, metal/core and mold/core area there is a continuous heat flow for which boundary condition of the fourth sort holds:

$$k_m \frac{\delta T_m}{\delta n} = k_k \frac{\delta T_k}{\delta n} \qquad (4)$$

$$k_m \frac{\delta T_m}{\delta n} = k_j \frac{\delta T_j}{\delta n} \qquad (5)$$

$$k_k \frac{\delta T_k}{\delta n} = k_j \frac{\delta T_j}{\delta n} \qquad (6)$$

Thermophysical properties of material. It has been asummed that thermal properties of mold, metal and core are temperature dependent[2]. (Appendix 3).

3. IMPLICIT METHOD OF VARIABLE DIRECTION

Differential heat flow equations (1) and (2) with corresponding initial and boundary conditions have been numerically solved by implicit method of variable direction[3]. The method utilize division of time interval into two steps. In the first half of time interval the equation is solved implicitly for z and explicitly for r direction. The procedure is reversed in the second half of time interval.

— za drugi $\Delta t/2$ vrijedi

$$2\frac{2T^{n+1}_{i,2}-2T^{n+1}_{i,1}}{(\Delta r)^2}+\frac{T^{n+1/2}_{i-1,1}-2T^{n+1/2}_{i,1}+T^{n+1/2}_{i+1,1}}{(\Delta z)^2}=$$

$$=\frac{1}{a_{i,1,n}}\frac{T^{n+1}_{i,1}-T^{n+1/2}_{i,1}}{\Delta t/2} \qquad (10)$$

Primjenom implicitne metode promjenljivog smjera dobije se sistem simultanih linearnih algebarskih jednadžbi, čije su nepoznanice $v_1, v_2, ..., v_n$, a koje imaju tridijagonalni oblik:

$$\begin{aligned}
b_1v_1+c_1v_2 &= d_1\\
a_2v_1+b_2v_2+c_2v_3 &= d_2\\
a_3v_2+b_3v_3+c_3v_4 &= d_3\\
&\cdots\cdots\\
a_iv_{i-1}+b_iv_i+c_iv_{i+1} &= d_i \qquad (11)\\
&\cdots\cdots\\
a_{N-1}v_{N-2}+b_{N-1}v_{N-1}+c_{N-1}v_N &= d_{N-1}\\
a_Nv_{N-1}+b_Nv_N &= d_N
\end{aligned}$$

Posebno efikasan algoritam za rješavanje tridijagonalnog sistema jednadžbi je:

$$v_N=\gamma_N \qquad (12)$$

$$v_i=\gamma_i-\frac{c_iv_{i+1}}{\beta_i},\ i=N-1,\ N-2,\ ...,\ 1 \qquad (13)$$

gdje se β i γ računaju iz rekurzivnih formula

$$\beta_1=b_1 \qquad (14)$$

$$\gamma_1=d_1/\beta_1 \qquad (15)$$

$$\beta_i=b_i-\frac{a_i}{ci-1}\beta_{i-1},\ =2,3,...,N \qquad (16)$$

$$\gamma_i=\frac{d_i-a_1\gamma_{i-1}}{\beta_i},\ i=2,3,...,N \qquad (17)$$

U Dodatku 4 navedeni su tridijagonalni koeficijenti koji daju algoritam procesa skrućivanja kućišta ventila u pješčanom kalupu.

4. DIJAGRAM TOKA

Na temelju prikazanog algoritma napisan je program u programskom jeziku ASCII FORTRAN koji je riješen na računalu SPERRY 1100. Detaljan dijagram toka prikazan je na **slici 2**. Osnovna karakteristika programa je da se koriste dvije matrice temperatura T i T*. Prva matrica sadrži temperature na početku i kraju vremenskog koraka, a druga matrica sadrži temperature na kraju prvog $\Delta t/2$. Na početku programa pridaju se početne vrijednosti pojedinim varijablama i konstantama. Potprogramom TYP pridaju se početne vrijednosti temperature pojedinim mrežnim točkama, a također se tipiziraju sve točke u kalupu, odljevku, jezgri i na njihovim međusobnim granicama. Nakon ispisa početne temperature raspodjele pomoću potprograma ISPIS1, sistem algevarskih tridijagonalnih jednadžbi rješava se prvo redak po redak (potprogram RED), a zatim stupac po stupac (potprogram STUP). Rezultati se periodički ispisuju po cijeloj geometriji odljevka, kalupa i jezgre (potprogram ISPIS1) ili samo po geometriji odljevka (potprogram ISPIS2) do unaprijed zadanog vremena t_{max}.

5. DISKUSIJA REZULTATA

Simulacija skrućivanja ventila od čeličnog lijeva s oko 0,25 % C u pješčanom kalupu provedena je uz prostorni korak $\Delta z=\Delta r=1$ cm i vremenski korak $\Delta t=10$ s do vre-

Consequently, for differential equation (1) and first half of time interval $\Delta t/2$ we have:

$$\frac{T^n_{i,j-1}-2T^n_{i,j}+T^n_{i,j+1}}{(\Delta r)^2}+\frac{T^n_{i,j+1}-T^n_{i,j-1}}{2r_j\Delta r+}$$

$$+\frac{T^{n+1/2}_{i-1,j}-2T^{n+1/2}_{i,j}+T^{n+1/2}_{i+1,j}}{(\Delta z)^2}=\frac{1}{a_{i,j,n}}\frac{T^{n+1/2}_{i,j}-T^n_{i,j}}{\Delta t/2} \qquad (7)$$

Whereas for the second t/2 we obtain:

$$\frac{T^{n+1}_{i,j-1}-2T^{n+1}_{i,j}+T^{n+1}_{i,j+1}}{(\Delta r)^2}+\frac{T^{n+1}_{i,j+1}-T^{n+1}_{i,j-1}}{2r_j\Delta r}+$$

$$+\frac{T^{n+1/2}_{i-1,j}-2T^{n+1/2}_{i,j}+T^{n+1/2}_{i+1,j}}{(\Delta z)^2}=\frac{1}{a_{i,j,n}}\frac{T^{n+1/2}_{i,j}-T^{n+1/2}_{i,j}}{\Delta t/2} \qquad (8)$$

Numerical solution of the differential equation (2) of heat flow for first $\Delta t/2$ is:

$$2\frac{2T^n_{i,2}-2T^n_{i,1}}{(\Delta r)^2}+\frac{T^{n+1/2}_{i-1,1}-2T^{n+1/2}_{i,1}+T^{n+1/2}_{i+1,1}}{(\Delta z)^2}=$$

$$=\frac{1}{a_{i,1,n}}\frac{T^{n+1/2}_{i,1}-T^n_{i,1}}{\Delta t/2} \qquad (9)$$

and for second $\Delta t/2$:

$$2\frac{2T^{n+1}_{i,2}-2T^{n+1}_{i,1}}{(\Delta r)^2}+\frac{T^{n+1/2}_{i-1,1}-2T^{n+1/2}_{i,1}+T^{n+1/2}_{i+1,1}}{(\Delta z)^2}=$$

$$=\frac{1}{a_{i,1,n}}\frac{T^{n+1}_{i,1}-T^{n+1/2}_{i,1}}{\Delta t/2} \qquad (10)$$

The use of implicit method of variable direction results in a system of simultaneous linear algebraic equations with variables $v_1, v_2...v_n$ of tridiagonal form:

$$\begin{aligned}
b_1v_1+c_1v_2 &= d_1\\
a_2v_1+b_2v_2+c_2v_3 &= d_2\\
a_3v_2+b_3v_3+c_3v_4 &= d_3\\
&\cdots\cdots\\
a_iv_{i-1}+b_iv_i+c_iv_{i+1} &= d_i \qquad (11)\\
&\cdots\cdots\\
a_{N-1}v_{N-2}+b_{N-1}v_{N-1}+c_{N-1}v_N &= d_{N-1}\\
a_Nv_{N-1}+b_Nv_N &= d_N
\end{aligned}$$

Specially efficient algoritm for the solving of tridiagonal system of equations is:

$$v_N=\gamma_N \qquad (12)$$

$$v_i=\gamma_i-\frac{c_iv_{i+1}}{\beta_i},\ i=N-1,\ N-2,\ ...,\ 1 \qquad (13)$$

where β and δ are calculated from recursive formulas

$$\beta_1=b_1 \qquad (14)$$

$$\gamma_1=d_1/\beta_1 \qquad (15)$$

$$\beta_i=b_i-\frac{a_i}{ci-1}\beta_{i-1},\ =2,3,...,N \qquad (16)$$

$$\gamma_i=\frac{d_i-a_1\gamma_{i-1}}{\beta_i},\ i=2,3,...,N \qquad (17)$$

Tridiagonal coefficients which give algorithm of valve housing solidification in sand mould are presented in Appendix 4.

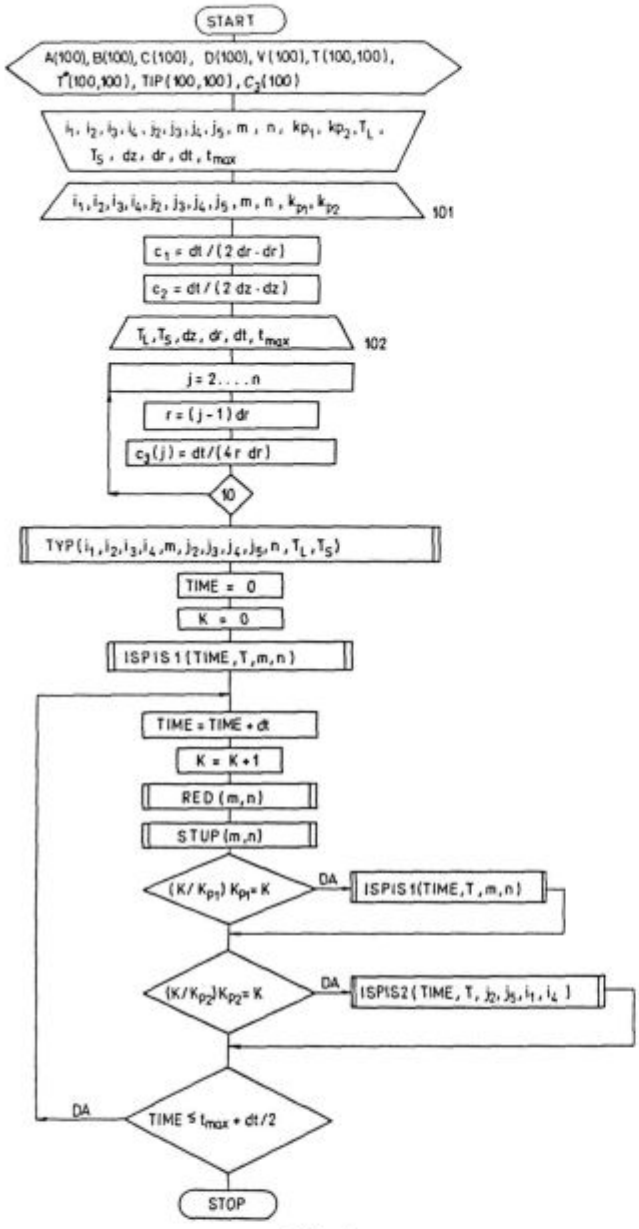

Slika 2
Dijagram toka.

Fig. 2
Flow diagram.

mena $t_{max} = 200$ s. Temperatura lijevanja bila je 1580°C a početna temperatura kalupa i jezgre 25°C. Na temelju sukcesivnih temperaturnih ispisa za pojedine mrežne točke dobije se vrijeme skrućivanja desnog toplinskog centra od 136 s i lijevog toplinskog centra 181 s, što ujedno predstavlja vrijeme skrućivanja cijelog odljevka. Na temelju pomicanja izosolidusa (**slika 3**) može se zaključiti da su mjesta moguće pojave defekta (lunkera) upravo mjesta gdje završava skrućivanje toplinskih centara, odnosno u blizini unutarnjeg ugla odljevka. Iz **slike 3** uočava se da jezgra bolje odvodi toplinu od kalupnog materijala jer su izosolidusi pomaknuti više prema periferiji odljevka.

Točnost simulacije skrućivanja čeličnog ventila u pješčanom kalupu ograničena je s tri aspekta: predpostavkama uvedenim pri definiranju matematičkog mode-

4. FLOW DIAGRAM

Based on the presented algorithm a computer program was written in ASCII FORTRAN and solved on SPERRY 1100 computer. A detailed flow diagram is seen on ***Fig. 2.*** *The main feature of the program is its use of two temperature matrixes namely T and T*. First matrix contains temperatures at the start and end of time step. The other contains temperature at the end of first $\Delta t/2$. Initial values are assigned to program variables and constants. Program module TYP provides for initial values of temperatures of particular net points as well as for standardization of all points in mold, casting, core and theirs boundary interfaces. Module ISPIS1 prints out initial temperature distribution. The system of tridiagonal equations is then solved firstly row by row (module RED) and then column by column (module STUP). Results are periodically printed over the whole geometry of casting, mold and core (module ISPIS1) or over the casting geometry only (module ISPIS2) untill the prescribed time t_{max}.*

5. DISCUSSION

Simulation of the solidification of 0.25% C steel valve housing casted in sand mold is carried out by space step $\Delta z = \Delta r = 1$ cm and time step $\Delta t = 10$ s till $t_{max} = 200$ s. Casting temperature was 1580°C whereas the initial temperature of mold and core was 25°C. On the basis of successive temperatures print out for particular net points, solidification time 136 s for the right and 181 s for the left heat centre is obtained. The later value is also solidification time for entire casting. By isosolidus shift as seen in ***Fig. 3*** *it can be concluded that potential defect sites are obviously the points of final solidification of heat centres i.e. in the vicinity of inner corner of the casting. From fig. 3 it can be seen that cooling rate of the core is higher than that of the mold since isosolidus curves are shifted outward.*

The accuracy of the simulation is limited depending on the assumptions utilized in mathematical model, method of numerical analysis and the utilized values of thermophysical material properties. Several assumptions have been used in the elaboration of the mathematical model. The most important are: the heat transfer rate is complete, the casting temperature is equal to initial temperature of metal in the mold and the mold/casting interfacial thermal contact is perfect. The first assumptions restrains the analysis to the mold-casting-

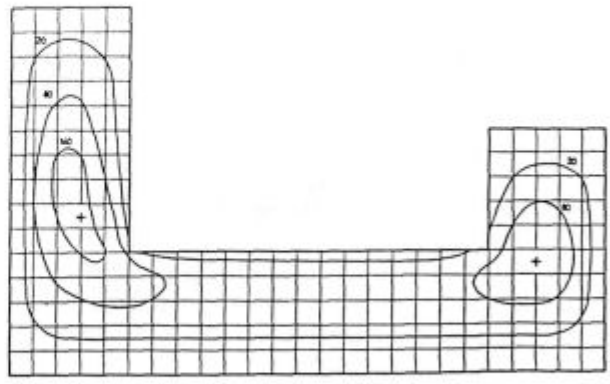

Slika 3
Napredovanje izosolidusa (1449°C) u odljevku za vremena 20, 80 i 140 s.

Fig. 3
Progress of isosolidus (1449°C) after 20, 80 and 140 s.

la, primjenjenoj metodi numeričke analize i korištenim vrijednostima toplofizičkih svojstava materijala. Pri postavljanju matematičkog modela krenulo se od više pretpostavki od kojih su najvažnije pretpostavka o potpunom provođenju topline, pretpostavka da je temperatura lijevanja jednaka početnoj temperaturi metala u kalupu i pretpostavka o savršenom toplinskom kontaktu na graničnoj plohi kalupa i odljevka. Prva pretpostavka ograničuje razmatranje skrućivanja na sistem kalup-odljevak-jezgra u kojem se toplina prenosi samo provođenjem, što znači da se ne razmatraju parcijalni procesi prijenosa topline vezani uz vlagu u kalupu i jezgri. Druga pretpostavka predstavlja pojednostavljenje uvedeno da se izbjegne kompleksno razmatranje protjecanja metala kroz uljevni sistem i kalupnu šupljinu povezano s prijelazom topline. Pretpostavka o savršenom toplinskom kontaktu na graničnoj plohi odljevka i kalupa prihvatljiva je iz razloga što se na graničnoj plohi tek djelomično javljaju plinski zazori, pa se pri matematičkoj formulaciji uzima da vrijedi granični uvjet četvrte vrste. Parcijalna diferencijalna jednadžba provođenja topline riješena je numeričkom metodom konačne razlike - implicitnom metodom promjenljivog smjera koja je odabrana iz razloga što ima veliku točnost pri aproksimaciji i prostora i vremena. Metoda je drugog reda s obzirom na diskretizaciju prostora i vremena. Nedovoljno poznavanje toplofizičkih svojstava materijala posebno pri visokim temperaturama značajno utječe na simulaciju skrućivanja. To se posebno odnosi na toplinska svojstva kalupnog materijala i jezgre, koja je moguće odrediti samo eksperimentalnim putem a pri visokim temperaturama pokazuje širok dijapazon rasipanja.

6. ZAKLJUČAK

U radu je provedena numerička simulacija skrućivanja kućišta ventila od niskougljičnog čeličnog lijeva na formuliranom matematičkom modelu. Modelni sistem je kompleksan jer se sastoji od triju materijala: kalupa, jezgre i odljevka relativno složene geometrije. Matematički model skrućivanja odljevka postavljen je uz pretpostavku da u sistemu postoji samo provođenje topline, što predstavlja fizikalno realnu pretpostavku. Diferencijalna jednadžba provođenja topline koja odgovara geometrijskom uzoru kućišta ventila odgovarajuće je modificirana i riješena numerički implicitnom metodom promjenljivog smjera s time da je uzeta u obzir temperaturna ovisnost toplofizičkih svojstava pojedinih materijala. Na temelju dobivenog algoritma napisan je program u programskom jeziku ASCII FORTRAN za računalo SPERRY 1100. Na temelju simulacije konstatirano je vrijeme skrućivanja od 181 s, a na temelju pomicanja izosolidusa moguće je odrediti tok skurćivanja te mjesta moguće pojave defekta u odljevku.

Dodatak 1

Popis oznaka korištenih u radu

a — temperaturna vodljivost materijala
a_i, b_i, c_i, d_i — koeficijenti uz nepoznanice u tridijagonalnom sistemu algebarskih jednadžbi
c_p — specifična toplina pri konstantnom tlaku
k — toplinska vodljivost materijala
n — normala
r — prostorna koordinata
t — vrijeme
T — temperatura
v_i — nepoznanica u sistemu simultanih algebarskih jednadžbi
z — prostorna koordinata

core system with heat conduction only, i.e. partial heat flows associated with mold and core moisture are not considered. The second assumptions is simplification introduced to avoid complex consideration of metal flow through gate system and mold cavity and matching heat transfer. The assumption of perfect thermal contact on the interface is acceptable since only partial appearance of gaseous clearance therefore in mathematical formulation the boundary condition of fourth kind is usually taken as valid. Partial differential equation for heat flow is solved by numerical method of finite difference - the implicit method of variable direction which was chosen due to its high accuracy at approximation of both time and space. The method is of the second order in respect to discretion of time and space. Insufficient knowledge of thermophysical properties of material specially at high temperatures has a strong influence on simulation of the solidification. It holds specially in respect to thermal properties of mold and core material which can be determined only by experiment. Moreover values for thermal properties at higher temperatures show considerable dissipation.

6. CONCLUSIONS

Numerical simulation of solidification of low carbon steel casting (valve housing) has been carried out on the basis of a suitable mathematical model. The complex model system is composed of three materials: mold, core and casting of comparatively complicated geometry. Mathematical model of solidification has been elaborated assuming thermal conduction as only heat flow in the system which is considered as a physically real assumption. Differential equation for heat flow suited to the geometry of valve housing has been modified and numerically solved by the use of implicit method of variable direction. Temperature dependence of thermophysical material properties has been taken into account. Based on the obtained algorithm a computer program written in ASCII FORTRAN for SPERRY 1100 computer was used for simulation of the solidification. It has been determined that complete solidification takes 181 seconds. The progress of solidification as well as hot spots i.e., sites of potential shrinkage cavities can be determined by shift of isosolidus.

Appendix 1

Abbreviations used:

a - temperature conductivity
a_i, b_i, c_i, d_i coefficients adjoining to unknowns in tridiagonal system of algebraic equations,
c_p - specific heat at constant pressure,
k - thermal conductivity,
n - vertical direction
r - space coordinate
t - time
T - temperature
v_i - unknown in system of simultaneous algebraic equations
z - space coordinate

Indices

i - space coordinate z, value for boundary mold/metal surface
j - space coordinate r, core
k - mold
L - casting
m - metal
s - room, interfacial

Indeksi

i — prostorna koordinata z, vrijednost na graničnoj plohi kalup-metal
j — prostorna koordinata r, jezgra
k — kalup
L — lijevanje
m — metal
s — sobno, površinski

Dodatak 2

Pri izvođenju jednadžbe za početnu temperaturnu raspodjelu na dodirnoj plohi kalupa i metala potrebno je riješiti parcijalnu diferencijalnu jednadžbu provođenja topline s odgovarajućim početnim i graničnim uvjetima

$$\frac{\delta T}{\delta t} = a\frac{\delta^2 T}{\delta x^2} \qquad (18)$$

$$T(x, O) = T_s$$
$$T(O, x) = T_1 \qquad (19)$$
$$|\,T(x, t)\,| < M$$

gdje je M - pozitivna realna konstanta.

Jednadžbu provođenja topline potrebno je riješiti za slučaj kontakta dvaju polubeskonačnih medija, kao što je prikazano na **slici 4**.

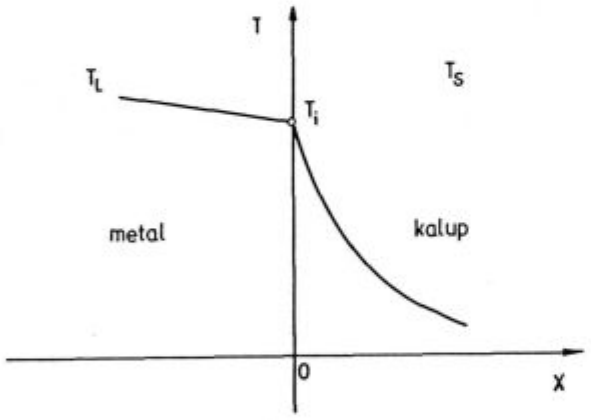

Slika 4
Početna temperatura na graničnoj plohi između kalupa i odljevka.

Fig. 4
Initial temperature on boundary mold/metal surface.

Parcijalnu diferencijalnu jednadžbu (18) potrebno je prevesti u običnu diferencijalnu jednadžbu, što omogućuju Laplaceove transformacije. Laplaceova transformacija definirana je kao:

$$\mathcal{L}\{T(x, t)\} = \theta(x, s) = \int_0^\infty e^{-st}\, T(x, t)\, dt \qquad (20)$$

Parcijalna diferencijalna jednadžba (18) u Laplaceovom području ima oblik:

$$\frac{d^2\theta}{dx^2} - \frac{1}{a}s\theta = -\frac{1}{a}T_s \qquad (21)$$

Rješenje jednadžbe (21) ima oblik:

$$\theta(x\ s) = c_1(s)e^{x\sqrt{s/a}} + c_2(s)\ e^{-x\sqrt{s/a}} + \frac{T_s}{s} \qquad (22)$$

Appendix 2

The following partial differential equation of heat flow with appropriate initial and boundary conditions must be solved in order to derive equation for temperature distribution on mold/metal interface.

$$\frac{\delta T}{\delta t} = a\frac{\delta^2 T}{\delta x^2} \qquad (18)$$

$$T(x, O) = T_s$$
$$T(O, x) = T_1 \qquad (19)$$
$$|\,T(x, t)\,| < M$$

where N is a positive real constant.

Equation of heat flow should be solved for case of the contact of two semi-infinite media as can be seen in ***fig. 4****.*

Partial differential equation (18) must be transformed into common differential equation by Laplace transformation defined as:

$$\mathcal{L}\{T(x, t)\} = \theta(x, s) = \int_0^\infty e^{-st}\, T(x, t)\, dt \qquad (20)$$

The equation (18) in Laplace region has the form:

$$\frac{d^2\theta}{dx^2} - \frac{1}{a}s\theta = -\frac{1}{a}T_s \qquad (21)$$

The solution of (21) has the form:

$$\theta(x\ s) = c_1(s)e^{x\sqrt{s/a}} + c_2(s)\ e^{-x\sqrt{s/a}} + \frac{T_s}{s} \qquad (22)$$

Because of temperature limitations $|T(x,t)| < M$ $c_1 = 0$ *for* $x \to \infty$, *i.e.*

$$\theta(x,s) = c_2\, e^{-x\sqrt{s/a}} + \frac{T_s}{s} \qquad (23)$$

For boundary condition $T(0,t) = T_i$ *i.e.*

$\theta(O,s) = c_2 + \frac{T_s}{s} = \frac{T_1}{s}$ *dobije se* $c_2 = \frac{1}{s}(T_i - T_s)$.

Final result in Laplace region is:

$$\theta(x,s) = \frac{T_i - T_s}{s}\, e^{-x\sqrt{s/a}} + \frac{T_s}{s} \qquad (24)$$

By going out of Laplace region into real space we have:

$$T(x,t) = (T_i - T_s)\ erfc\ \left(\frac{x}{2\sqrt{at}}\right) + T \qquad (25)$$

$$odnosno\ \frac{T - T_i}{T_s - T_i} = erf\ \left(\frac{x}{2\sqrt{at}}\right) \qquad (25')$$

where the error function is defined as:

$$erf\,(t) = \frac{2}{\sqrt{\pi}}\int_0^t e^{-u^2}\,du \qquad (26)$$

Temperature gradient along x - axis is:

$$\frac{\delta T}{\delta x} = \frac{T_s - T_i}{\sqrt{\pi at}}e^{-x^2/4at} \qquad (27)$$

$$odnosno\ \left(\frac{\delta T}{\delta x}\right) x = o = \frac{T_s - T_i}{\sqrt{\pi at}} \qquad (28)$$

Two semi-infinite media (mold and metal) are in interfacial contact and the boundary condition of fourth kind is valid:

Zbog ograničenosti temperature, odnosno $|T(x,t)| < M$ slijedi $c_1 = 0$ za $x \to \infty$, odnosno

$$\theta(x,s) = c_2 e^{-x\sqrt{s/a}} + \frac{T_s}{s} \quad (23)$$

Korištenjem graničnog uvjeta $T(0,t) = T_i$, odnosno

$\theta(O,s) = c_2 + \frac{T_s}{s} = \frac{T_i}{s}$ dobije se $c_2 = \frac{1}{s}(T_i - T_s)$.

Konačni rezultat u Laplaceovom području je

$$\theta(x,s) = \frac{T_i - T_s}{s} e^{-x\sqrt{s/a}} + \frac{T_s}{s} \quad (24)$$

Prijelazom iz Laplaceovog područja u realno područje dobije se

$$T(x,t) = (T_i - T_s)\ \mathrm{erfc}\ \left(\frac{x}{2\sqrt{at}}\right) + T \quad (25)$$

$$\text{odnosno } \frac{T - T_i}{T_s - T_i} = \mathrm{erf}\ \left(\frac{x}{2\sqrt{at}}\right) \quad (25')$$

pri čemu je funkcija pogreške definirana kao

$$\mathrm{erf}\ (t) = \frac{2}{\sqrt{\pi}} \int_0^t e^{-u^2} du \quad (26)$$

Temperaturni gradijent u smjeru osi x je:

$$\frac{\delta T}{\delta x} = \frac{T_s - T_i}{\sqrt{\pi at}} e^{-x^2/4at} \quad (27)$$

$$\text{odnosno } \left(\frac{\delta T}{\delta x}\right)_{x=o} = \frac{T_s - T_i}{\sqrt{\pi at}} \quad (28)$$

Na graničnoj plohi u kontaktu su dva polubeskonačna medija (kalup i metal) pri čemu vrijedi granični uvjet četvrte vrste:

$$-k_k \left(\frac{\delta T_k}{\delta x}\right)_{x=0} = -k_m \left(\frac{\delta T_m}{\delta x}\right)_{x=0} \quad (29)$$

Uvrštavanjem odgovarajućih gradijenata temperature dobije se

$$k_k \frac{T_i - T_s}{\sqrt{\pi a_k t}} = k_m \frac{T_L - T_i}{\sqrt{\pi a_m t}} \quad (30)$$

Sređivanjem jednadžbe (30) dobije se početna temperaturna raspodjela na graničnoj plohi između kalupa i odljevka

$$T_i = T_s + \frac{T_L + T_s}{1 + \frac{k_k}{k_m}\sqrt{\frac{a_m}{a_k}}} \quad (31)$$

Dodatak 3

Toplofizička svojstva materijala

a) Niskougljični čelični lijev (oko 0,25 % C)

Toplinska vodljivost, W/mK

$T \geq 1499^0$ C $\quad k = 25{,}96$
$1499^0\text{C} > T \geq 1449^0$ C $\quad k = 207{,}54 - 0{,}12114\ T$
$1499^0\text{C} > T \geq 893^0$ C $\quad k = 26{,}6 + 0{,}00374\ T$
$893^0\text{C} > T \quad k = 50{,}31 - 0{,}0225\ T$

Specifična toplina, J/kgK

$$-k_k \left(\frac{\delta T_k}{\delta x}\right)_{x=0} = -k_m \left(\frac{\delta T_m}{\delta x}\right)_{x=0} \quad (29)$$

By including proper temperature gradients:

$$k_k \frac{T_i - T_s}{\sqrt{\pi a_k t}} = k_m \frac{T_L - T_i}{\sqrt{\pi a_m t}} \quad (30)$$

Finally, initial temperature distribution on the boundary mold/metal surface is obtained:

$$T_i = T_s + \frac{T_L + T_s}{1 + \frac{k_k}{k_m}\sqrt{\frac{a_m}{a_k}}} \quad (31)$$

Appendix 3

Thermo-physical properties of the materials

a) Low carbon (0.25 % C) casted steel

Thermal conductivity, W/mK

$T \geq 1499^0$ C $\quad k = 25{,}96$
$1499^0\text{C} > T \geq 1449^0$ C $\quad k = 207{,}54 - 0{,}12114\ T$
$1499^0\text{C} > T \geq 893^0$ C $\quad k = 26{,}6 + 0{,}00374\ T$
$893^0\text{C} > T \quad k = 50{,}31 - 0{,}0225\ T$

Specific heat, J/kgK

$T \geq 1499^0$ C $\quad c_p = 879{,}2$
$1499^0\text{C} > T \geq 1474^0$ C $\quad c_p = 652273{,}5 - 434{,}585\ T$
$1474^0\text{C} > T \geq 1449^0$ C $\quad c_p = 436{,}258\ T - 631251{,}9$
$1449^0\text{C} > T \geq 982^0$ C $\quad c_p = 421{,}36 + 0{,}28712\ T$
$982^0\text{C} > T \geq 704^0$ C $\quad c_p = 1502{,}8 - 0{,}81391\ T$
$704^0\text{C} > T \geq 427^0$ C $\quad c_p = 143{,}76 + 1{,}11535\ T$
$427^0\text{C} > T \quad c_p = 458{,}86 + 0{,}37681\ T$

b) Core
Thermal conductivity, W/mK
$k = 3.246 \times 10^{-6}\ T^2 - 3.894 \times 10^{-3} T + 3.052$
Temperature diffusivity, m^2/s
$a = 1.689 \times 10^{-12}\ T^2 - 2.174 \times 10^{-9} T + 1.785 \times 10^{-6}$

c) Mold

Thermal conductivity, W/mK
$k = 3.937 \times 10^{-6} T^2 - 3.57 \times 10^{-3} T + 3.421$
Temperature diffusivity, m^2/s
$a = 1.957 \times 10^{-12} T^2 - 1.8 \times 10^{-9} T + 1.913 \times 10^{-6}$

Appendix 4

Constants which appear in tridiagonal coefficients

$$p_1 = \frac{a\,\Delta t}{2\,(\Delta r)^2}$$

$$p_2 = \frac{a\,\Delta t}{4 r_f \Delta r}$$

$$p_3 = p_1 - p_2$$

$$p_4 = p_1 + p_2$$

$$p_5 = \frac{\Delta t\,(k_A + k_B)}{2\,c\,(\Delta r)^2}$$

$$p_6 = \frac{\Delta t\,(k_A + k_B)}{4\,c\,r_f \Delta r}$$

$$c = \frac{k_A}{a_A} + \frac{k_B}{a_B}$$

$T \geq 1499^0C \quad c_p = 879{,}2$
$1499^0C > T \geq 1474^0C \quad c_p = 652273{,}5 - 434{,}585\ T$
$1474^0C > T \geq 1449^0C \quad c_p = 436{,}258\ T - 631251{,}9$
$1449^0C > T \geq 982^0C \quad c_p = 421{,}36 + 0{,}28712\ T$
$982^0C > T \geq 704^0C \quad c_p = 1502{,}8 - 0{,}81391\ T$
$704^0C > T \geq 427^0C \quad c_p = 143{,}76 + 1{,}11535\ T$
$427^0C > T \quad c_p = 458{,}86 + 0{,}37681\ T$

b) Jezgra

Toplinska vodljivost, W/mK
$k = 3{,}246 \cdot 10^{-6}\,T^2 - 3{,}894 \cdot 10^{-3}T + 3{,}052$
Temperaturna vodljivost, m^2/s
$a = 1{,}689 \cdot 10^{-12}T^2 - 2{,}174 \cdot 10^{-9}\,T + 1{,}785 \cdot 10^{-6}$

c) Kalup

Toplinska vodljivost, W/mK
$k = 3{,}937 \cdot 10^{-6}\,T^2 - 3{,}57 \cdot 10^{-3}\,T + 3{,}421$
Temperaturna vodljivost, m^2/s
$a = 1{,}957 \cdot 10^{-12}\,T^2 - 1{,}8 \cdot 10^{-9}\,T + 1{,}913 \cdot 10^{-6}$

Dodatak 4

Konstante koje se javljaju u tridijagonalnim koeficijentima

$$p_1 = \frac{a\,\Delta t}{2\,(\Delta r)^2}$$

$$p_2 = \frac{a\,\Delta t}{4 r_j \Delta r}$$

$$p_3 = p_1 - p_2$$

$$p_4 = p_1 + p_2$$

$$p_5 = \frac{\Delta t\,(k_A + k_B)}{2\,c\,(\Delta r)^2}$$

$$p_6 = \frac{\Delta t\,(k_A + k_B)}{4\,c\,r_j \Delta r}$$

$$c = \frac{k_A}{a_A} + \frac{k_B}{a_B}$$

$$q_1 = \frac{a\Delta t}{2\,(\Delta z)^2}$$

$$q_2 = \frac{K_A \Delta t}{c\,(\Delta z)^2}$$

$$q_3 = \frac{k_A \Delta t}{c\,(\Delta z)^2}$$

$$q_4 = \frac{\Delta t\,(k_A + k_B)}{2\,c\,(\Delta z)^2}$$

$$q_5 = \frac{K_A sa40D^t}{c\,(\Delta r)^2}$$

$$q_6 = \frac{k_B \Delta t}{c\,(\Delta r)^2}$$

Tridijagonalni koeficienti
1. Točka (i,j) u kalupu, metalu odnosno jezgri
— prvi $\Delta t/2$:

$$q_1 = \frac{a\Delta t}{2\,(\Delta z)^2}$$

$$q_2 = \frac{K_A \Delta t}{c\,(\Delta z)^2}$$

$$q_3 = \frac{k_A \Delta t}{c\,(\Delta z)^2}$$

$$q_4 = \frac{\Delta t\,(k_A + k_B)}{2\,c\,(\Delta z)^2}$$

$$q_5 = \frac{K_A sa40D^t}{c\,(\Delta r)^2}$$

$$q_6 = \frac{k_B \Delta t}{c\,(\Delta r)^2}$$

Tridiagonal coefficients
1. Point (i,j) in the mold, metal or core; first $\Delta t/2$:

$a_i = c_i = -q_1$
$b_i = 1 + 2\,q_1$
$d_i = p_3\,T^n_{i,j-1} + (1 - 2p_1)\,T^n_{i,j} + p_4 T^n_{i,j+1}$ (32)

— second $\Delta t/2$:

$a_j = -p_3$
$b_i = 1 + 2\,p_1$
$c_j = -p_4$
$d_i = q_1\,T^{n+1/2}_{i-1,j} + (1 - 2q_1)\,T^{n+1/2}_{i,j} + q_1\,T^{n+1/2}_{i+1,j}$ (33)

2. Point (i,j) on the boundary surface parallel to r axis separating the material A (left) and B (right).

— first $\Delta t/2$:

$a_i = -q_2$
$b_i = 1 + q_2 + q_3$
$c_i = q_3$
$d_i = (p_5 - p_6)\,T^n_{i,j-1} + (1 - 2p_5)\,T^n_{i,j} + (p_5 + p_6)\,T^n_{i,j+1}$ (34)

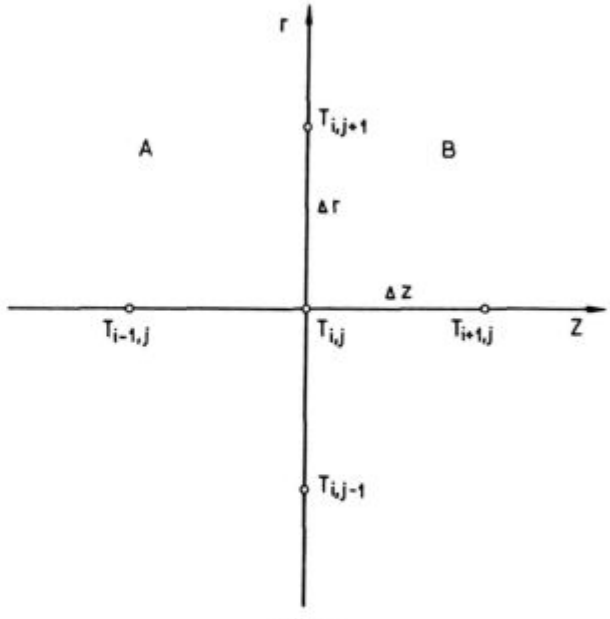

Slika 5
Mrežna točka (i,j) na vertikalnoj graničnoj plohi.
Fig. 5
Net point (i,j) on vertical boundary surface.

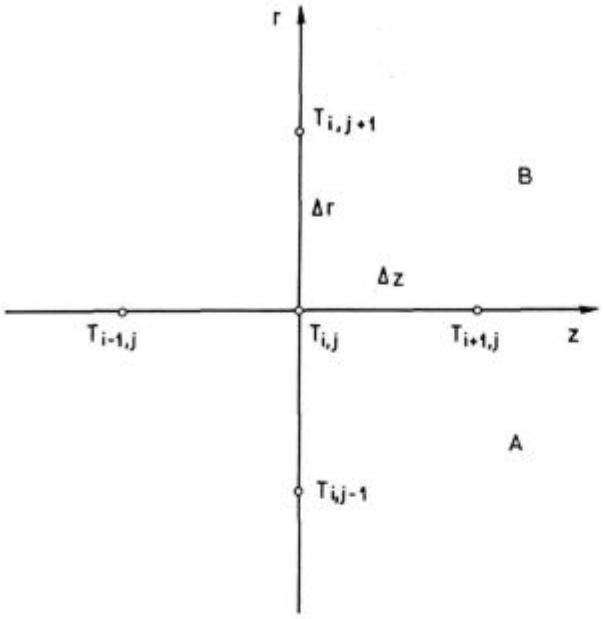

Slika 6
Mrežna točka (i,j) na horizontalnoj graničnoj plohi.
Fig. 6
Net point (i,j) on horizontal boundary surface.

$a_i = c_i = -q_1$
$b_i = 1 + 2\,q_1$
$d_i = p_3\,T^n_{i,j-1} + (1-2p_1)\,T^n_{i,j} + p_4 T^n_{i,j+1}$ (32)

— drugi $\Delta t/2$:

$a_j = -p_3$
$b_j = 1 + 2\,p_1$
$c_j = -p_4$
$d_j = q_1\,T^{n+1/2}_{i-1,j} + (1-2q_1)\,T^{n+1/2}_{i,j} + q_1\,T^{n+1/2}_{i+1,j}$ (33)

2. Točka (i,j) na graničnoj plohi paralelno r osi koja odvaja materijal A (lijevo) i B (desno)
— prvi $\Delta t/2$:

$a_i = -q_2$
$b_i = 1 + q_2 + q_3$
$c_i = q_3$
$d_i = (p_5 - p_6)\,T^n_{i,j-1} + (1-2p_5)\,T^n_{i,j} + (p_5 + p_6)\,T^n_{i,j+1}$ (34)

— drugi $\Delta t/2$:
$a_j = -(p_5 - p_6)$
$b_j = 1 + 2\,p_5$
$c_j = -(p_5 + p_6)$
$d_j = q_2\,T^{n+1/2}_{i-1,j} + (1-q_2-q_3)\,T^{n+1/2}_{i,j} + q_3\,T^{n+1/2}_{i+1,j}$ (35)

3. Točka (i, j) na graničnoj plohi paralelno z osi koja dijeli materijal A (dolje) i B (gore)

— prvi $\Delta t/2$:
$a_i = c_i = -q_4$
$b_i = 1 + 2q_4$
$d_i = (q_5 - q_6)\,T^n_{i,j-1} + (1-2p_5)\,T^n_{i,j} + (q_6 + p_6)\,T^n_{i,j+1}$ (36)

— drugi $\Delta t/2$:
$a_j = p_6 - q_5$
$b_j = 1 + 2p_5$
$c_j = -(q_6 + p_6)$
$d_j = q_4\,T^{n+1/2}_{i-1,j} + (1-2q_4)T^{n+1/2}_{i,j} + q_4\,T^{n+1/2}_{i+1,j}$ (37)

— *second* $\Delta t/2$:
$a_j = -(p_5 - p_6)$
$b_j = 1 + 2\,p_5$
$c_j = -(p_5 + p_6)$
$d_j = q_2\,T^{n+1/2}_{i-1,j} + (1-q_2-q_3)\,T^{n+1/2}_{i,j} + q_3\,T^{n+1/2}_{i+1,j}$ (35)

3. Point (i,j) on the boundary surface parallel to z axis separating the material A (down) and B (up).
— *first* $\Delta t/2$:
$a_i = c_i = -q_4$
$b_i = 1 + 2q_4$
$d_i = (q_5 - q_6)\,T^n_{i,j-1} + (1-2p_5)\,T^n_{i,j} + (q_6 + p_6)\,T^n_{i,j+1}$ (36)

— *second* $\Delta t/2$:
$a_j = p_6 - q_5$
$b_j = 1 + 2p_5$
$c_j = -(q_6 + p_6)$
$d_j = q_4\,T^{n+1/2}_{i-1,j} + (1-2q_4)T^{n+1/2}_{i,j} + q_4\,T^{n+1/2}_{i+1,j}$ (37)

4. Point (i,1) out of boundary surface; first $\Delta t/2$:

$a_i = c_i = -q_1$
$b_i = 1 + 2q_1$
$d_i = (1-4p_1)\,T^n_{i,1} + 4p_1\,T^n_{i,2}$ (38)

— *second* $\Delta t/2$:

$b_j = 1 + 4p_1$
$c_j = 4p_1$
$d_j = q_1\,T^{n+1/2}_{i-1,1} + (1-2q_1)\,T^{n+1/2}_{i,1} + q_1\,T^{n+1/2}_{i+1,1}$ (39)

5. Point (i,1) on the boundary surface which separate material A (left) and B (right)

— *first* $\Delta t/2$:
$a_i = -q_2$
$b_i = 2q_4 + 1$
$c_i = -q_3$
$d_i = (1-4p_5)\,T^n_{i,1} + 4p_5\,T^n_{i,2}$ (40)

— *second* $\Delta t/2$:

$b_j = 4p_5 + 1$
$c_j = -4p_5$
$d_j = q_2\,T^{n+1/2}_{i-1,1} + (1-2q_4)\,T^{n+1/2}_{i,1} + q_3\,T^{n+1/2}_{i+1,1}$ (41)

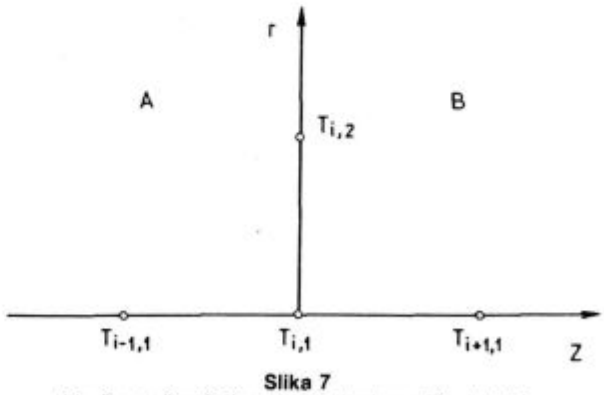

Slika 7
Mrežna točka (i,1) na vertikalnoj graničnoj plohi.
Fig. 7
Net point (i,1) on vertical boundary surface.

4. Točka (i, 1) koja nije na granici

— prvi $\Delta t/2$:

$$a_i = c_i = -q_1$$
$$b_i = 1 + 2q_1$$
$$d_i = (1 - 4p_1)\, T^n_{i,1} + 4p_1\, T^n_{i,2} \qquad (38)$$

— drugi $\Delta t/2$:

$$b_j = 1 + 4p_1$$
$$c_j = 4p_1$$
$$d_j = q_1\, T^{n+1/2}_{i-1,1} + (1 - 2q_1)\, T^{n+1/2}_{i,1} + q_1\, T^{n+1/2}_{i+1,1} \qquad (39)$$

5. Točka (i, 1) na graničnoj plohi koja dijeli materijal A (lijevo) i B (desno)

— prvi $\Delta t/2$:

$$a_i = -q_2$$
$$b_i = 2q_4 + 1$$
$$c_i = -q_3$$
$$d_i = (1 - 4p_5)\, T^n_{i,1} + 4p_5\, T^n_{i,2} \qquad (40)$$

— drugi $\Delta t/2$:

$$b_j = 4p_5 + 1$$
$$c_j = -4p_5$$
$$d_j = q_2\, T^{n+1/2}_{i-1,1} + (1 - 2q_4)\, T^{n+1/2}_{i,1} + q_3\, T^{n+1/2}_{i+1,1} \qquad (41)$$

LITERATURA / *REFERENCES*

1. E. R. G. Eckert, R. M. Drake, Analysis of Heat and Mass Transfer, McGraw-Hill Kogakusha, Tokyo, 1972.
2. R. D. Pehlke, A. Jeyarajan, H. Wada, Summary of Thermal Properties for Casting Alloys and Mold Materials, University of Michigan, Ann Arbor, 1982.
3. J. Douglas, H. H. Rachford, Trans. Amer. Math. Soc. 82 (1956), 421.

Vsebina — *Contents*

Grozdanič V., J. Črnko

Kompjutorska simulacija skrućivanja odljevaka kompleksne geometrije

Železarski zbornik 25 (1991) 4 s 149—158

Numeriča simulacija, skrućivanje, niskougljični čelični lijev, kućište ventila

U radu je provedena simulacija skrućivanja odljevka relativno kompleksne geometrije — kućišta ventila od niskougljičnog čeličnog lijeva na formuliranom matematičkom modelu. Postavljeni matematički model temelji se na fizikalno realnim pretpostavkama i riješen je numeričkom metodom konačne razlike — implicitnom metodom promjenljivog smjera. Simulacija skrućivanja provedena je tako da je latentna toplina kristalizacije inkorporirana u jednadžbu za specifičnu toplinu metala s time da je uzeta temperaturna ovisnost toplofizičkih svojstava svih materijala u sistemu kalup-odkljevak-jezgra. Simulacija skrućivanja kućišta ventila, odnosno odljevka relativno složene geometrije koji je često primjer u ljevaoničkoj praksi, omogućuje da se unaprijedi naše saznanje o procesu skrućivanja takvih odljevaka te da se na suvremen i znanstveni način ukaže na mjesta moguće pojave defekta a da se pri tome ne odlije ni jedan odljevak.

Grozdanič V., J. Črnko

Solidification Simulation of Castings of Complex Geometry

Železarski zbornik 25 (1991) 4P 149—158

Numerical simulation, solidification, low-carbon steel, valve housing

The solidification simulation of the casting of relatively complex geometry, low-carbon steel valve housing, has been presented in the paper. Mathematical model has been based on physical realistic assumptions, and has been solved by finite difference method — implicit alternating directions method. Simulation of solidification has been performed so that the latent heat of solidification has been incorporated in the equation for specific heat of metal, and the temperature dependence of thermal properties of all materials in the system mould-casting-core has been taken. The solidification simulation of valve housing, that is the casting of relatively complex geometry which is a common example in foundry practice, enables the improvement of our knowledge about solidification process in these castings, and points in a modern and scientific way to the points where defects occurrence is possible and in this way the casting is not necessary.

Železarski zbornik, 25, 1991, 1—4

1. KRONOLOŠKO KAZALO

2. AVTORSKO KAZALO

SLOVENSKE ŽELEZARNE

ŽELEZARNA ŠTORE

ŠTORE

PROIZVODNI PROGRAM

Toplo valjani profili
- kvalitetno in plemenito ogljikovo jeklo ter
- kvalitetno in plemenito nizko legirano jeklo v okrogli, ploščati in kvadratni obliki,
- specialni profili po načrtih

Hladno oblikovani profili
- vlečeno in brušeno jeklo v vseh kvalitetah v okrogli, ploščati in specialni izvedbi

Livarski proizvodi
- ulitki iz sive litine,
- ulitki iz nodularne (KGR) litine,
- kontinuirno liti profili,
- litoželezni valji,
- jeklarske kokile,
- priklopna sedla,
- mehanski sklopi,
- strmoramenska platišča

Industrijska oprema
- industrijski gorilniki, industrijske peči za ogrevanje, žarenje itd.,
- indukcijske peči,
- rekuperativna toplotna tehnika,
- plinski oskrbovalni sistemi za ZP in zamenljive mešanice

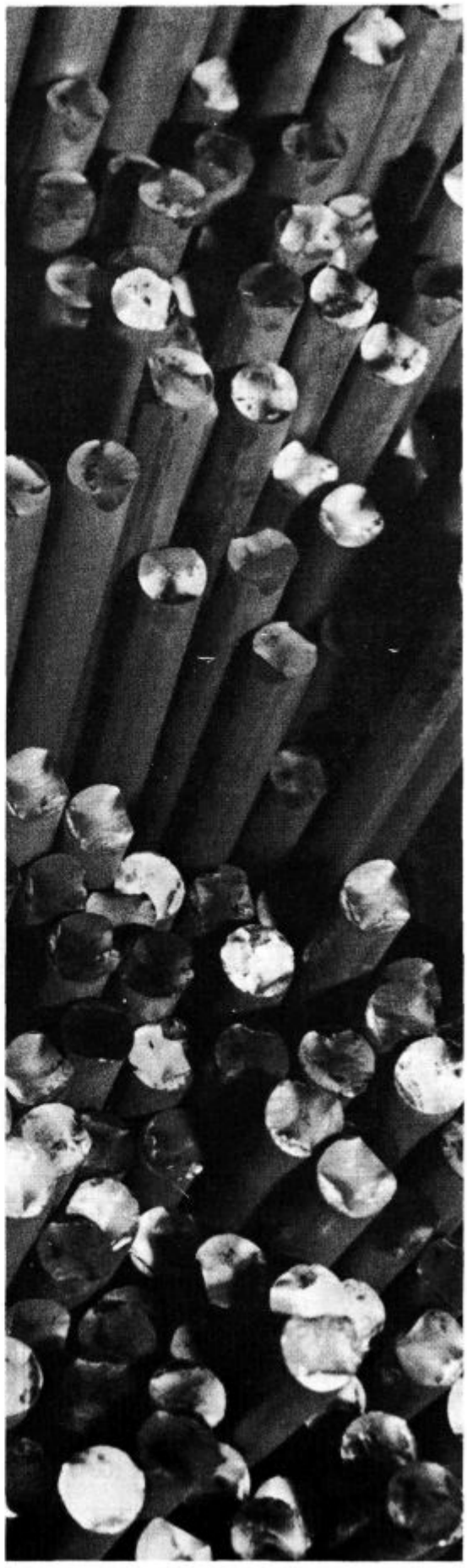

Vlečene palice kakovostnega jekla